

Dissertation

**Exploring the Pathophysiology of Vocal Fold Inflammation:
The Molecular Impact of Vibration**

submitted by

Dr.med.univ. David HORTOBAGYI

for the Academic Degree of

Doctor of Medical Science (Dr. scient. med.)

at the

Medical University of Graz

Division of Phoniatics, ENT Hospital

under the Supervision of

Univ.-Prof. Priv.-Doz. Dr.med.univ.et scient.med. Markus

GUGATSCHKA

2022

Statutory Declaration

I hereby declare that this thesis is my own original work and that I have fully acknowledged by name all of those individuals and organizations that have contributed to the research for this thesis. Due acknowledgement has been made in the text to all other material used. Throughout this thesis and in all related publications I followed the “Standards of Good Scientific Practice and Ombuds Committee at the Medical University of Graz”.

Graz, 01.01.2022

Disclosures

Part of this thesis has been published in *PLoS One*,

In vitro mechanical vibration down-regulates pro-inflammatory and pro-fibrotic signaling in human vocal fold fibroblasts (1)

David Hortobagyi, Tanja Grossmann, Magdalena Tschernitz, Magdalena Grill, Andrijana Kirsch, Claus Gerstenberger, Markus Gugatschka

Division of Phoniatics, Medical University of Graz, Graz, Austria

All co-authors agreed to the use of their data in the thesis and the respective publication:

Contributions of co-authors to the thesis and the respective publication:

Tanja Grossmann supervised the experiments and contributed to project design as well as data acquisition.

Magdalena Tschernitz contributed to performing the experiments.

Magdalena Grill gave input in project design and methodology.

Andrijana Kirsch supported in investigatory processes and project design.

Claus Gerstenberger was responsible for the development of the phonomimetic bioreactor.

Markus Gugatschka was the project supervisor and therefore was involved in conceptualization, visualization as well as project administration.

Acknowledgements

Initially I would like to express my gratitude to all the team members of the LTTEG (Laryngo Tracheal Tissue Engineering Graz) research group without whom this work would not have been possible. In particular I would like to express my sincere appreciation to Prof. Markus Gugatschka, who encourages me to have a look on things from different perspectives, helps me improve my professional as well as my general knowledge, makes me keep an eye on the bigger picture and promotes my creativity.

My sincere thanks also go to Prof. Barbara Obermayer-Pietsch and Prof. Christian Wadsack, who gave important inputs to improve my work.

Furthermore, I would like to thank the Medical University of Graz, who funded the publication of my paper through the Doctoral School "Molecular Medicine and Inflammation" and who gave me the possibility to take multiple great courses in order to become a better scientist and medical doctor.

Last but not least I would like to thank my family and friends, especially Anna-Maria Haas whose unconditional love makes me to a better person and without whom I would have never made it this far. Because of her and our son Leon I wake up every day as one of the happiest persons in the world.

Table of contents

ABBREVIATIONS AND DEFINITIONS	9
LIST OF FIGURES	12
LIST OF TABLES	13
ABSTRACT IN GERMAN	14
ABSTRACT IN ENGLISH	16
INTRODUCTION	17
Vocal fold composition	18
Epithelium	18
Basement membrane	19
Lamina propria	19
Vocal fold muscle	21
Physiology	21
Myoelastic-aerodynamic theory	21
Body-cover-theory	22
Source filter theory	22
Mechanotransduction	23
Wound healing	25
Inflammatory phase	25
Proliferative Phase	25
Remodeling	26
Scar formation	26
Diagnostic methods	27

VF scar treatment options	27
Medialization thyroplasty	28
Injection laryngoplasty	28
Experimental approaches	28
Growth factors	28
Cell therapy	29
Tissue engineering.....	29
Gene editing	30
Vocal rest	31
Bioreactors	32
2D-Bioreactors	35
3D-Bioreactor	35
Present bioreactor/Graz prototype.....	35
MATERIALS AND METHODS	38
Cell culture	38
Selection of genes and molecules	40
ECM-related molecules.	40
Inflammatory and fibrogenic markers.....	44
Lactate dehydrogenase (LDH) assay	47
.....	48
Isolation of RNA and Reverse Transcription-quantitative Polymerase Chain Reaction (RT-qPCR)	49
Western blot analysis	52
Magnetic Luminex assay	52
Enzyme-linked immunosorbent assay (ELISA)	53
Statistical analysis	53
RESULTS	55

Preliminary trials	55
Genotypic alterations	55
Phenotypic alterations	56
Four hours of vibration per day	57
Fibroblast viability	57
Gene expression and protein synthesis	58
Phenotypic alterations	61
Eight hours of vibration per day	63
Fibroblast viability	63
Gene expression	64
DISCUSSION	67
<i>In vivo</i> studies	67
<i>In vitro</i> studies	68
Effects of vibration and cytokine-stimuli on VFF	69
MAPK/Erk	71
Limitations	72
Conclusion	73
REFERENCES	75
SUPPLEMENTARY APPENDIX	90
Supplementary file 1: raw data from statistical tests four hours of vibration per day	90
qPCR	90
Luminex	97
Western Blot	101
ELISA.....	102
Supplementary file 2: raw data from statistical tests - eight hours of vibration per day	103
qPCR	103
1-way ANOVA.....	105

Kruskal-Wallis	105
Man-U-Whitney.....	105
Tukey-post hoc	106
Supplementary file 3: Catalogue numbers.....	109
General laboratory equipment.....	109
LDH Assay	111
qPCR	111
Western Blot	111
Supplementary file 4: Standard Curves of Luminex Samples - four hours of vibration per day	112
COL1A1	112
FN1	112
TIMP1	113
VEGF A	113
VEGF C	115
bFGF	115
IL11	117

Abbreviations and Definitions

2D	two-dimensional
3D	three-dimensional
ACTA	alpha smooth muscle actin
ASC	adipose tissue derived stem cells
α-SMA	alpha smooth muscle actin
B2M	beta-2 microglobulin
bFGF	basic fibroblast growth factor
BM	basement membrane
BMSC	bone marrow derived stem cells
Cas	CRISPR-associated
cDNA	complementary deoxyribonucleic acid
COL	collagen
COX	cyclooxygenase
CRISPR	clustered regularly interspaced short palindromic repeats
crRNA	CRISPR RNA
CT	cycle threshold
DAMP	damage associated molecular patterns
DMEM	Dulbecco's Modified Eagle's Medium
ECM	extracellular matrix
EDTA	ethylenediaminetetraacetic acid
EGF	epidermal growth factor
ELISA	enzyme-linked immunosorbent assay
ELN	elastin
Erk	extracellular signal-regulated kinase
FAK	focal adhesion kinase
FBS	fetal bovine serum
Fc	Ficoll
FGFR	fibroblast growth factor receptor
FN	fibronectin
GAG	glycosaminoglycan
GAPDH	glyceraldehyde phosphate dehydrogenase
gDNA	genomic DNA
GRBAS	grade, roughness, breathiness, asthenia, strain
HA	hyaluronic acid

HAS	hyaluronan synthase
HGF	hepatocyte growth factor
HMGB1	major sources of high-mobility group box
(h)VFF	(human) vocal fold fibroblast
HYAL	hyaluronidase
IL	interleukin
JNK	c-Jun NH2- terminal kinase
LDH	lactate dehydrogenase
LDV	laser doppler vibrometry
LP	lamina propria
LXSAHM	Human Magnetic Luminex Assays
MAPK	mitogen-activated protein kinases
MCP-1	monocyte chemoattractant protein-1
MEK	Mitogen-activated protein/extracellular signal-regulated kinase
MM	macromolecules
MMC	macromolecular crowding
MMP	matrix metalloproteinase
mRNA	messenger RNA
OA	Optical absorbance
PAMP	pathogen associated molecular patterns
PBS	phosphate buffered saline
PEB	protein extraction buffer
PDGF	platelet derived growth factors
PIGF	placental growth factor
POM	polyoxymethylene
qPCR	quantitative polymerase chain reaction
RISC	RNA-induced silencing complex
RNAi	RNA interference
RT	reverse transcription
SERPINH1	Serpin peptidase inhibitor clade H, member 1
siRNA	small interfering ribonucleic acid
TALENs	transcription activator-like effector nucleases
TERT	telomerase reverse transcriptase

TGF	transforming growth factor
TIMP	tissue inhibitor of metalloproteinase
tracrRNA	trans-activating crRNA
UXT	ubiquitously expressed transcript protein
VEGF	vascular endothelial growth factor
VEGFR	VEGF-receptors
VF	vocal fold
VHI	voice handicap index

List of figures

FIGURE 1 SCHEMATICAL VOCAL FOLD STRUCTURE.....	18
FIGURE 2: HISTOLOGICAL STRUCTURE OF THE HUMAN VOCAL FOLD (PERIODIC ACID ALCIAN BLUE STAINING).....	19
FIGURE 3: HISTOLOGICAL STRUCTURE OF THE HUMAN VOCAL FOLD (HEMATOXYLIN-EOSIN STAINING).....	21
FIGURE 4: ILLUSTRATION OF POSSIBLE WAYS OF MECHANOTRANSDUCTION.....	24
FIGURE 5: DESIGN OF THE LOUDSPEAKER WITH MOUNTING BEARING A SIX-WELL PLATE ON THE TOP.....	37
FIGURE 6: SCHEMATIC REPRESENTATION OF THE BIOREACTOR WITH ITS COMPONENTS...37	
FIGURE 7: EXPERIMENTAL SETUP.....	39
FIGURE 8: SCHEMATIC ILLUSTRATION OF HYALURONIC ACID DISACCHARIDE UNIT (A) AND CHEMICAL STRUCTURE (B).....	43
FIGURE 9: LASER DOPPLER VIBROMETER MEASUREMENTS.....	48
FIGURE 10: ALTERATIONS OF GENE EXPRESSION UNDER INFLAMMATORY CONDITIONS OVER TIME.....	55
FIGURE 11: MORPHOLOGICAL CHANGES AFTER DIFFERENT DURATION OF CYTOKINE TREATMENT.....	56
FIGURE 12: EFFECT OF VIBRATION (4 HOURS PER DAY) AND/OR CYTOKINE EXPOSURE ON CELL VIABILITY AND GENE EXPRESSION.....	57
FIGURE 13: EFFECT OF VIBRATION WITH/WITHOUT CYTOKINE EXPOSURE ON HA METABOLISM.....	58
FIGURE 14: EFFECT OF VIBRATION WITH/WITHOUT CYTOKINE EXPOSURE ON ECM-RELATED MOLECULES.....	59
FIGURE 15: EFFECT OF VIBRATION WITH/WITHOUT CYTOKINE EXPOSURE ON ECM-RELATED MOLECULES, GROWTH FACTORS AND ANGIOGENIC FACTORS.....	60
FIGURE 16: EFFECT OF VIBRATION WITH/WITHOUT CYTOKINE EXPOSURE ON INFLAMMATORY AND FIBROGENIC MARKERS.....	62
FIGURE 17: EFFECT OF VIBRATION (8 HOURS PER DAY) AND/OR CYTOKINE EXPOUSRE ON CELL VIABILITY AND GENE EXPRESSION.....	63
FIGURE 18: EFFECT OF VIBRATION WITH/WITHOUT CYTOKINE EXPOSURE ON HA METABOLISM.....	64
FIGURE 19: EFFECT OF VIBRATION WITH/WITHOUT CYTOKINE EXPOSURE ON ECM-RELATED MOLECULES.....	65
FIGURE 20: EFFECT OF VIBRATION WITH/WITHOUT CYTOKINE EXPOSURE ON INFLAMMATORY AND FIBROGENIC MARKERS.....	66

FIGURE 21: ILLUSTRATION OF POSSIBLE MAPK/ERK PATHWAY.....72

List of tables

TABLE 1: SUMMARY OF DIVERSE BIOREACTORS.....33
TABLE 2 MEMBRANE DEFLECTION.....46
TABLE 3: PRIMER SEQUENCES USED FOR RT-QPCR.....51

Abstract in German

Einführung

Die biologische Grundlage von Stimmruhe nach traumatischen Ereignissen wie Stimmüberlastung oder phonochirurgischen Eingriffen ist bis heute nicht geklärt, da die Durchführung rein explorativer invasiver Eingriffe an den Stimmlippen (SL) beim Menschen aus ethischen Gründen nicht möglich ist. Ziel dieser Studie war es, das zelluläre Verhalten humaner Stimmlippenfibroblasten (hSLF), als zellulären Hauptbestandteil der Lamina propria, unter dynamischen („Stimmbelastung“) und statischen („Stimmruhe“) Bedingungen nach einem entzündlichen Reiz zu untersuchen.

Methoden

hSLF wurden auf six-well-plates mit flexibler Membran kultiviert und, mit Hilfe eines phonometrischen Bioreaktors, einem vordefinierten mechanischen Reiz ausgesetzt. Zusätzlich wurde, durch Zugabe von Interleukin (IL)1 β und transforming growth factor (TGF) β 1 in das Nährmedium, ein Entzündungsreiz nachgeahmt. Die mechanische Stimulation wurde über einen Zeitraum von 72 Stunden für acht bzw. vier Stunden täglich ausgeübt. Anschließend wurden die Zellen geerntet und Änderungen sowohl der Genexpression, als auch bestimmter Proteinkonzentrationen von Komponenten der Extrazellulärmatrix, angiogenetischen Faktoren sowie entzündlichen und fibrogenen Markern bestimmt.

Ergebnisse

Auf epigenetischer Ebene zeigte sich während einer Entzündungsreaktion eine signifikante Zunahme der Expression verschiedener Schlüsselproteine, was die Wirksamkeit dieser Stimuli widerspiegelt. Zusätzlich konnte unter proinflammatorischen Bedingungen eine signifikante Reduktion von IL11 sowie des Myofibroblasten-Markers alpha smooth muscle actin (α -SMA) durch zusätzliche Vibration über vier Stunden pro Tag nachgewiesen werden. Die Hyaluronsäurekonzentration war nach Zytokinbehandlung zwar erhöht, wurde durch zusätzliche Vibration jedoch nicht vermindert.

Diskussion

Klinische Empfehlungen und Behandlungsstrategien sollten auf biologischen Mechanismen basieren. In der Laryngologie stellt dies ein schwieriges Unterfangen dar da die SL beim Menschen nicht wiederholt biopsiert werden können. Die in dieser Publikation beschriebenen Versuche zeigten eine signifikante Reduktion proinflammatorischer bzw. profibrotischer Proteine

durch zusätzliche mechanische Stimulation. Diese Ergebnisse sind im Einklang mit klinischen Studien, die eine frühe Stimmaktivierung nach einem akuten Ereignis empfehlen.

Abstract in English

Introduction

The biological basis of voice rest following a traumatic event, such as vocal overuse, or phonosurgery, remains unanswered as purely explorative invasive interventions of the vocal folds in humans cannot be carried out due to ethical reasons. Aim of our study was to study the cellular behavior of human vocal fold fibroblasts (hVFF), being the main cellular component of the lamina propria, under dynamic ('vocal load') and static ('voice rest') conditions following an inflammatory stimulus.

Methods

hVFF were seeded onto flexible membraned six-well-plates and exposed to a predefined vibrational stress pattern by using a phonomimetic bioreactor. Additionally, inflammatory and profibrotic stimuli were induced by adding interleukin (IL)1 β and transforming growth factor (TGF) β 1. Mechanical stimulation was applied for eight and four hours daily, over a period of 72 hours. Outcome measurements comprised assessment of extracellular matrix (ECM)-related components, angiogenic factors, and inflammatory and fibrogenic markers on gene expression and protein levels.

Results

Quantitative polymerase chain reaction (qPCR) showed a significant increase in the expression of different key proteins during an inflammatory reaction, reflecting that these stimuli were effective. Under inflammatory conditions, the inflammatory cytokine IL11, as well as the myofibroblast marker alpha smooth muscle actin (α -SMA) were significantly reduced when additional vibration, for four hours per day, was applied. The desirable anti-fibrotic extracellular matrix component hyaluronic acid was increased following cytokine treatment, was however not diminished following vibration.

Discussion

Clinical recommendations and treatment strategies need to be based on biological mechanisms, however remaining an unmet goal, as human VF cannot be repeatedly biopsied. Our experiments showed the effect of vibrational stress on hVFF in an inflammatory state. Elevated levels of certain pro-inflammatory/pro-fibrotic factors could be mitigated by additional vibrational excitation in an *in vitro* setting. These findings corroborate clinical studies, recommending early voice activation following an acute event.

Introduction

The vocal folds (VF) are the core structure of the larynx and the main source of verbal communication. In a superficial contemplation it may seem as if phonation follows a simple mechanism. However, it is one of the most complex processes in the human body. This complexity is also reflected by the unique molecular histological tissue structure, being extremely fragile. Disruption of the VF mucosa as well as traumatic stress due to vocal overload lead to an upregulation of inflammatory cytokines and enzymes in the VF. (2) (3) These inflammatory processes have a significant impact on VF metabolism and tissue remodelling and may, in the worst-case, result in a permanent impairment of the viscoelastic properties leading to VF scarring and dysphonia. Understanding and modelling these processes have important clinical implications, including recommendations of voice rest following phonosurgery or phonotrauma. Endolaryngeal surgery of the VF is an established treatment option for benign and malignant VF lesions and is nowadays routinely carried out in many countries of the world. While many lesions can be treated surgically, there is still insecurity about the postoperative management, more precisely the role of voice rest. Different concepts dealing with this issue exist, yet a commonly accepted recommendation is not available, reflecting the scarce amount of profound data. Some authors postulated that voice rest may have a beneficial effect on wound healing (4) (5), while others did not. (3) (6) (7) Similar to other medical fields, where a rapid mobilisation after a surgical intervention is recommended to achieve an early recovery, there is a tendency during the past years to decrease the interval of voice rest following phonomicrosurgery. (8) (9) However, there barely is any evidence about the influence of voice rest following phonotrauma/VF surgery on different vocal and laryngoscopic parameters. This might also be due to the fact that the healing process itself is triggered by multiple factors, which makes it difficult to estimate the influence of a single factor. These comprise the size of the VF lesion and hence the extend of surgery (uni-/bilateral lesion, polyp/Reinke's edema etc.), laryngo-pharyngeal reflux, smoking status, sex, age etc. It is furthermore virtually impossible to follow postinterventional changes on a cellular level in humans, as the VF are a small structure where every biopsy carries with it the risk of scarring. However, in order to get a profound understanding of VF physiology and pathophysiology it is mandatory to explore mechanisms on a molecular level.

It is known that vocal fold fibroblasts (VFF) respond to vibration by altering their extracellular matrix (ECM) production, but the impact of vibration on VFF in an inflammatory state is still not fully elucidated. (10) Our recently designed phonomimetic bioreactor allows us to apply any vibrational pattern to human vocal fold fibroblasts (hVFF) in culture. (11) The present study

aims to reveal the impact of mechanical stress by means of vibrational forces on hVFF during an acute inflammatory reaction putting an emphasis on the molecular and cellular level. (1)

Vocal fold composition

The VF extend between the thyroid and the arytenoid cartilages of the larynx. They are multi-layered structures composed of the epithelium, basement membrane (BM), lamina propria (LP) and the vocal muscle. The epithelium, the BM and the LP are designated VF mucosa (see Figure 1).

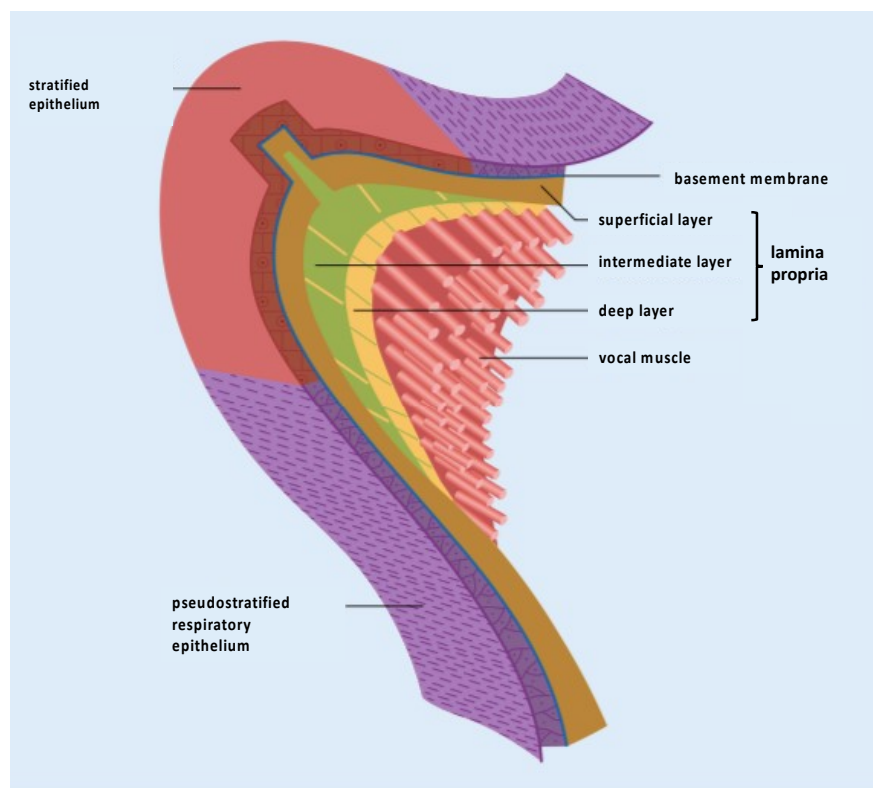


Figure 1 Schematic vocal fold structure; This figure was reproduced and adapted from(12) and (13). With permission of HNO/Springer.

Epithelium

The epithelial cells of the VF are closely juxtaposed and form a stratified epithelium consisting of five to ten cell layers. The remaining parts of the larynx are covered by a pseudostratified respiratory epithelium. This difference in structure might be owed to the fact that the VF are exposed to immense mechanical forces during phonation. Mechanical stability is not only reflected on a cellular level but also on a molecular one. The cells are tightly connected to each

other as well as to the BM via adherence junctions. Since the space between the VF, called glottis, is the narrowest part of the upper airways in adults, a turbulent airflow occurs. Consequently, the VF epithelium, representing the outermost layer, is particularly exposed to biological and chemical pollutants. As protection against these they are covered by mucous. The adhesion of the laryngeal secrete is ensured by innumerable microscopic wrinkles and grooves in the mucosa. These mucosal folds facilitate the movement of the mucosal wave during phonation (see Figure 2). (14)(15)(16)(17)

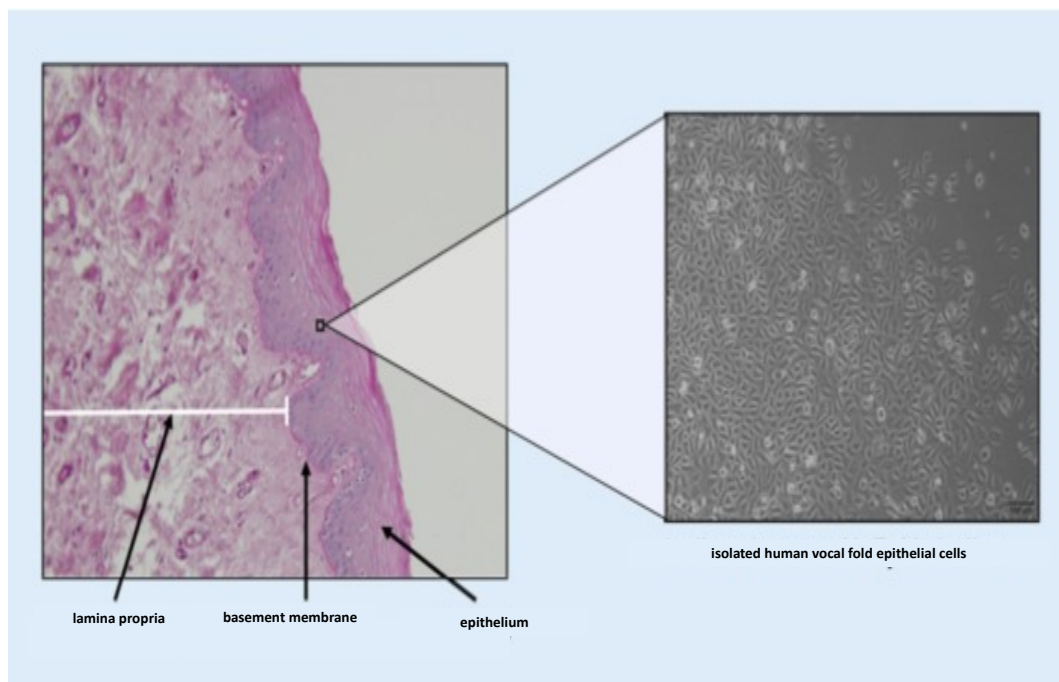


Figure 2: Histological structure of the human vocal fold (periodic acid Alcian Blue staining) with a light microscope image of isolated human vocal fold epithelial cells (10x magnification). This figure was reproduced and adapted from (13). With permission of HNO/Springer.

Basement membrane

The zone between epithelium and LP is called BM. It anchors these two layers to each other primarily by means of collagen (COL) type IV and VII. The amount of these anchoring fibers depends, on the one hand, on the localization, since higher amounts are described in the membranous part of the VF. On the other hand, genetic predisposition seems to play an important role, which might also explain an interindividual disposition to dysphonia. (18)

Lamina propria

In contrast to the epithelium, the cell density in the LP is by far lower. Consequently, this layer is mainly composed of extracellular matrix (ECM). Nevertheless, VFF, the most abundant cell-

type in the LP, play an important role since it is assumed they are primarily responsible for the production of the macromolecules (MM) throughout this layer. VFF not only produce the components of the LP, but also various enzymes, some of them being important for the degradation of ECM components. Therefore, the ECM is not a rigid scaffold where cells are embedded in, but a dynamic and adaptive three-dimensional network. Furthermore, many other functions than cell adhesion are known, such as enabling migration and proliferation of cells. (19)

The distribution of the MM differs across the LP. As a consequence, the LP can be subdivided into three layers which smoothly merge into one another. The cause of this phenomenon has not yet been elucidated in detail but mechanotransductive processes seem to play a pivotal role. The homeostasis of the MM and the integrity of the layered structure of the LP is essential for an optimal oscillation and consequently for voice production.

The superficial layer resembles a viscous fluid and is pervaded from loose connective tissue. Besides the VFF there are also macrophages and myofibroblasts located in the LP. Even though all layers of the LP are populated with cells, macrophages and myofibroblasts are more abundant in the superficial layer. Higher amounts of the former might be due to higher exposure to mucosal irritants. Greater levels of the latter likely reflect a higher exposition to mechanical forces. Additionally, myofibroblasts seem to be essential in wound healing as they are held responsible for increased COL exposition as well as wound contraction which deteriorate oscillatory properties of the VF. (16)(20)

The transition to the middle layer of the LP is distinctive, since compared to the more superficial part there is an appreciably higher concentration of elastin, which is an elastic protein. Towards the anterior and posterior ends of the VF the amount increases, which again can be traced back to higher mechanical stress during phonation. This area is called macula flava. Special types of VFF were found there and named after their shape as stellate cells. It has been suggested that they act as an endogenous stem cell population. (21)(22)

Going deeper across the LP, the concentration of ELN gradually decreases while the amount of COL increases. When reaching an area where the ratio between COL and ELN is 2:1 in favor of COL type I one speaks about the deep layer. Due to its high COL proportion, it resembles a ligamentous structure, hence the name vocal ligament.

Aside from these two fibrous proteins, many other MM can be found in the LP, such as proteoglycans and glycoproteins. Of particular interest is hyaluronic acid (HA), a glycosaminoglycan (GAG). HA is a polar molecule which is able to bind high amounts of water. Consequently, this MM has a great impact on viscosity of the VF and plays a decisive role for optimal oscillation from a biomechanical perspective (see Figure 3). (15) (23)

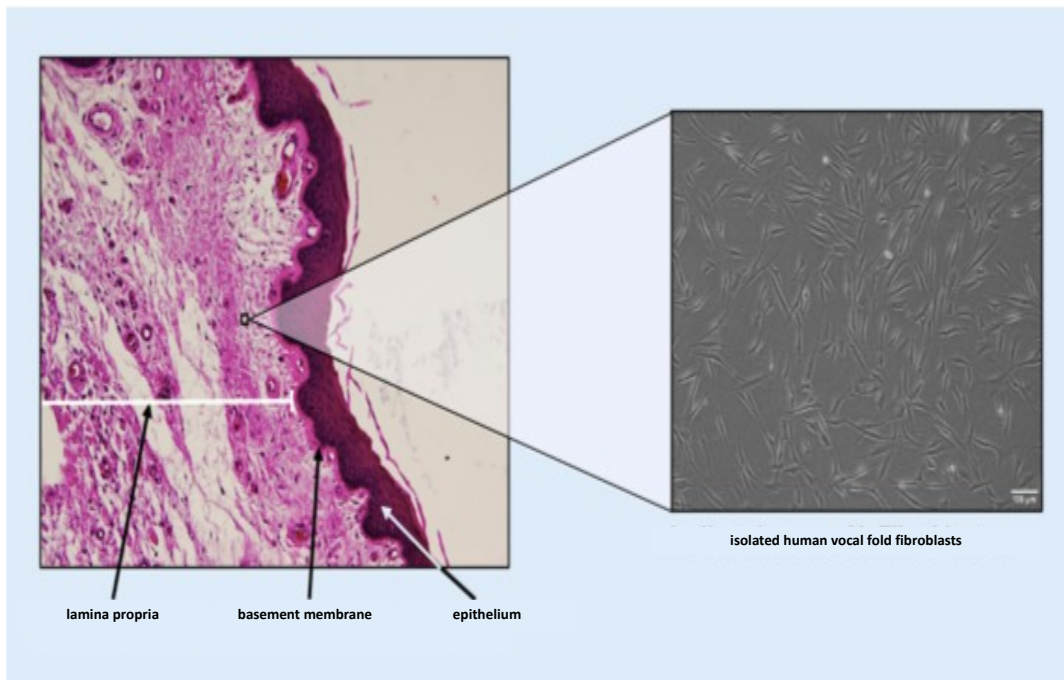


Figure 3: Histological structure of the human vocal fold (hematoxylin-eosin staining) with a light microscope image of isolated human vocal fold fibroblasts (10x magnification). This figure was reproduced and adapted from (13). *With permission of HNO/Springer.*

Vocal fold muscle

The VF muscle can be seen as the superficial portion of the thyroarytaenoid muscle. It possesses a high density of muscle spindles which measure the degree of strain in the muscle, supporting the assumption that it is particularly important for the fine-tuning of the VF tension and consequently for the pitch. Furthermore, the fibers have a high proportion of mitochondria, which indicates the need for high energy supply. (24)

Physiology

Myoelastic-aerodynamic theory

Until the mid-20th century two contradicting theories existed which explained the mechanism behind phonation. The neuromuscular hypothesis claimed that transverse muscle fibers would pull on the vocal ligament and cause rhythmic contraction as a response to stimuli by the recurrent laryngeal nerve. Since muscle fibers have an absolute refractory period of 3-4 msec., polyphasic contractions of the fibers for frequencies above 500 Hz were postulated. However, many other anatomic and physiologic aspects could not be explained by the neuromuscular

theory. Hans von Leden therefore rejected it and favored the still valid myoelastic theory of Müller. The latter was further expanded to the myoelastic-aerodynamic theory. (25)

According to this theory and in contrast to the neuromuscular hypothesis, VF oscillation is a passive process. During phonation, the VF approximate each other and the glottis narrows. The pressure below the closed VF, referred to as subglottal pressure, results from the exhaled air created by the lungs. Once the air pressure below the glottis has exceeded the threshold, the air displaces the loosely attached epithelium and air passes the VF. Driven by different factors, the glottis immediately closes again and only a small amount of air passes at once. One component causing closure is the elastic property of the VF tissue, which tend to regain its initial, closed position. Secondly, Bernoulli's principle plays a role in restoring the glottis to its narrowed position. As already mentioned, the glottis is the narrowest part of the upper airways. Owed to this fact the air stream is accelerated between the VF generating a negative pressure, leading to a suction effect and achieving VF closure. However, these factors were overestimated for a long time. Titze described in detail that due to the geometric properties of the VF, continuous energy transfer from the airflow to the tissue results in a self-sustained oscillation, thereby overcoming frictional energy loss.

This alternating process of VF closure and opening is frequently repeated during phonation and leads to periodic compression of the air. (26)1/1/2022 4:10:00 PM(27)

Body-cover-theory

The myoelastic-aerodynamic theory bases to a certain extend on the unique configuration of the VF. Beside the previously mentioned histological perspective of the VF structure, M. Hirano described in the 1970s the functional aspect which can be considered as the other side of the same coin. He divided the VF into three functional units with different mechanical properties. The body represents the fundament and comprises the vocal muscle and the deep layer of the LP. The most superficial part is the cover, including the epithelium, the BM and the superficial layer of the LP. The remaining intermediate layer of the LP is designated as transition zone which enables a smooth displacement of the cover relative to the body during phonation. (28)(29)

Source filter theory

The former two sections describe the origin and therefore the source of the primary larynx sound in humans. However, this sound deviates from the sound which is commonly considered as voice. This can be explained by the fact that VF vibration does not produce a pure tone but a spectrum of frequencies, called harmonics. The organs cranially to the VF, summarized as

the vocal tract, form a resonance chamber which functions as a filter, where the amplitude of some frequencies is intensified while others are damped. Changes in the shape of the vocal tract result in the formation of different vowels but also of turbulent airstreams and consequently of consonants. (30)(31)

Mechanotransduction

As stated above, the LP can be divided into three layers. VFF are ubiquitous in all these layers and mainly responsible for the production of ECM components. Since all VFF have an identical genome, epigenetic factors and in particular mechanotransductive processes, are held responsible for the development of the three-layered structure.

The term mechanotransduction refers to the translation of mechanical stimuli into biochemical signals. It can take place in a number of ways and multiple steps are involved in these processes. First of all, an external mechanical stimulus has to be transmitted to a cell capable of perceiving these forces, called mechanotransmission and mechanosensing. Conformational changes of the ECM are the predominant way how mechanical impulses are conducted to the cells. This can happen via transmembrane proteins, e.g. integrins which are connected to the cytoskeleton. Alternatively, channels in the cellular membrane can be activated by stretching and thereby initiate the next step, referred to as biomechanical coupling. This means transferring the mechanical stimulus into a biochemical or electrochemical signal. These signals in turn may influence transcription factors, which bind to certain segments of the DNA and affect the translation of genes into mRNA and as a further consequence the transcription into proteins (see Figure 4). (19)(32)(33)(34) Fibroblasts in general, as well as hVFF in particular, are well known to be mechanosensitive. There are roughly two groups of genes which are responsive to mechanical stimulation: 1) ECM-related genes coding for example for COL and 2) inflammation-related genes possessing the genetic blueprint proteins such as cyclooxygenase (COX) -2. This explains why mechanotransduction plays a pivotal role in various diseases. Several studies have demonstrated that mechanical stress can result in pathologies including cardiomyopathies, muscular dystrophies or cancer progression. (19)(35)(36) However, mechanotransductive processes may also have beneficial effects in wound healing by enhancing angiogenesis and stem cell recruitment. (19)(37)(38)(39) This may explain why in other medical fields, such as orthopedics, an early postoperative mobilization has shown to have a beneficial impact on patient's recovery and is already incorporated in clinical routine. (8)(9)(33)

It is known that mechanotransductive processes also play a role in embryonic development. Since the LP in newborns is homogenous it is assumed that the formation of the three-layered structure might also be associated with mechanical stimulation as a consequence of phonation. (32)(40)

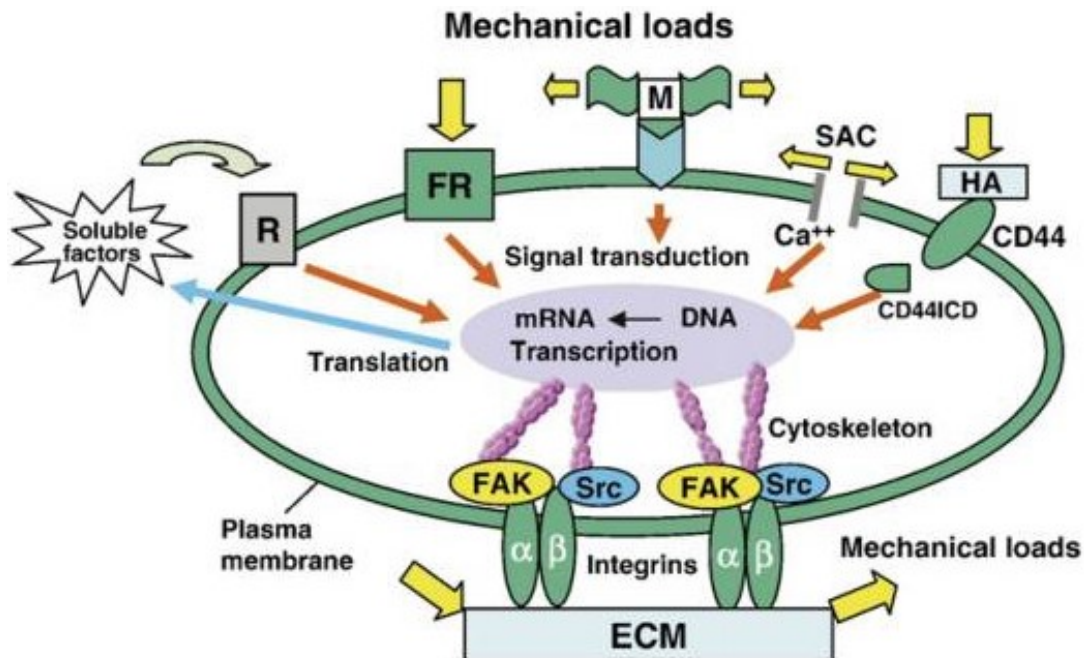


Figure 4: Illustration of possible ways of mechanotransduction. This figure was reproduced from (34) with permission of Elsevier. This figure was published in *Gene*, 391, Wang, Thampatty, Lin, Im, *Mechanoregulation of gene expression in fibroblasts*, pages 1-15, Copyright Elsevier (2007). ECM: extracellular matrix; FAK: focal adhesion kinase; FR: force receptor; HA: hyaluronan; M: domain of an extracellular protein; R: receptor; SAC: stretching-activated channels

Wound healing

Disruption of the VF mucosa, due to surgery or phonotrauma, initiates a signaling cascade which in turn triggers wound healing. Wound healing is an essential physiological process to regain integrity of the organ and trying to restore tissue to their pre-injury state. (41) Therefore, an accurate temporospatial coordination of the involved cells and molecules is required. Otherwise, it may lead either to an exuberant reaction with the formation of keloids or to insufficient recovery and consequently chronic wounds. Three partially overlapping phases of wound healing are distinguished, the inflammatory, proliferative and remodeling phase. (42)

Inflammatory phase

The inflammatory phase is characterized by hemostasis and an inflammatory reaction in order to avoid further blood loss and invasion of pathogens as well as to clean the wound from cell debris. It lasts for about 72 hours after the injury. (42)

Trauma induces the release of various factors and COL fibers which enable the adhesion of thrombocytes which form a blood clot. This is important for the prevention of blood loss, for the formation of a first new barrier against pathogens, for the creation of a matrix for the intruding cells and serves as a reservoir for growth factors. (43)

Studies investigating wound healing after skin injury have revealed that interleukin (IL) -1 leads to a degranulation of thrombocytes and the excretion of growth factors such as epidermal growth factor (EGF), platelet derived growth factors (PDGF) and transforming growth factor (TGF)- β . IL-1 is the body's signal to tissue damage, released by disrupted keratinocytes.

Besides the pathogen associated molecular patterns (PAMPs) from infectious agents, there are also large amounts of damage associated molecular patterns (DAMPs) present in the wound area. Cells, originating primarily from the innate immune system, migrate alongside the increasing gradient of these factors. Neutrophil granulocytes are the first cells reaching the wound site. They intensify the immune response by secreting even more pro-inflammatory cytokines. (41)(42)(43)(44)(45)(46)(47)

An *in vivo* study in rats by Lim et al. suggests that these cytokines signaling processes are similar in VF. (48)

Proliferative Phase

Resident macrophages as well as monocytes play the major role in the transition to the proliferative phase. The transformation of monocytes into macrophages is induced by TGF- β . Since

wound healing increases the energy metabolism, a sufficient blood and nutrient supply is crucial. This is enabled by pro-angiogenic factors which contribute to the vascularization of the tissue. (47)(49)

The replacement of the blood clot and the reepithelization can last several weeks. In order to accomplish this, keratinocytes migrate to the wound edges and fibroblasts differentiate into myofibroblasts. The latter achieve a contraction of the wound and therefore facilitate the closing process. (45)(50) The accumulation of inflammatory cells, fibroblasts, keratinocytes and vessels embedded in a loose matrix of COL, ELN, glycoproteins and HA is referred to as granulation tissue. (42)(45)

Remodeling

The final phase is the tissue remodeling and takes several months to years. A mature scar is formed by replacing the granulation tissue. This phase is characterized by the degradation of the excess ECM components. (42)(45)

Scar formation

As described above, wound healing is an important process enabling tissue repair. However, the healed tissue is usually accompanied by loss of functions. In many fields of medicine, scientists have been undertaking considerable efforts to investigate how complete tissue regeneration can be achieved. (51) Researchers have been focusing on fetal wound healing, since studies in the field of dermatology have shown that fetal wounds are capable of regeneration to normal dermal architecture. (42)(52) Differences were identified particularly in the inflammatory reaction showing a decreased inflammatory response and a shift in favor of anti-inflammatory cytokines. They concluded, that the inflammatory phase of wound healing must be essential in scar formation. (42)(53)

Due to ethical reasons, it is barely possible to study VF scars in humans. Consequently, our current knowledge derives mainly from animal trials.

Since VFF are majorly responsible for the ECM composition, their transformation into myofibroblasts may have great impact on the altered ECM composition in scarred tissue. Myofibroblasts are assumed to produce substantial amounts of COL type I, which deposit in an unorganized manner throughout the LP. An increase in the concentration of the glycoprotein fibronectin (FN) could be shown in VF scars as well, participating in cell-to-matrix interactions and in adhesion of ECM proteins amongst each other. This might increase tissue viscosity. Moreover, decreased concentrations of HA, decorin and ELN were revealed. All these changes may result in impaired oscillatory capacities and glottal insufficiency due to scar formation leading

to irregular VF vibration and dysphonia. Gaining a deeper knowledge on the wound healing process in the VF might help to develop therapeutic strategies to prevent VF scarring. (54)(55)(56)(57)(58)

Diagnostic methods

It is not the scarring per se but the consequent dysphonia which leads to a reduced quality of life. A comprehensive medical history and examination of the larynx may point out the cause of dysphonia. Particularly, videostroboscopy is an important tool to examine VF oscillation. It uses synchronized flashlights with the aid of which the rapid mucosal waves pretend to oscillate in slow-motion. This enables an assessment of different phases of the VF movements. (59)

These methods however do not examine the voice itself. Therefore, various other diagnostic methods have been developed to assess the degree of hoarseness.

In order to objectivize the degree of voice impairment of the patient in everyday life numerous questionnaires, such as the voice handicap index (VHI), can be used. They focus on intrapsychic, communicative and social factors.

Besides these, speech therapists may assess the patients voice with the help of the GRBAS scale (0 = normal – 3 = severe impairment).

Moreover, computer-assisted measurements allow an objective evaluation of the voice by quantifying the frequency (jitter) and amplitude (shimmer) fluctuations. They also include parameters like for instance normalized-noise-energy or harmonics-to-noise-ratio.

In order to gain a holistic view, indices have been developed which incorporate different parameters. Nevertheless, also the objective measurements have their limitations such as intertest-reliability and lack of correlation with the subjective sensation. (60)(61)(62)(63)(64)

VF scar treatment options

The treatment of VF scars still poses a major challenge in laryngology. To date voice therapy and the associated but controversially discussed voice rest is the fundament of the postoperative management and will be discussed later.

Depending on the severity of symptoms and the patient's preferences, further intervention to improve the outcome might be necessary.

Medialization thyroplasty

Medialization thyroplasty bases on the idea to push the scarred VF medially thereby narrowing the glottis. The main application area comprises VF paralysis, but the use of this technique in VF scars seems reasonable. The major advantage is, that this method does not intervene directly on the VF, avoiding further trauma. Besides hydroxyapatite and silicone, the usage of titanium implants is popular, because it is an inert material, has a high plasticity and can hence be adjusted individually to the patient's larynx. Furthermore, it is not ferromagnetic and therefore suitable for magnetic resonance imaging. (56)(65)(66)(67)

Injection laryngoplasty

Based on the same principle, in injection laryngoplasty a filler substance is applied directly into the VF, augmenting them to decrease the glottal gap. Two groups of injectable materials can be distinguished. Alloplastic materials are created synthetically and are not biodegradable, resulting in a permanent augmentation of VF. Autologous substances in contrast, most commonly fat and fascia, are absorbable. In order to achieve durable improvement of voice quality, repeated injections are needed, causing recurrent trauma. However, the advantage is that the injected tissue derives from the patient him-/herself, thus being not immunogenic. Conversely, xenogenic materials have their origins in another species such as the bovine based substances. (56)

Experimental approaches

The above-mentioned therapies represent the approaches currently applied, being only symptomatic. Much effort is put into the development of causal approaches, with the most promising being described below. None of them is however used in clinical routine at present.

Growth factors

In order to ensure survival, cells are in need of nutrition and growth factors. In addition to the aforementioned substances, growth factors can also be applied directly into the LP and are often used in regenerative medicine. They decrease the glottal gap and improve viscoelastic properties.

A frequently applied growth factor is the basic fibroblast growth factor (bFGF). It seems to reduce the production of COL I and increase HA. In a recent study Okui et al. examined 53 patients suffering from age-related VF atrophy whom bFGF was locally applied. Acoustic as well as aerodynamic parameters improved after injection. (68)(69)

Similarly, to bFGF, hepatocyte growth factor (HGF) is attributed to obtain the same effect, namely a decrease of COL I and an increase in HA concentration. A difficulty to struggle with is the insufficient retention period. Ohno et al. tried to circumvent this issue by developing a hydrogel delivering system, which continuously, over two weeks, releases HGF *in vivo*. In a canine model a significant improvement of vibratory properties of scarred VF was described. (70)

Cell therapy

Another strategy is the local injection of cells. To avoid a rejection reaction of the body after the implantation of allogenic cells, autologous cells are primarily eligible. Buccal fibroblasts were used in canine models because of their similarity and facile accessibility. Improvements in histology and functional mucosal waves could be seen. Dermal fibroblasts however appear to be less appropriate because of their limited ability to produce HA.

Furthermore, pluripotent stem cells, particularly bone marrow derived stem cells (BMSC) and adipose tissue derived stem cells (ASC), caught scientist's attention. Both cell types revealed promising results in *in vivo* animal trials. (69)(71)(72)

Tissue engineering

Tissue engineering can be seen as a combination of the above-mentioned methods. It aims to create a tissue, which is undistinguishable from the healthy local tissue by replacing the injured one. The simplest form of tissue engineering has been introduced above and refers to the exclusive injection of cells. Engineering an entire tissue piece *in vitro* is regarded as the supreme challenge. Three essential factors to succeed this difficulty are the choice of the right cell type, developing a scaffold and using an appropriate mixture of growth factors.

The selection of the appropriate cell types and growth factors has already been discussed previously. Equal attention is given to the right frame. It is not possible to fabricate an ECM by stringing the different molecules together, because of the complex LP structure. Therefore, scaffolds, consisting of only one of these ECM molecules, have been developed.

Polymerized COL is popular in different fields of tissue engineering because of its abundance in various tissues. Another advantage of COL-fibers is their ability to form a stable three-dimensional structure. Nevertheless, due to the inherent stiffness of this scaffold, COL matrices are not ideal for the replacement of VF tissue. Fibrin polymer is regarded as a suitable alternative. It occurs naturally in blood clots and plays an essential part during coagulation. Embedded in adipose derived stem cells, fibrin polymer supports ELN transcription as well as

deposition and has superior biomechanical properties. Forming a scaffold out of other molecules has not been fruitful yet. HA for example plays an essential role in VF pliability. However, it is not possible to create a solid three-dimensional structure with HA alone. Moreover, synthetic elastic materials did not manage to reflect the complex micro-architecture of the LP.

A more elegant way is the use of a decellularized organ matrix. In the decellularization process, not only cells but also several other water-soluble molecules are eluted from the matrix. Finally, a delicate structure, mainly composed of COL, remains. However, this structure, would still not meet the biomechanical requirements of the VF tissue. It provides a habitat for cells, which can be seeded onto the matrix and generate other ECM components. Since this decellularized matrix theoretically is free of antigens, an interindividual implantation may be applicable. (71)(73)

An impressive innovation succeeded the group of Welham which has managed to engineer a piece of VF mucosa *in vitro*. They harvested hVFF and VF epithelial cells from cadaver six hours *post mortem* and from patients who underwent laryngectomy without pathologies of the VF. Afterwards, they cultivated them separately and merged them again after several days. Polymerized COL provided the cells as three-dimensional scaffold. After ten to fourteen days the co-cultivated cells formed an around 50µm tissue engineered mucosa. It was then transplanted *ex vivo* into a larynx of a rabbit for measuring its biomechanical resilience and properties. Thereby the researchers could show that engineered mucosa is able to withstand the mechanical forces which occur during vibration. Moreover, aerodynamic, high-speed digital imaging and acoustic data revealed that the engineered and native tissue were indistinguishable. Another obstacle in tissue engineering is the immunological compatibility. This was investigated by transplanting the tissue *in vivo* into a mouse larynx. Since it did not cause an immune response, the authors concluded that this method might be also feasible for allotransplantation. (74)

Gene editing

Another, highly sophisticated method is genome editing. It bases on the precise manipulation of genes. Various mechanisms have been developed to achieve this aim. The most popular include the following four groups, which can be summed up under the term targeted nucleases: zinc finger nucleases, transcription activator-like effector nucleases (TALENs), meganucleases and the CRISPR/Cas system. The latter technique is very promising and was first observed in the bacterial immune system, which enables a defense against invading viruses. Short parts of the pathogen's nucleic acid are integrated into the specific region of the hosts

genome called clustered regularly interspaced short palindromic repeats (CRISPR). This integrated sequence is further transcribed into CRISPR RNA (crRNA) which in turn binds to a trans-activating crRNA (tracrRNA). Together they link to an endonuclease called CRISPR-associated (Cas) protein. This complex is able to cleave a specific site in the virus-genome. Further research has revealed that the CRISPR/Cas molecule also enables a modification of the mammalian genome. With the aid of this method, it is not only possible to cause deletions in certain DNA sequences but also to insert a desired sequence. (75)

Besides genome modification, the possibility to silence mRNA via RNA interference (RNAi) exists. The long double stranded RNA is introduced into the cell and subsequently cleaved into siRNA. The siRNA is then incorporated into an RNA-induced silencing complex (RISC). This complex binds to a specific mRNA and inhibits its translation. (76)1/1/2022 4:10:00 PM

In laryngology Kishimoto et al. utilized this principle in order to avoid VF scarring in an *in vivo* rat model. One important step in COL maturation is its specific folding. This process requires a chaperone known as Serpin peptidase inhibitor clade H, member 1 (SERPINH1). Studies have shown that the suppression of SERPINH1 reduces COL accumulation and improves organ functions.

For this reason, the group injected an siRNA targeting SERPINH1 into previously injured rat VF. The results revealed a reduced COL abundance in the VF mucosa and had a beneficial effect on wound healing. (77)

Vocal rest

The formation of benign VF lesions can be prevented with the help of voice therapy and can in some cases, as for example with VF nodules, function as primary treatment. In most of these lesions vocal training serves as an additional therapy to an operation. (78)(79) A question, which has to date still not been fully answered is when to start with voice therapy postoperatively. Tang et al. were able to show, that presurgical vocal training has a positive impact on subjective voice parameters. (80) State of the art today for benign as well as malignant VF lesions is the endolaryngeal surgery, finding application all over the world in daily routine. Despite its successful implementation and the positive postoperative outcome in many cases, it remains unclear how to support patients during their postoperative rehabilitation. The role of voice rest after a laryngeal surgery remains much debated. The medical recommendation bases on the hypothesis, that mechanical strain has a negative impact on tissue repair. A distinction is made between absolute and relative voice rest. The former is defined as a complete avoidance of any strain on the VF, hence instructing the patient not to phonate. Relative voice

rest is, to date, not clearly defined. In other medical disciplines, such as for example orthopaedics, a quick postoperative mobilization is aimed at in order to achieve a fast recovery. As a result, there has, over the past years, been a tendency to reduce the voice rest interval after phonomicrosurgery. (8)(9) Obviously, a great difference lies between the objectives of rehabilitation of, for example, a joint and the VF. While resilience is the predominant aim in orthopaedics, pliability is of utmost importance in VF wound healing. Nevertheless, the known anti-fibrotic effect of early mobilization might also be beneficial in the field of laryngology. (81) Randomized controlled studies, which have recently been published, did not show any advantages of an absolute voice rest compared to a reduction in phonation postoperatively, based on subjective (e.g. VHI) as well as acoustic and aerodynamic parameters. (82)(83) This topic is still much debated and a commonly accepted consensus not agreed on. (3)(4)(6)(5)(7)(82)(84)

Bioreactors

One possibility to gain more information about cellular processes is the deduction from animal experiments. Particularly rodents have been proven to be a good alternative because of their similarities to human VF LP. (85) But according to the three R's concept (reduce, refine, replace), in vivo experiments are tried to be reduced to a minimum and replaced by in vitro trials. For a long time, the lack of an appropriate in vitro model being able to simulate VF oscillation impeded laryngological knowledge acquisition.

For this purpose, the development of different bioreactors, attempting to imitate vocal stresses in vitro, was enhanced in the past years. (see Table 1)

Table 1: summary of diverse bioreactors. The table was reproduced and adapted from (11). With permission of PLoS1.

Publication	Titze et al. (10)	Wolchok et al. (86)	Kutty and Webb (87)	Gaston et al. (88)	Farran et al. (89)	Latifi et al. (90)	Kim et al. (91)	Present Bioreactor (11)
Reactor type	3D-axial and vibratory stimulation	3D-substrate vibratory stimulation	3D-vibratory stimulation	3D-axial and vibratory stimulation	2D-electro-acoustically driven	3D-perfusion phonation-induced stimulation	2D- vibratory stimulation	2D- electro acoustically driven
Source of vibration	voice coil actuator	voice coil actuator	voice coil actuator	voice coil actuator	loudspeaker	variable speed centrifugal air blower	linear actuator	loudspeaker
Cell type	Human laryngeal fibroblasts	Human laryngeal fibroblasts	Human dermal fibroblasts	Human vocal fold fibroblasts, bone marrow mesenchymal stem cells	Neonatal foreskin fibroblasts	Human vocal fold fibroblasts	Human vocal fold fibroblasts	Human vocal fold fibroblasts
Culture substrate	Tecoflex substrate	Tecoflex substrate	Methacrylated hyaluronate hydrogel	Fibronectin coated Tecoflex substrate	Collagen-I coated silicone membranes	HA-Ge hydrogel	Collagen-I coated Bioflex plate	Pronectin coated Bioflex plate
Duration of experiment	6 hours	3 days /21 days	1/3/5/10 days	1 day	1 day	2 days	2/6/10 hours	2days
Stimulation/vibration frequency	20% axial strain/ 100 Hz	100 Hz	100 Hz	20% axial strain/ 200 Hz	60/110/300 Hz	~100 Hz	205 Hz	50-250Hz
Stimulation per day	6 hours	6 hours	2 hours	8 hours	1 hour	2 hours	2/6/10 hours	8h
Stimulation pattern	continuous	1 s vibration/ 2 s static	2 s vibration/2 s static	continuous	continuous	1 h phonation/15 min rest/1 h phonation	continuous	1 min vibration/1 min static for 16 hours
tested frequency range of reactor	20-200 Hz	100-200 Hz	not discussed	0-2727 Hz	0-400 Hz	0,5-100 Hz	not discussed	50-2500 Hz

Biological effects of vibration compared to static conditions

collagen-I	1.5-fold gene upregulation	1.7-fold increased protein expression	20 % reduction of total collagen protein (d5)	no effect	1.2-fold gene upregulation (60 Hz), 0.75-fold downregulation (110 Hz)	5-fold increased protein expression	no effect	1.8-fold gene upregulation, 1.5-fold increased protein expression
collagen-III	NA	NA		NA	NA	2.4-fold increased protein expression	NA	1.5-fold gene upregulation
HA synthase 2	2.5-fold gene upregulation	NA	5-fold gene upregulation (d3)	NA	NA	NA	10-20 % gene downregulation	1.6-fold gene upregulation
fibronectin	~2.3-fold gene upregulation	~2-fold increased protein expression	NA	no effect	no effect	NA	no effect	1.3-fold gene upregulation

MMP1	~3-fold gene upregulation	NA	2-fold gene upregulation (d5)	NA	10% gene downregulation 60 Hz	NA	no effect	no effect
TGF-β1	NA	2 -fold increased protein expression in medium	NA	no effect	NA	NA	NA	1.5-fold gene upregulation

2D-Bioreactors

Farran et al. constructed a 'two-dimensional' electro-acoustically driven bioreactor. They seeded neonatal foreskin fibroblasts onto circumferentially-anchored silicone membranes which were set into vibration by air pressure changes below the plate. Stimulation was applied for one hour. They observed a frequency-dependent up- and down-regulation of *COL-1* at 60 Hz and 110 Hz, respectively. (89)

Kim et al. built dynamic culture systems where cells were seeded onto flexible membranes which were then oscillated by linear actuators which triggered a down-regulation of hyaluronan synthase (*HAS*) 2. (91) A 'two-dimensional' reactor type is characterized by the fact that the utilized cells in the experiment are single-layered.

3D-Bioreactor

Besides the mentioned 'two-dimensional' approaches, there has also been progress in the development of three-dimensional bioreactors. (10)(86)(87)

Kutty et al. exposed human dermal fibroblasts encased in a methacrylated hyaluronate hydrogel to a vibratory pattern of 100 Hz for one to ten days. Five days of stimulation caused an upregulation of *matrix metalloproteinase (MMP)1*, *HAS2*, *decorin*, and *fibromodulin*. (87)

Titze et al. seeded human laryngeal fibroblasts onto a three-dimensional tecoflex matrix, subjected to axial and vibratory stresses and described an upregulation of *COL-1*, *HAS2*, *FN* and *MMP-1*. (10)

The group around Latifi et al. constructed a bioreactor, which at the moment best imitates the in vivo situation. They injected a scaffold of hVFF into silicone VF replicas, with the aim of imitating all mechanical forces, which act on VFF during phonation. The cells in the scaffolds are oscillated by an airflow coming from beneath, imitating the mechanical strain the human VF are exposed to during phonation. After the mechanical stimulation of two hours per day for four days cells were harvested. *COL-I* and *COL-III* were increased compared to the unphonated controls. (90)

Zhang et al. were able to show, that the inflammatory reaction caused by cigarette smoke is reduced with the utilization of periodic tensile strain on hVFF. (92) A profound knowledge on the effect of vibration on hVFF in an inflammatory setting is still missing.

Present bioreactor/Graz prototype

The above-mentioned constructions are subjected to some limitations as well. The major difficulties are their restricted frequency range and their sophisticated structure. The latter complicates examinations under different conditions, such as proinflammatory ones. To overcome

these issues, we designed a special phonomimetic bioreactor. It is composed of a portable media player being additionally connected to a power amplifier and a loudspeaker. The loudspeaker, being fully enclosed in an incubator, has a circumferential polyoxymethylene (POM) mounting with cell culture plate fixation elements. Flexible bottomed six-well-plates can be placed on the mounting and oscillated by aerodynamic pressure fluctuation (see Figures 5 and 6). The advantage of this construction is its ability to expose the cells in culture to specific patterns of vibration. This device allows to investigate cellular processes of hVFF under static as well as dynamic conditions during an inflammatory and pro-fibrotic stimuli for the first time. By the combination of these factors, we seek to imitate an inflammatory reaction after phonosurgical interventions as precisely as possible, in order to deepen our knowledge in the impact of (voice) rest versus vibration on inflammatory and fibrogenic markers, angiogenic factors as well as on ECM-related molecules. (1)(11)

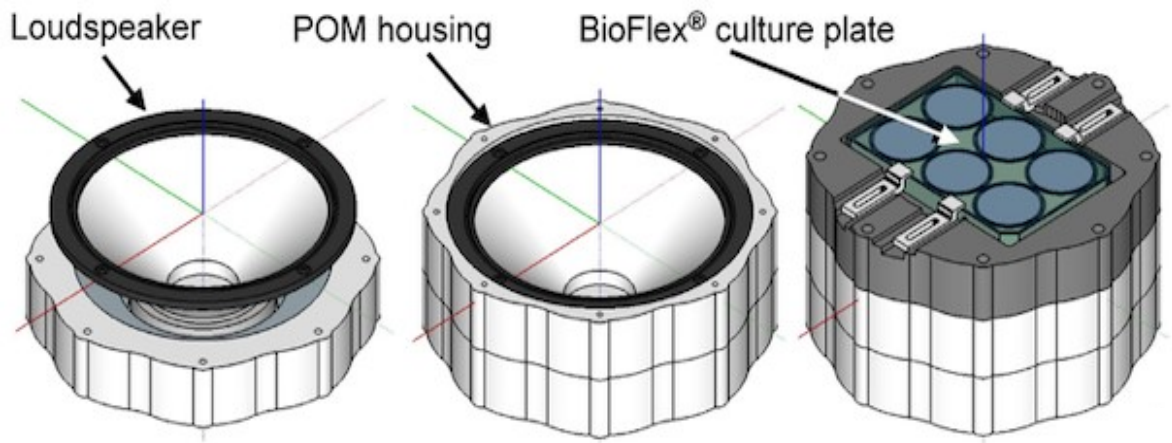


Figure 5: Design of the loudspeaker with mounting bearing a six-well plate on the top. The figure was reproduced and adapted from (10). With permission of PLoS1.



Figure 6: Schematic representation of the bioreactor with its components. The figure was reproduced and adapted from (11). With permission of PLoS1.

Materials and methods

Cell culture

Immortalized hVFF, which have been supplied by Prof. S. Thibeault (University of Wisconsin-Madison, USA), were cultivated in standard medium consisting of Dulbecco's modified Eagle's medium (DMEM, 4.5g/L glucose, Sigma Aldrich, Vienna, AT) supplemented with 10% fetal bovine serum (FBS, Biowest, Nuaille', FR) and 0.2% Normocin (Invivogen, San Diego, CA, USA) as previously described by Graupp et al..(93)

The density of the cells on the two flexible-bottomed, prolectin coated BioFlex culture plates (Flexcell International, Burlington, NC, USA), was 144000 cells per well, except indicated otherwise. 24 hours later, the medium was changed to a serum-free medium for starvation. Another 24 hours later, cells were exposed to various settings and thus split into four groups, namely static with cytokines, static without cytokines, dynamic with cytokines and dynamic without cytokines. Additionally, a replacement of the starvation medium to a basal medium consisting of DMEM, 0.5% FBS, 0.2% Normocin, and 100µM ascorbic acid (all Sigma Aldrich) was performed. The cells in the static group were preserved in a separate incubator. Two different experimental setups were performed, differing only in the duration of vibration per day. In the first setup, vibration was applied for eight hours daily, based on a previous publication of our group.(11) In the second setup vibration was applied for four hours per day, while the pattern remained the same in order to assess the impact of a lower mechanical strain as well. The pattern remained the same and is described below. After a total of 73 hours, in detail 72 hours of treatment or control conditions and one hour of rest, the cells were harvested (see Figure 7). The qPCR was then carried out for the harvested material. In the four-hour vibration groups, one well of each condition was used for ELISA, Western Blot and Luminex as described in more detail below. The primary focus was laid on ECM-related proteins, proangiogenic factors and profibrotic as well as proinflammatory markers. The justification for this gene and molecule selection can be found below. The repetition for all experiments was four times per setup. In the first setup the mean number of cell passages of the four experiments was 137 while in the second this number was 125.

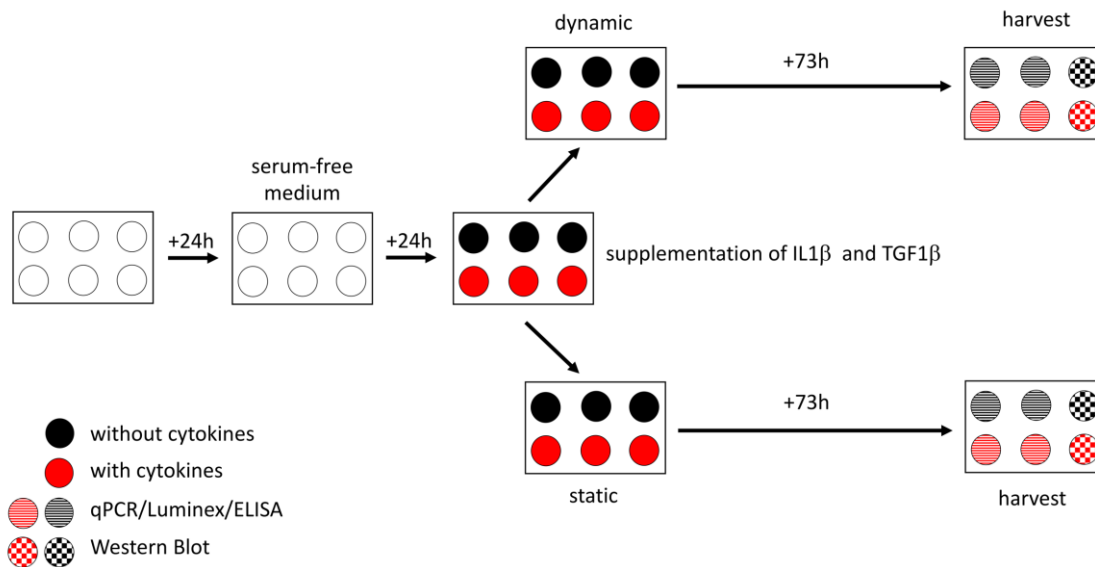


Figure 7: Experimental setup. One day after seeding the cells, a serum-free medium was used for starvation. Twenty-four hours later, cells were exposed to various settings and thus split into four groups (with or without cytokines—static or dynamic). Two different setups were performed, with four experiments each, differing only in the duration of mechanical stimulation per day (four hours and eight hours). The cells were harvested another 73 hours later. In the group of eight hours of vibration per day only a qPCR was performed using four wells per plate, the remaining two wells were left empty. In the other setup (four hours of vibration per day) two wells of each condition were used for qPCR, ELISA as well as Luminex and one for Western Blot. All samples were considered in the LDH assays. The figure was reproduced from (1), with permission of PLoS1.

Inflammatory reaction

By adding IL-1 β and TGF- β 1 (both at a concentration of 5ng/mL, R&D Systems, Minneapolis, MN, USA) to the basal medium inflammatory and pro-fibrotic culture conditions were simulated in vitro. This cytokine combination and their concentration were based on preliminary trials from our group as well as previous publications. (1)(94)(95)(96)(97)

Prior to the present study we conducted trials to evaluate whether TGF- β 1, IL-1 β or a combination of both was the most appropriate to simulate an acute inflammatory reaction. Therefore, 144.000 hVFF were seeded per well of 6-well plate. After 24 hours the medium was changed to a serum-free medium for starvation. After another day, cells were exposed either to 5ng/mL TGF- β 1 or 5ng/mL IL-1 β , to a combination of both or, for control, to standard medium without any cytokines. Cells were then harvested after four hours, 24 hours and 72 hours. The cell harvesting, RNA isolation and RT-qPCR procedures were identical to the ones of the present

study. Gene expression of ECM-related proteins (*HAS1*, *HAS2*, *HAS3*, *COL1A1*) and pro-inflammatory/pro-fibrotic markers (*IL6* and *TGF-β1*) were measured. Moreover, we looked for morphological changes of the fibroblasts under the microscope, as a consequence of cytokine treatment. The experiments were in total performed three times.

Macromolecular crowding

Moreover, the addition of inert MM to the culture medium improves the deposition of COL and other ECM components. This is essential to get a deeper knowledge on pathophysiology of fibrosis. (98)(99) For this reasons, all trials were conducted under crowded conditions. Therefore, the basal medium was supplemented with MM, in more detail a mixture of 37.5mg/mL 70 kDa Ficoll (Fc) with 25 mg/mL 400 kDa Fc5, 400μL L-Glutamine 1x and 100μM ascorbic acid (all Sigma-Aldrich St. Louis,MO,USA). (1)(98)

Selection of genes and molecules

ECM-related molecules.

The term ECM-related molecules refers to enzymes, that play a pivotal role in the ECM homeostasis as well as to components of the extracellular network and hence are fundamental in scar development. For the vocal fold lamina propria, HA and COL are two functionally relevant ECM components. (1)

Collagen

COL is the most abundant protein in the human body. More than 20 types of collagens are known. They all have in common that they consist of three peptide chains, called α -chains, which coil upon each other and form a triple helix. The composition of the α -chains, however, differs between the various types. For example, the α 1-chain of COL type VII is different to the α 1-chain of COL type VIII. Furthermore, there are COL which consist of different α -chains. COL I for instance contains two α 1-chains and one α 2-chain. In contrast to the only of one type of α -chains consisting homotrimeric COL (e.g. collagen III), COL I belongs to the so-called heterotrimers. (100)(101)

Like for every other protein, the blueprint of COL is encoded on the DNA. Since COL I and COL III are the most common types in the VF, in the present publication the expression of *COL1A1* (coding for the α 1-chain of COL I), *COL1A2* (coding for the α 2-chain of COL I) and *COL3A1* (coding for the α 1-chain of COL III) were determined. These genes are first transcribed into mRNA and then translated into procollagen α -chains, the progenitor molecules.

These molecules go through numerous posttranslational changes and finally form a procollagen triple helix. This is secreted into the ECM and undergoes some more modifications. N-proteinases and C-proteinases cleave the N- and C-propeptide ends from the triple-helix to form tropocollagen. Many of these tropocollagen molecules unite to COL fibrils and finally enable the formation of a crosslinked network of COL-fibers.

In healthy VF these fibers are parallelly organized, whereas in scar tissue there is an increased disorganized deposition. In order to determine COL deposition, both, intra- and extracellular proCOL1 and COL1 α 1-chains were measured by Western Blot and Luminex, respectively.

(101)(102) 1/1/2022 4:10:00 PM

MMP1 and TIMP1

Besides COL production, also its breakdown is essential in order to maintain homeostasis. Particularly the matrix metalloproteinase (MMP) and their antagonists, the tissue inhibitor of metalloproteinase (TIMP), play a pivotal role in orchestrating the ECM composition.

MMP belong to a group of enzymes, the metzincins, which require zinc, a metal ion, for their catalytic activity. Depending on their substrate specificity, soluble MMP can be assigned to four classes: collagenases (MMP1, MMP8, MMP13), gelatinases (MMP2, MMP9) stromelysins (MMP3, MMP10, MMP11) and a fourth heterogenous group containing the remaining MMP. The membrane anchored MMP are allocated to a separate class. (103) Originally it was thought that they were solely responsible for the conversion of the ECM by proteolytic degradation. However, they also participate in the release of biologically active proteins (e.g. growth factors and cytokines) called shedding. MMP are multidomain proteins. Via the cysteine switch mechanism, a cysteine component of the prodomain prevents a water molecule from binding to the zinc ion and keeps the proenzyme in its inactive form. During activation, the substrate expels the water molecule. The carboxylate group of the glutamate in the active region retains a proton from the water molecule and the polarized water molecule hydrolysis the substrate's carbonyl group of the peptide bond.

Furthermore, the hemopexin domain, which is not part of every MMP, is of significant importance. Its structure is reminiscent of a four-bladed propeller and responsible for the degradation of the collagen triple-helix. MMP1 is able to degrade various molecules, including collagen I and III, as it is one of the MMP containing the hemopexin domain.

An *in-vivo* rabbit phonation model revealed a significant upregulation of *MMP1* gene expression and therefore is mechanoresponsive. (102)(103)(104)

If they are dysregulated, MMP are involved in many pathologies, such as wound healing disorders and fibrotic diseases. In order to avoid these, there exist different regulatory mechanisms. Besides important epigenetic processes, there are two types of endogenous enzymes, α 2-macroglobulines and TIMP, which are capable of inhibiting the activated MMP. Four TIMP families are known, each of them is able to inhibit every MMP, however the efficacy is variable. TIMP1 for example is a strong inhibitor of MMP1. Due to its wedge-shaped structure, it blocks the active center of MMP prevents the substrate to bind. The expression of MMP1 as well as TIMP1 were measured by qPCR. (102)1/1/2022 4:10:00 PM(104)(105)(106)

Hyaluronic acid

HA is an ubiquitous non-sulfated GAG composed of repetitive units of a uronic sugar and an amino sugar, namely D-glucuronic acid and N-acetylglucosamin respectively. Under physiological conditions, the carboxyl groups are in a negatively charged state. This causes an attraction of cations (e.g. Na^+ , K^+ , Ca^{2+} , Mg^{2+}) and in further consequence of water molecules. Therefore, at physiologic pH, HA is present as anion and form salts which are referred to as hyaluronate. Due to its capacity of storing large amounts of water, it has a significant effect on tissue elasticity and is of particular importance in the VF. *In vivo* animal studies have revealed that acute VF trauma comes along with reduced concentrations of HA which has a negative impact on functional measures of phonation. (107)

In contrast to other GAG HA is not synthesized in the Golgi apparatus but by enzymes, located at the inner surface of the membrane called hyaluronan synthases (HAS) and afterwards secreted to the ECM. Of these three isoenzymes HAS1, HAS2 and HAS3, with different kinetic properties, are known. Their counterparts, responsible for HA degradation are the hyaluronidases (HYAL) belonging to the endoglycosidases. Six genes are known in the human genome, encoding for the different HYAL isoenzymes. In this publication, we measured the expression of all three *HAS* and the *HYAL-2* genes in order to assess HA metabolism (see Figure 8). (108)(109)(110)(111)

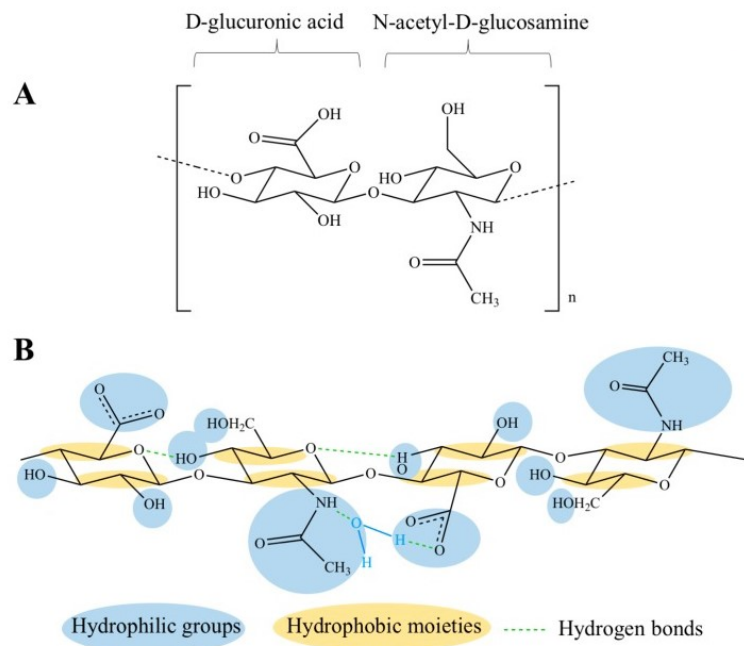


Figure 8: Schematic illustration of hyaluronic acid disaccharide unit (A) and chemical structure (B). Figure was reproduced from (110), with permission of Dr. Manfredini.

Fibronectin

Fibronectin (FN) is a dimeric glycoprotein, where each monomere consists of almost identical repeating subunits, referred to as FN repeats. Although FN is encoded on one gene, many different variants arise from alternative splicing of the pre-mRNA. Basically, two different manifestations of FN are distinguished: a soluble plasma form and the less-soluble intracellular form. FN contributes to diverse processes, including angiogenesis, cell migration and differentiation but also influences gene expression. By its outstanding ability to mediate cell-to-cell and matrix-to-cell adhesion it lives up to its name of an “extracellular glue”. The RGD region of FN plays a major role since it is mainly responsible for binding to the transmembrane proteins, especially to $\alpha_5\beta_1$ -integrins. Particularly in the superficial layer of the LP high concentrations of FN were found, indicating its importance during phonation. Besides *FN1*-gene expression additionally extracellular FN1 concentration was determined via qPCR and Luminex, respectively. (57)(112)(113)

Pro-angiogenic factors

A sufficient blood supply of the injured region is essential for wound healing. Vascular endothelial growth factors (VEGF) contribute significantly to the re-vascularization. Particularly the hypoxic conditions in inflamed tissue promote VEGF mRNA expression. Different proteins are

part of the VEGF family, including VEGF-A, VEGF-B, VEGF-C, VEGF-D and placental growth factor (PlGF). While VEGF-C and VEGF-D are mainly responsible for lymphangiogenesis, VEGF-A is known to be essential for the *de-novo* synthesis of blood vessels. The different VEGF bind with variable affinity to the different VEGF-receptors (VEGFR), which are tyrosine-kinase receptors. VEGFR-2 for example, particularly expressed in endothelial cells, is the main signaling receptor of VEGF-A. In this way it induces mitogenesis and vessel permeability. (114)(115)(116)

Even though, most of the current knowledge about VEGF bases on oncological and ophthalmological studies, a previous trial by our group showed that these proteins may also be relevant in VF pathologies, such as Reinke's edema. We investigated the impact of cigarette smoke extract on VFF. A significant increase of VEGF-A and C in combination with mechanical stimulation could be shown. (117) With this background knowledge and in order to assess potential alterations due to vibration and cytokine treatment, we included these two proangiogenic factors in the present study,

Inflammatory and fibrogenic markers

α -SMA and ACTA2

The cytoskeleton can be considered as the intracellular scaffold. However, similarly to the ECM, it is not a rigid but a very dynamic structure which is subject to constant conversion. Actins are, besides microtubules and intermediate filaments, one of the three main types of polymers of which the cytoskeleton is composed of. These polymers fulfill important functions such as giving the cells a spatial structure but also in the transmission of biomechanical stimuli. Of particular importance during inflammatory processes is the α -smooth muscle actin (α -SMA). It is a well-established myofibroblast marker and significantly contributes to wound contraction. From a pathophysiological perspective this makes sense, since it impedes the penetration of pathogens, however in the VF it has undesired effects on the oscillatory properties. α -SMA as well as its encoding gene alpha smooth muscle actin (*ACTA*) 2 were measured by Western Blot and qPCR, respectively. (58)(94)(118)(119)

IL-1 β , IL-6, IL-11, COX-2 and TGF- β 1

Cytokines are a heterogeneous group of proteins which are essential for the inflammatory reaction. Generally, many different cytokines act simultaneously and interact with each other. Depending on the type of immune response, they can have pro- as well as anti-inflammatory regulatory functions, which are very complex processes and their description would go beyond the scope of this work.

They are primarily secreted by antigen presenting cells, but some of them may also be produced by other cells such as fibroblasts. The most important representatives include interleukins and various growth-factors such as TGF- β 1. In addition to these proteins, however, arachidonic acid derivatives, namely prostaglandins, thromboxane A2 and leukotriens, play also a decisive role during inflammation. The enzyme COX catalyzes the formation of thromboxane A2 and prostaglandins. (120)(121)(122)

This study only considered a limited subset of the above-mentioned inflammation-regulating molecules, in the knowledge that many more could be relevant. Gene expressions of *IL-1 β* , *IL-6*, *COX-2* and *TGF- β 1* were included since many studies have previously reported about their important role in acute inflammatory reactions, also in VF. (48) (123)

Additionally, the concentration of IL-11, a member of the IL-6 family, was determined by Luminex since this cytokine is known to be mechanoresponsive and is also involved in the pathogenesis of tissue fibrosis. (124)(125)(126)

bFGF

Basic fibroblast growth factor (bFGF), also known as fibroblast growth factor 2, is a member of the fibroblast growth factor family. Frequently, bFGF is linked to heparin or heparan sulfate which does not influence the bFGFs molecular structure but increases the affinity to the FGF receptors (FGFR). Binding to the FGFR induces autophosphorylation of the receptor and causes the activation of intracellular signaling pathways which finally leads to various biological effects such as cell migration and proliferation. (127)(128)

In *in vitro* experiments, bFGF showed an anti-inflammatory effect by downregulating COL production and upregulating HA production. *In vivo* studies in a rat model revealed improvements in phonatory functions supporting that bFGF might have beneficial effects on VF wound healing. (129) bFGF concentrations were quantified by Luminex assay.

Mechanical stimulation

Mechanical stimulation was applied by using a phonomimetic bioreactor, which was developed and realized by our group. In brief, the flexible bottoms of the 6-well plates were set into oscillation by aerodynamic pressure fluctuations generated by a loudspeaker underneath the plates. One of the most important prerequisites for ensuring reproducibility and comparability is the uniform stimulation of all 6 membranes. With the aid of a laser doppler vibrometer (LDV) fundamental frequencies and membrane displacements were measured (see table 2). They were first determined without any fluid on it. For this purpose, the laser beam was focused at the center of the membrane and afterwards at 3, 6, 9, 12, 15 and 17.5 mm radially from the center. Multiple measurements were conducted at each of the mentioned distances and the resulting amplitude spectra were averaged. These revealed a fundamental frequency at 180 ± 3 Hz and the first harmonic at 310 ± 5 Hz. Afterwards, displacements were assessed having added 2,5mL of cell culture medium. Due to the increase of inertia the fundamental frequency dropped to 55 ± 2 Hz and the first harmonic to 150 ± 4 Hz. Marginal deviations between the different membranes are traced back to slight differences of clamping and/or thickness of the membranes (see figure 9). (1)(11)(130)

Table 2 Membrane deflection. Table was reproduced (11). With permission of PLoS1.

	Without medium (excitation 180 Hz)	With medium (excitation 55 Hz)
Voltage (V)	Membrane deflection (mm)	
0.08	0.063 ± 0.004	0.055 ± 0.011
0.25	0.195 ± 0.010	0.162 ± 0.082
0.5	0.405 ± 0,021	0.267 ± 0.066
1	0.864 ± 0.050	0.437 ± 0.071
1.5	1.316 ± 0.088	0.559 ± 0.090
2	1.691 ± 0.119	0.658 ± 0.041
2.5	1.950 ± 0.133	0.703 ± 0.030
3		0.759 ± 0.032
3.3		0.785 ± 0.045

Since the inflammatory phase of wound healing lasts for around three days, the mechanical stimulation on hVFF was equally distributed over a time period of 72 hours. (2)(5) The stimulatory pattern of our study was a sinusoidal chirp sound ranging from 50 Hz to 250 Hz. This frequency range corresponds to the primary larynx sound in humans. The central part of the membranes of the well were displaced on average $82 \mu\text{m} \pm 5 \mu\text{m}$, depending on the applied frequency. The input voltage (V) was set to 1.1 V on the loudspeaker. First, mechanical stimulation was applied for eight hours per day, basing on our previous study. (11) Afterwards, the stimulatory pattern was reduced to four hours daily, according to a publication of Titze et al. (131) To date only a few publications exist, which deal with human VF displacements (horizontal and vertical) during phonation. These report a broad spectrum of values, depending on the measurement method and/or the setting. Our bioreactor is able to simulate these displacements and complies with the maximal displacement in humans. (132) The cells in the static group were preserved in a separate incubator, in order to exclude any interferences. (1)

Lactate dehydrogenase (LDH) assay

The activity of the lactate dehydrogenase (LDH) was measured in the supernatants, using the Pierce™ LDH Cytotoxicity Assay Kit (Thermo Scientific), in order to evaluate cell viability. For this purpose, it is necessary to determine the maximum LDH activity. This was achieved by seeding the cells in two wells of a 24-well-plate parallel and at the same density to the 6-well-plates. The change of the medium was performed identically to the experimental cells. Additionally, two wells with standard medium \pm cytokines without any cells served as blanks. Half an hour before the harvest, the cell-seeded wells were enriched with 10x lysis buffer and further incubated at 37 °C. Following the manufacturer's instructions, 50 μ L of supernatants were obtained from all wells and processed in duplicates. Absorbances at 680nm and 490nm were determined using the Spectramax Plus 384 Microplate Reader (Molecular Devices, San Jose, CA, USA). First the absorbance at 680nm was subtracted from the absorbance at 490nm and the mean of each duplicate computed. Finally, the differences of this value and the blank values were calculated. The LDH activity was defined as percentage of the maximal LDH activity. (1)

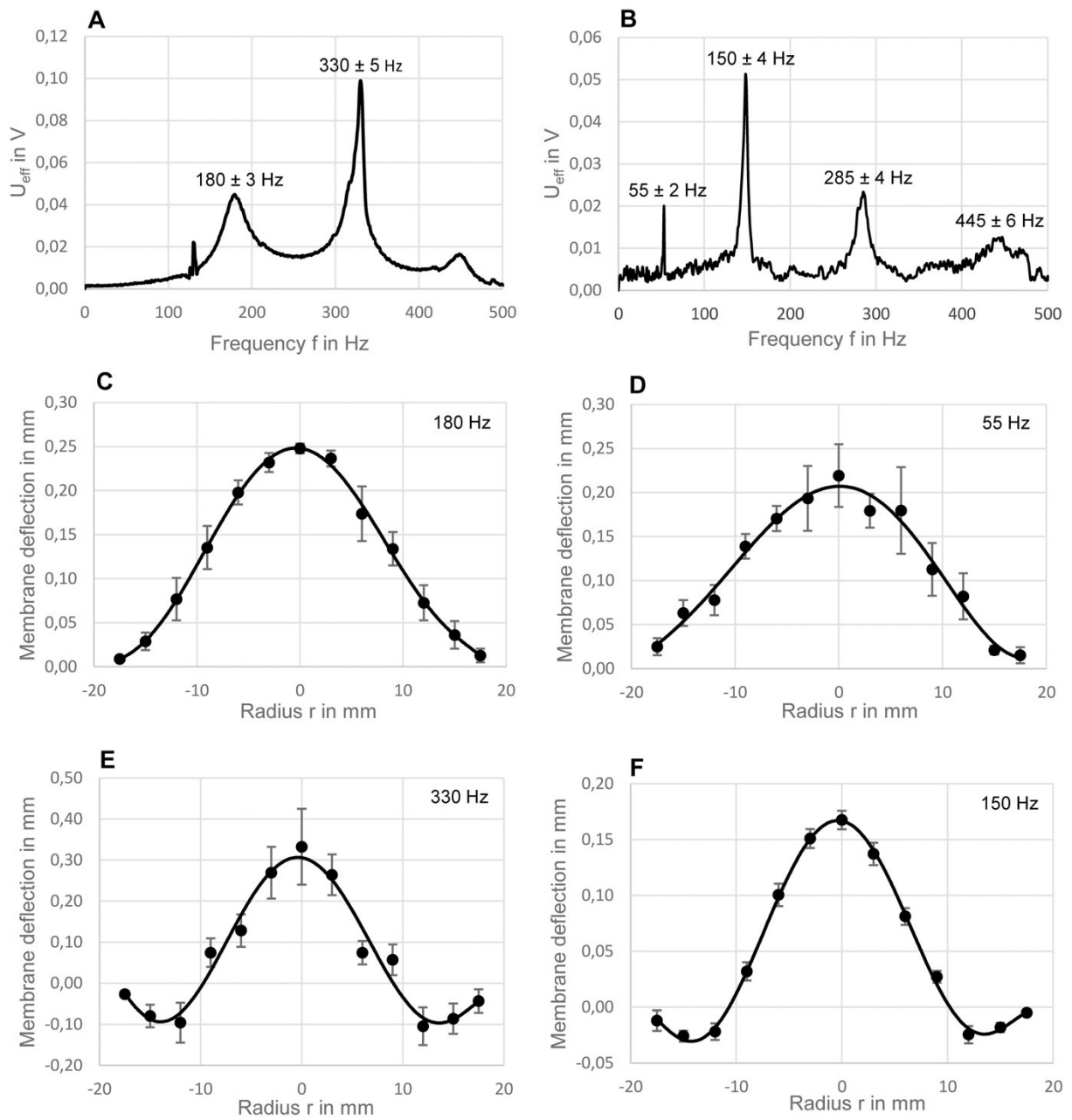


Figure 9: Laser Doppler Vibrometer Measurements. A, C and E represent the vibration amplitude spectra and the corresponding vibration modes without medium; B, D and F represent the vibration amplitude spectra and the corresponding vibration modes with 2,5mL medium. A and B show the frequency spectra, plotted for the central position of the membrane. C and D show the fundamental modes of the membranes at an excitation frequency of 180Hz and 55Hz respectively. E and F present the first harmonic modes of the membranes at an excitation frequency 330 Hz and 150 Hz, respectively. All measurements were averaged values from all 6 membranes of one cell culture plate. Table was reproduced from (11), with permission of PLoS1.

Isolation of RNA and Reverse Transcription-quantitative Polymerase Chain Reaction (RT-qPCR)

From each six-well-plate, four wells were harvested for RT-qPCR. The culture medium was removed and 700 μL QIAzol Lysis Reagent (Qiagen, Hilden, GER) was added in each well. After five minutes the suspension was thoroughly mixed in order to gain as many RNA as possible and finally transferred into a tube.

Next RNA was isolated with the aid of an miRNeasy Mini Kit (Qiagen, Hilden, GER). For this purpose, 140 μL chloroform were added and the samples vigorously shaken for 30 seconds. Subsequently, the tubes were left at room temperature for three minutes. Then they were centrifuged for 15 minutes at 4°C and 12000 rpm. This causes a separation of RNA from other molecules. RNA was obtained using a pipette and transferred into another tube, where it was gently mixed with 450 μL of 100% ethanol. 700 μL of this solution were pipetted into a spin column with a collection tube. These were centrifuged at room temperature and 9000rpm for 15 seconds. The solution in the collection tube was poured off. This step was repeated once. 700 μL of RWT were added and centrifuged at room temperature and 9000rpm for 15 seconds. This cycle was repeated with 500 μL of RPE buffer. Finally, spin columns were recentrifuged at room temperature and 13000rpm for two minutes. The collection tube was replaced by a new one the samples were repeatedly centrifuged, after having added 30 μL of RNase free water, again at room temperature and 9000rpm for one minute. By using a NanoDrop 2000c UV-Vis spectrophotometer (Thermo Scientific, Waltham, MA) RNA concentration was determined. 1 μL of RNase free water was taken for blank. In order to determine RNA purity, the ratio of the absorbances at 280nm and 260nm were calculated. $A_{260}/A_{280} > 1,8$ was considered to be pure. (1)

Reverse transcription of RNA into complementary DNA (cDNA) was achieved using the QuantiTect Reverse Transcription Kit (Qiagen). Of each sample 1 μg total RNA was diluted with the appropriate amount of RNase free water to eventually obtain 12 μL in total. Genomic DNA (gDNA) was removed by adding 2 μL of gDNA wipe-out buffer, centrifugating these suspensions and incubating them for 2 minutes at 42°C in a water bath. 4 μL solution, containing 10ng cDNA, were mixed with 6 μL of Primer- SYBR Master Mix (Promega/USA) containing 5 μL GoTaq Master Mix (Promega/USA) and 1 μL (200nM each) Primer F&R. RT-qPCR was conducted in technical triplicates utilizing the LightCycler 480 system (Roche, Vienna, AT). Denaturation, amplification and the melting curve analysis were achieved by the following program: 2 min/95°C, 45 cycles of 10 s/95°C, 1 min/60°C and finally the temperature was constantly increased at a rate of 2.5°C/min from 55°C to 95°C. (133) CT values were computed using the AbsQuant^{2nd} Derivative Max method of the LightCycler 480 software. Relative quantification

of gene expression levels was calculated by using the geometric mean of ubiquitously expressed transcript protein (*UXT*) and beta-2 microglobulin (*B2M*) as housekeeping genes. (134)(135) Validation of the internal references was done according to Dheda et al. (136) Finally the gene expression of pro-inflammatory/pro-fibrotic markers (*ACTA2*, *IL-1 β* , *IL-6*, *IL-11*, *COX-2* and *TGF- β 1*) and ECM-related proteins *HAS1*, *HAS2*, *HAS3*, *HYAL2*, *COL1A1*, *COL1A2*, *COL3A1*, *FN1*, *MMP1* and *TIMP1* was determined. *TIMP1* and *IL-11* were only determined in the four-hour of vibration setup. (1)

In the third run of the eight hours of vibration setup, two samples (deriving from the two middle wells of the dynamic plate) were inadvertently mixed up during the preparation for qPCR and consequently not considered for statistical analysis. Primer sequences are listed in table 3.

Table 3: Primer sequences used for RT-qPCR. Table was reproduced and adapted from (11). With permission of PLoS1.

Gene	Gene symbol	Forward primer	Reverse primer
Alpha smooth muscle actin	<i>ACTA2</i>	CGTTACTACTGCTGAGCGTGA	GCCCATCAGGCAACTCGTAA
Beta-2-microglobulin	<i>B2M</i>	AGGCTATCCAGCGTACTCCA	CGGATGGATGAAACCCAGACA
Collagen I α 1	<i>COL1A1</i>	CCCCGAGGCTCTGAAGGT	GCAATACCAGGAGCACCATTG
Collagen I α 2	<i>COL1A2</i>	ACCACAGGGTGTTCAAGGTG	CAGGACCAGGGAGACCAAAC
Collagen III α 1	<i>COL3A1</i>	GACCTGGAGAGCGAGGATTG	GTCCATCGAAGCCTCTGTGT
Prostaglandin-endoperoxide synthase 2	<i>PTGS2/COX2</i>	AGTGCGATTGTACCCGGACAGGA	TGCACTGTGTTTGGAGTGGGTTTCA
Fibronectin 1	<i>FN1</i>	CTGCAAGCCCATAGCTGAGA	GAAGTGCAAGTGATGCGTCC
Hyaluronan synthase 1	<i>HAS1</i>	CTTCCTAAGCAGCCTGCGAT	TATATAGGCCTAGAGGACCGCTG
Hyaluronan synthase 2	<i>HAS2</i>	ATGCTTGACCCAGCCTCATC	TTAAATCTGGACATCTCCCCAA
Hyaluronan synthase 3	<i>HAS3</i>	ATCATGCAGAAGTGGGGAGG	GAGTCGCACACCTGGATGTA
Hyaluronidase 2	<i>HYAL2</i>	CGTGGTCAATGTGTCCTGGG	CCCAGGACACATTGACCACG
Interleukin 1 beta	<i>IL1β</i>	GATGGCTTATTACAGTGGCAATGA	GGTCGGAGATTTCGTAGCTGG
Interleukin 6	<i>IL6</i>	AACCCCAATAAATATAGGACTGGA	CCGAAGGCGCTTGTGGA
Matrix metalloproteinase 1	<i>MMP1</i>	CACGCCAGATTTGCCAAGAG	GTTGTCCCGATGATCTCCCC
Metalloproteinase inhibitor 1	<i>TIMP1</i>	GGAATGCACAGTGTTCCTG	GGAAGCCCTTTTCAGAGCCT
Transforming growth factor beta 1	<i>TGFβ1</i>	TACCTGAACCCGTGTTGCTC	GCTGAGGTATCGCCAGGAAT
Ubiquitously expressed transcript protein	<i>UXT</i>	GCAGCGGGACTTGCGA	TAGCTTCTGGAGTCGCTCA

Western blot analysis

Western Blot analysis measured the intracellular changes of α -SMA, which is a myofibroblast marker, as well as COL. (58) Two wells from each plate, with or without cytokines, were taken to gain protein lysates. Firstly, the culture media was removed by aspiration. Ice-cold PBS was used to wash the cells. Then, 90 μ L of the protein extraction buffer (PEB), containing ice-cold RIPA buffer (Cell Biolabs San Diego, CA, USA), 5mM EDTA solution and 1x HaltProtease and Phosphatase Inhibitor Cocktail (both from Thermo Fisher Scientific) were added for cell lysis. Cells adherent to the membrane were scraped using a cell scraper under ice. The PEB-cell suspension was transferred into a tube. In order to increase the yield, this step was repeated once. With the help of an ultrasound homogenizer, each lysate was sonicated three times for 10 seconds adhering to a 30 second pause between each cycle. Finally, the tubes were centrifuged for 10 minutes at 13000 rpm and 4°C. The determination of the total protein concentration was performed with the Pierce BCA Protein Assay Kit (Thermo Fisher Scientific), following the manufacturer's protocol. Of each sample 25 μ g of total protein were obtained, the appropriate amount of DTT and 4x Laemmli Buffer (Bio-Rad, Hercules, CA, USA) were added and boiled for 5 min at 95°C. Subsequently the samples were applied to SDS-PAGE using 4–20% Mini PROTEAN TGX gels (Bio-Rad). Afterwards the proteins were blotted onto a nitrocellulose membrane (Bio-Rad). A blockage of the blots was performed using 5% milk for two hours and then incubated with the primary antibody against glyceraldehyde phosphate dehydrogenase (GAPDH, Cell Signaling, Danvers, MA, USA, #2118S, 1:5000); COL1A1 (Nordic Bio Site, Ta'by,SE, ABB-2670, 1:2000); or α -SMA (Sigma-Aldrich, A5228, 1:1000) at 4°C overnight. After washing, the appropriate secondary antibodies Goat Anti-rabbit IgG H&L (Abcam, abb6721, polyclonal, 1:5000 for COL1A1 and GAPDH) and Goat Anti-mouse IgG H&L (Abcam, Cambridge, UK, abb6789, monoclonal, 1:5000 for α -SMA) were added to the blots for another cycle of incubation. The SuperSignal West Pico Chemiluminescent Substrate (Thermo Fisher Scientific) was used for signal detection and ChemiDoc Touch system (Bio-Rad) enabled image acquisition. Densitometric analyses were performed using ImageLab software (Bio-Rad). Western Blot was only performed in the plates with four hours of vibration per day. (1)

Magnetic Luminex assay

For quantifying selected proteins in the supernatant, and therefore extracellularly, the Human Magnetic Luminex Assays (LXSAHM, R&D Systems) were used. The custom-designed multiplex assays, which measure TIMP1, pro-angiogenic factors (VEGF A, VEGF C), COL1A1, IL-11, FN1 and bFGF were conducted following the manufacturer's instructions. The manufacturer supplied standards for each analyte and included them in the kit. These were used with

the purpose of preparing standard curves. Additionally, standard mediums with and without cytokines were used as blank. The estimation of the sample dilutions for the chosen markers was done on the basis of previous Luminex measurements by our group (e.g. Gugatschka et al 2019, Grossmann et al. 2020). (117) (130) Pre-diluted 1:50 samples were used for TIMP1, FN1 and COL1A1 measurements, while the determination of all other analytes were performed with undiluted samples. The measurements and calculations of the assays were carried out using the Bio-Plex 200 assay reader (Bio- Rad) and the Bio-Plex Manager Software Version 6.2 (Bio- Rad), respectively. Luminex was only performed for the plates with four hours of vibration per day. (1)

Enzyme-linked immunosorbent assay (ELISA)

For the determination of the HA levels in the supernatant, the sandwich enzyme immunoassay Quantikine1 ELISA Kit (DHYAL0, R&D Systems) was used following the manufacturer's instructions. Briefly, an HA standard provided in the kit was utilized and diluted with calibrator diluent RT5-18, serving simultaneously as the zero standard. HA standard curves were prepared with concentrations ranging from 0.625 to 40 ng/mL. Standard medium with and without cytokines were used as blanks. For predilution, Calibrator Diluent RD5-18 was added to the blanks and all samples in a 1:100 ratio. These were assayed with HA standards on the same plate in technical duplicates. Using the Spectramax Plus 384 Microplate Reader (Molecular Devices), optical absorbance (OA) values were measured and the differences calculated (OA values at 540nm were subtracted from those at 450nm). The sample concentrations were assessed from the calibration curve and the corresponding blank value deducted. Resulting numbers were multiplied by the dilution factor (x100). ELISA was only performed for the plates with four hours of vibration per day. (1)

Statistical analysis

Statistical analysis was conducted with SPSS (Version 25). Shapiro-Wilk test was performed in order to assess normal distribution. The four different conditions (static or dynamic, each with or without cytokines) were defined as independent variables. If the data was normally distributed, a one-way ANOVA was performed in order to evaluate significant differences. To further specify between which of the conditions there was a significant difference, a Tukey post-hoc test was used.

However, in cases of significant Shapiro-Wilk test, indicating not normally distributed data, a Kruskal-Wallis test was performed. Mann-Whitney-U test was performed for pairwise compar-

isons when Kruskal-Wallis test revealed a significant difference. A p-value < 0.05 was considered as statistically significant. Values are described as means \pm standard deviation (S.D.). Effect size was determined by calculating partial eta squared (η^2). (1)

Results

Preliminary trials

Genotypic alterations

Since no duplicates existed in these trials, a statistical analysis would not have been reasonable, therefore focusing on trends. Even though, the combination of the cytokines did not show the greatest change in each case, in our opinion these results were the most promising (see Figure 10).

Since these pre-trials used different 6-well-plates than the present study and did not apply macromolecular crowding (MMC), a direct comparison of the results is not possible. (1)

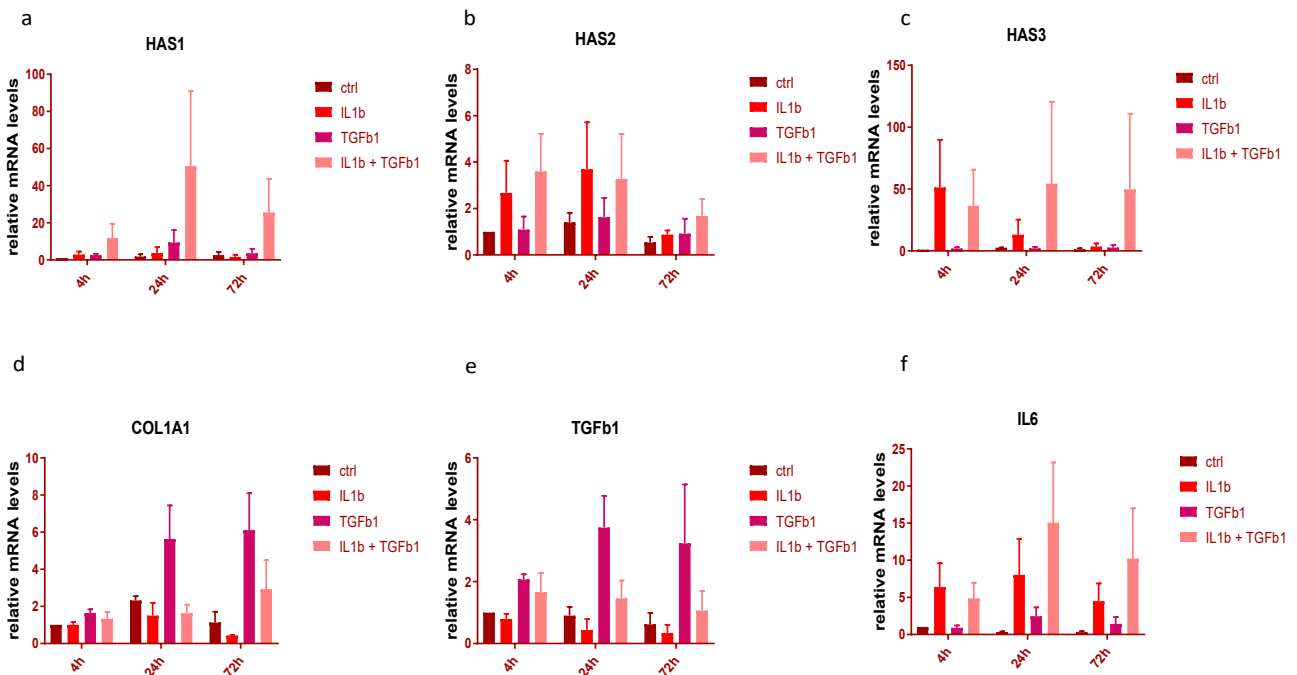


Figure 10: Alterations of gene expression under inflammatory conditions over time. This figure elucidates the impact of TGFβ1, IL1β and their combination on the gene expression of ECM-related proteins and cytokines when compared to an untreated control group. ctrl (control), HAS1 (hyaluronan synthase 1), HAS2 (hyaluronan synthase 2), HAS3 (hyaluronan synthase 3), COL1A1 (collagen 1 alpha 1), IL6 (interleukin 6), TGFβ1 (transforming growth factor beta 1). This figure was reproduced from (1), with permission of PLoS1.

Phenotypic alterations

Besides the molecular changes we could also observe morphological changes in the fibroblasts under the light microscope. VFF are spindle-shaped cells.(20) This structure remained the same under all conditions at any point of observation. The nucleus differed however when exposed to TGF- β 1 and IL-1 β simultaneously. A more prominent nucleus with a granulous structure compared to the untreated control group could be observed. These changes could be suspected already after four hours of treatment but were most obvious after 72 hours. (See figure 11)

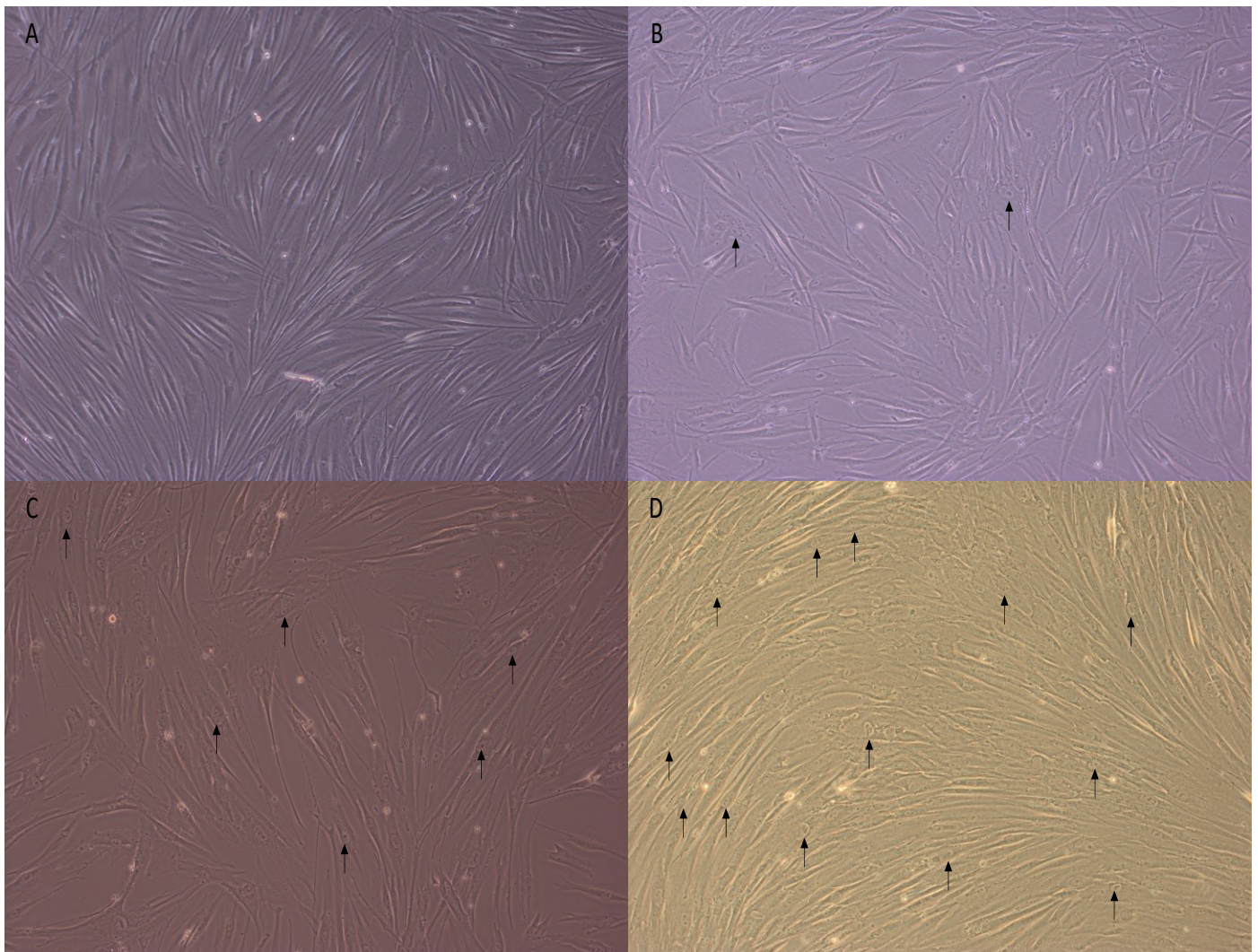


Figure 11: Morphological changes after different duration of cytokine treatment (B-D) compared to untreated control (A). A shows the untreated control group after 72 hours of observation. B-D show the cells exposed to IL-1 β and TGF- β 1 for four hours (B), 24 hours (C) and 72 hours (D). Arrows are indicating some of the altered nuclei.

Four hours of vibration per day

Fibroblast viability

Comparing the different conditions LDH activity did not show any significant differences. ($p = 0.966$). (see Figure 12). (1)

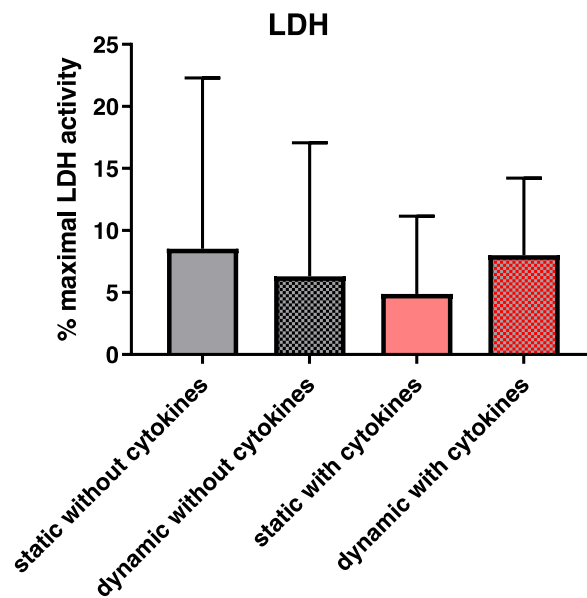


Figure 12: Effect of vibration (4 hours per day) and/or cytokine exposure on cell viability and gene expression. After a total of 73 hours, in detail 72 hours of treatment or control conditions and one hour of rest, supernatants were obtained for LDH activity assay. The LDH activity is shown as percentage of the maximal LDH activity. A p -value <0.05 was considered statistically significant. This figure was reproduced from (1), with permission of PLoS1.

Gene expression and protein synthesis

ECM-related molecules and angiogenic factors.

Statistically significant differences were found in HA concentration ($p = 0.008$; $\eta^2 = 0.850$), and expression of HAS1 ($p = 0.043$; $\eta^2 = 0.243$) and HAS3 ($p = 0.000$; $\eta^2 = 0.792$). Tukeys post hoc comparison revealed significant increase of HA concentration in the supernatants as a consequence of inflammatory stimuli, however additional mechanical strain did not show any effects (see Figure 13). Consistent with these results, gene expression of HAS1 and HAS3 were also significantly increased due to cytokine exposure (see Figure 13). Gene expression of HAS2 revealed a similar trend, hence not reaching statistical significance ($p = 0.125$; $\eta^2 = 0.369$) (see Figure 13). HYAL2 mRNA levels stayed unaffected ($p = 0.155$; $\eta^2 = 0.343$) (see Figure 13). (1)

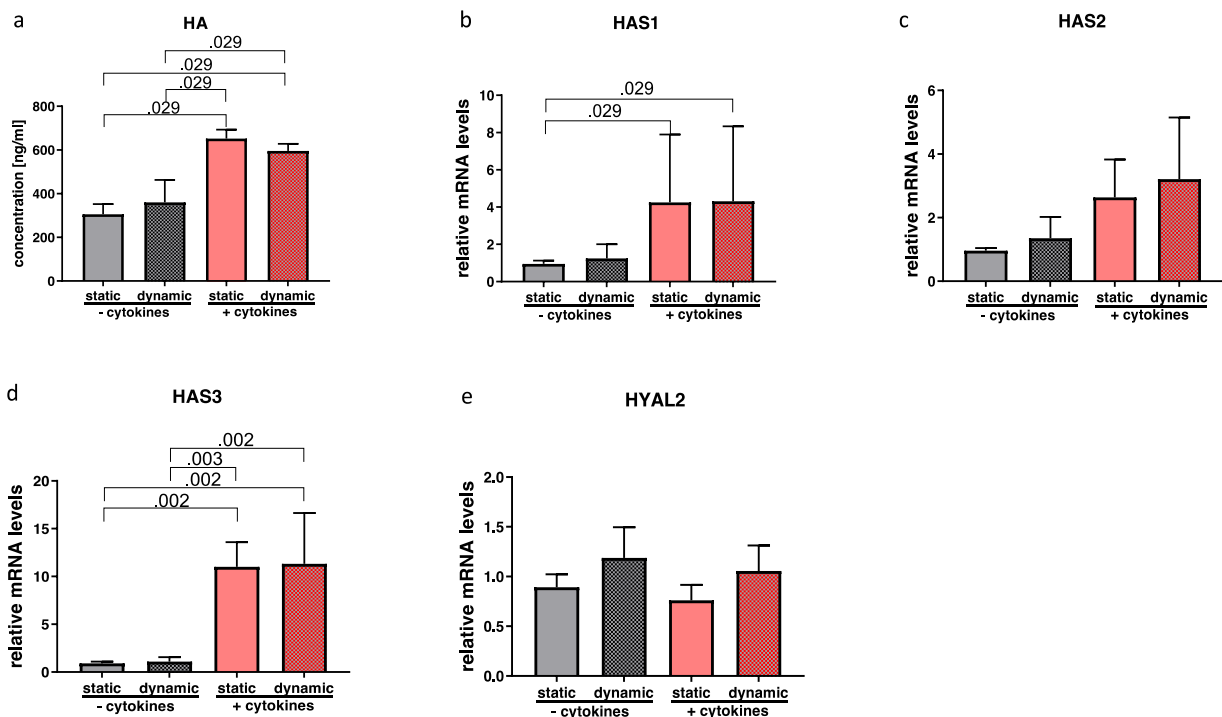


Figure 13: Effect of vibration with/without cytokine exposure on HA metabolism. Supernatants were obtained for ELISA to evaluate the HA concentration(a). qPCR was performed in order to analyze the HA-related gene expression (b-e). The results of the four independently conducted experiments ($N = 4$) are indicated as mean \pm S.D. A one-way ANOVA, when the data was normally distributed or Kruskal-Wallis test, when the data was non-parametric, were used for statistical analyses. A p -value < 0.05 was considered statistically significant. In case of statistical significance, p -values from post-hoc tests are represented as decimal numbers above the bars; p -values which are not shown in this figure, are complemented in the supplementary file 1. HA (hyaluronic acid), HAS1 (hyaluronan synthase 1), HAS2 (hyaluronan synthase 2), HAS3 (hyaluronan synthase 3), HYAL2 (hyaluronidase 2). This figure was reproduced from (1), with permission of PLoS1.

ANOVA revealed significant changes of COL1A1 ($p = 0.000$; $\eta^2 = 0.825$); COL1A2 ($p = 0.000$; $\eta^2 = 0.795$) and COL3A1 ($p = 0.005$; $\eta^2 = 0.640$). Pairwise comparison showed a statistically significant upregulation of the three COL subtypes as a consequence of cytokine exposure, whereas vibration did not show any additional effects (see Figure 14). Similarly, intracellular COL1A1 protein level was increased, however did not meet statistical significance ($p = 0.076$; $\eta^2 = 0.451$), while extracellular protein content was significantly increased (see Figure 14). In the post hoc tests, again the inflammatory stimuli significantly increased COL1 concentration in the supernatant compared to the static group without cytokine exposure (see Figure 14). The mRNA expression *MMP1* was significantly changed as well ($p = 0.009$; $\eta^2 = 0.604$). In the post hoc comparisons, a decrease was observable after cytokine exposure compared to the non-inflammatory groups (see Figure 14). Neither inflammatory nor mechanical stimuli had an effect on TIMP1 expression ($p = 0.629$; $\eta^2 = 0.130$) (see Figure 15). (1)

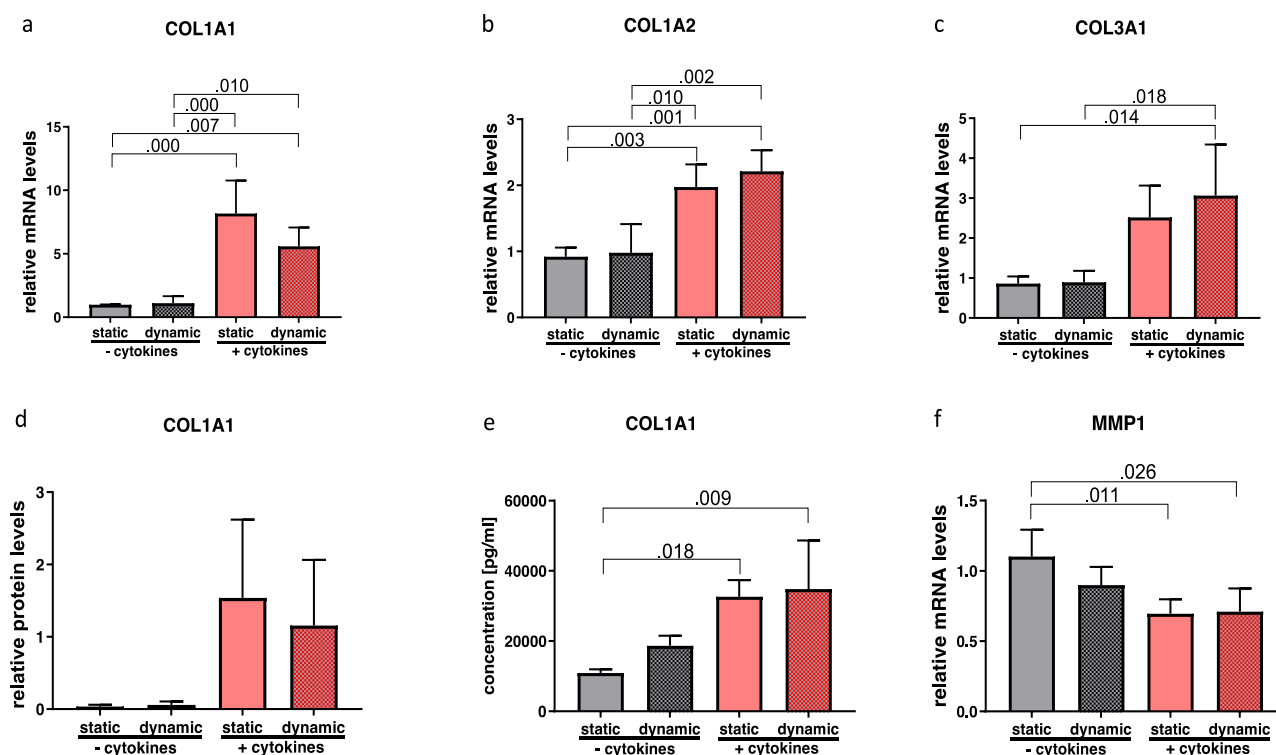


Figure 14: Effect of vibration with/without cytokine exposure on ECM-related molecules. qPCR, Western blot and Luminex were performed in order to analyze mRNA (a-c and f) and protein levels (d and e) of ECM-related molecules, respectively. The results of the four independently conducted experiments ($N = 4$) are indicated as mean \pm S.D. A one-way ANOVA, when the data was normally distributed or Kruskal-Wallis test, when the data was non-parametric, were used for statistical analyses. A p -value < 0.05 was considered statistically significant. In case of statistical significance, p -values from post-hoc tests are represented as decimal numbers above the bars; p -values which are not shown in this figure, are complemented in the supplementary file 1. COL1A1 (collagen 1 alpha 1), COL1A2 (collagen 1 alpha 2), COL3A1 (collagen 3 alpha 1), MMP1 (matrix metalloproteinase 1). This figure was reproduced from (1), with permission of PLoS1.

Having performed statistical tests on FN1 gene expression ($p = 0.000$; $\eta^2 = 0.804$) as well as on FN1 protein concentration ($p = 0.012$; $\eta^2 = 0.790$), the null hypothesis was rejected. Post hoc tests revealed a significant increase of gene expression due to inflammatory stimuli, but no alterations were found with additional mechanical stimulation (see Figure 15). FN1 protein levels were also elevated by cytokine exposure but significant changes were only reached when compared to the static group. (see Figure 15). (1)

One way ANOVA revealed significant alterations of extracellular bFGF concentration ($p = 0.000$; $\eta^2 = 0.859$). Pairwise comparison showed a significant increase due to cytokine exposure. (see Figure 15). Neither condition had an impact on the pro-angiogenic factors VEGF A ($p = 0.763$; $\eta^2 = 0.089$) and VEGF-C ($p = 0.481$; $\eta^2 = 0.180$) (see Figure 15). (1)

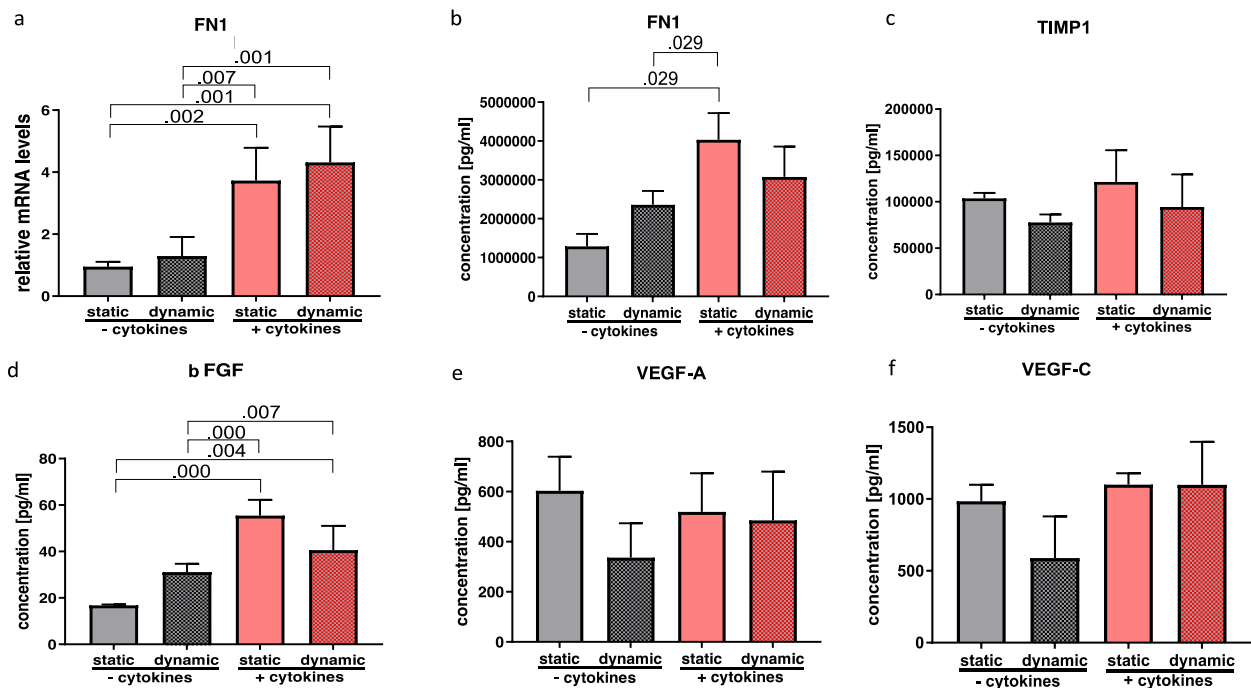


Figure 15: Effect of vibration with/without cytokine exposure on ECM-related molecules, growth factors and angiogenic factors. qPCR and Luminex were performed in order to analyze mRNA (a) and protein levels (b-d) of ECM-related molecules as well as growth- and angiogenic factors, respectively. The results of the four independently conducted experiments ($N = 4$) are indicated as mean \pm S.D. A one-way ANOVA, when the data was normally distributed or Kruskal-Wallis test, when the data was non-parametric, were used for statistical analyses. A p -value < 0.05 was considered statistically significant. In case of statistical significance, p -values from post-hoc tests are represented as decimal numbers above the bars; p -values which are not shown in this figure, are complemented in the supplementary file 1. FN1 (fibronectin 1), TIMP1 (Tissue inhibitor of metalloproteinase), bFGF (basic fibroblast growth factor), VEGF A (vascular endothelial growth factor A), VEGF C (vascular endothelial growth factor C). This Figure was reproduced from (1), with permission of PLoS1.

Inflammatory and fibrogenic markers.

One-way ANOVA showed significant alterations of the gene expression of *IL-1 β* ($p = 0.016$; $\eta^2 = 0.564$), *IL-6* ($p = 0.003$; $\eta^2 = 0.670$), *TGF- β 1* ($p = 0.012$; $\eta^2 = 0.587$), *ACTA2* ($p = 0.001$; $\eta^2 = 0.754$) and protein concentration of IL-11 ($p = 0.000$; $\eta^2=0,861$) protein concentration as well as α -SMA ($p = 0.000$; $\eta^2 = 0.798$). Post hoc comparisons revealed a significant increase of *IL-1 β* between the dynamic inflammatory group and the non-inflammatory groups (see Figure 16). *IL-6* was also significantly increased under inflammatory conditions, however vibration had no effect (see Figure 15). Statistical tests showed a significant increase of IL-11 concentration in the supernatant after cytokine exposure, whereas additional vibration led to a significant reduction of the IL-11 concentration (see Figure 16). (1)

TGF- β 1 expression was significantly upregulated by cytokine exposure under static conditions, but was not influenced by vibration (see Figure 16). Similarly, *ACTA2* expression was significantly increased after cytokine treatment alone. The combination of cytokine treatment and vibration however, did not show a significant alteration. (see Figure 15). In contrast, concentration of α -SMA was significantly increased by cytokine treatment but reduced by vibration (see Figure 16). (1)

Neither condition had a significant influence on *COX-2* expression ($p = 0.506$; $\eta^2 = 0.027$). (1)

Phenotypic alterations

Similarly, to the preliminary trials, we could see morphological changes of the nuclei as a consequence of cytokine exposure in both setups. However, additional mechanical stimulation did not visibly affect cell morphology under the light microscope.

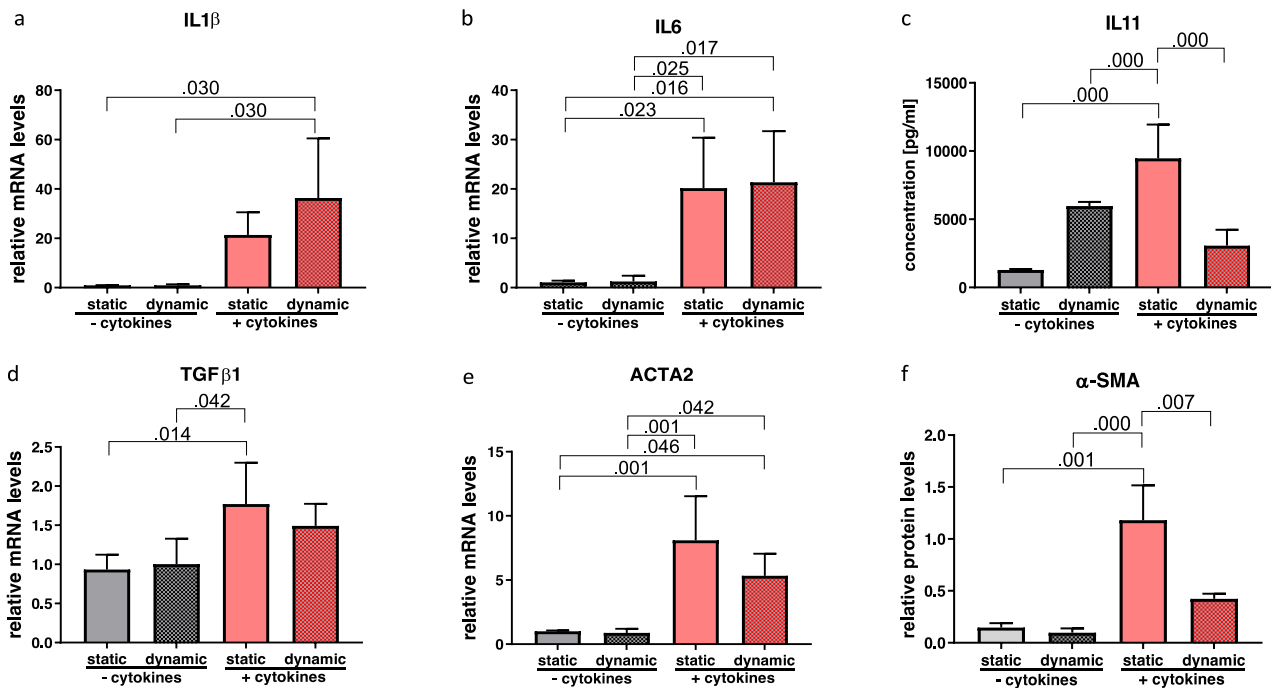


Figure 16: Effect of vibration with/without cytokine exposure on inflammatory and fibrogenic markers. qPCR, Western blot and Luminex were performed in order to analyze mRNA (a, b, d, e) and protein levels (c and f) of inflammatory and fibrogenic markers, respectively. The results of the four independently conducted experiments ($N = 4$) are indicated as mean \pm S.D. A one-way ANOVA, when the data was normally distributed or Kruskal-Wallis test, when the data was non-parametric, were used for statistical analyses. A p -value <0.05 was considered statistically significant. In case of statistical significance, p -values from post-hoc tests are represented as decimal numbers above the bars; p -values which are not shown in this figure, are complemented in the supplementary file 1. IL1 β (interleukin 1 β), IL6, IL11, TGF β 1 (transforming growth factor beta 1), ACTA2 (alpha smooth muscle actin), α -SMA (alpha smooth muscle actin). Figure was reproduced from (1), with permission of PLoS1.

Eight hours of vibration per day

Fibroblast viability

Comparing the different conditions LDH activity did not show any significant differences. ($p = 0.212$). (see figure 17).

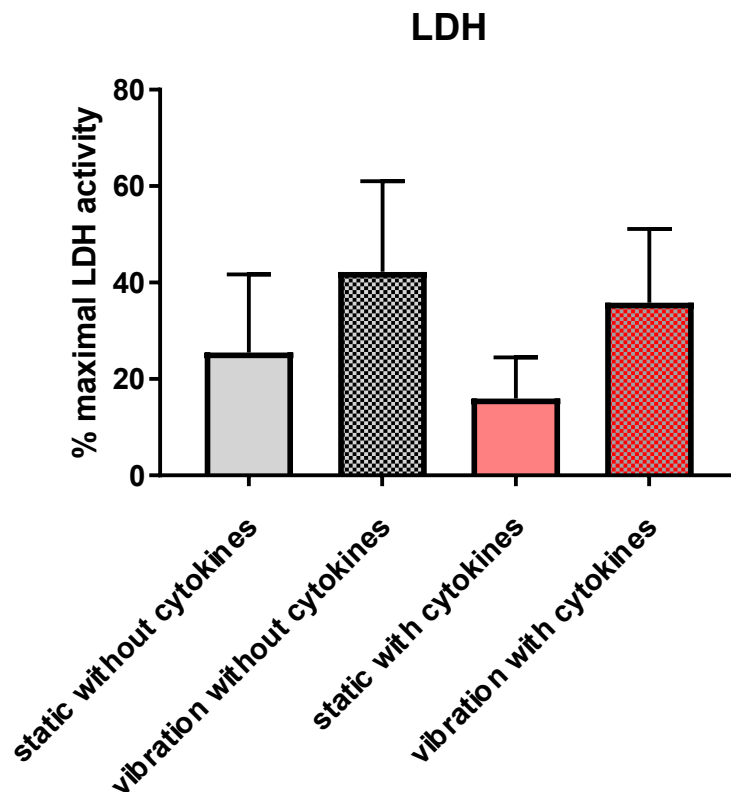


Figure 17: Effect of vibration (8 hours per day) and/or cytokine exposure on cell viability and gene expression. After a total of 73 hours, in detail 72 hours of treatment or control conditions and one hour of rest, supernatants were obtained for LDH activity assay. The LDH activity is shown as percentage of the maximal LDH activity. A p -value <0.05 was considered statistically significant.

Gene expression

ECM-related molecules

Statistical analysis revealed significant alterations of HAS3 ($p = 0.000$; $\eta^2 = 0,766$) COL1A1 ($p = 0.000$; $\eta^2 = 0.892$); COL1A2 ($p = 0.010$; $\eta^2 = 0.601$), COL1A3 ($p = 0.006$; $\eta^2 = 0.530$) FN1 ($p = 0.002$; $\eta^2 = 0.704$) and HYAL2 ($p = 0.000$; $\eta^2 = 0.803$). The Tukey post hoc comparison showed a statistically significant alteration as a consequence of cytokine exposure as well as vibration in COL1A1 and HYAL2. In COL1A2 and FN1 only cytokine exposure caused changes in mRNA expression. In the Man-U-Whitney post hoc comparison a significant alteration of HAS3 due to cytokine exposure was observed. (see figure 18 and 19)

In the eight hours of vibration setup, HAS1 could not be detected in some wells during the third and the fourth run, probably due to contamination (3rd run: dynamic conditions wells 1 and 2; 4th run: static condition well 1 and dynamic condition well 2). In this case statistical analysis was performed with the remaining values, which impedes the interpretation of HAS1 in this setup substantially.

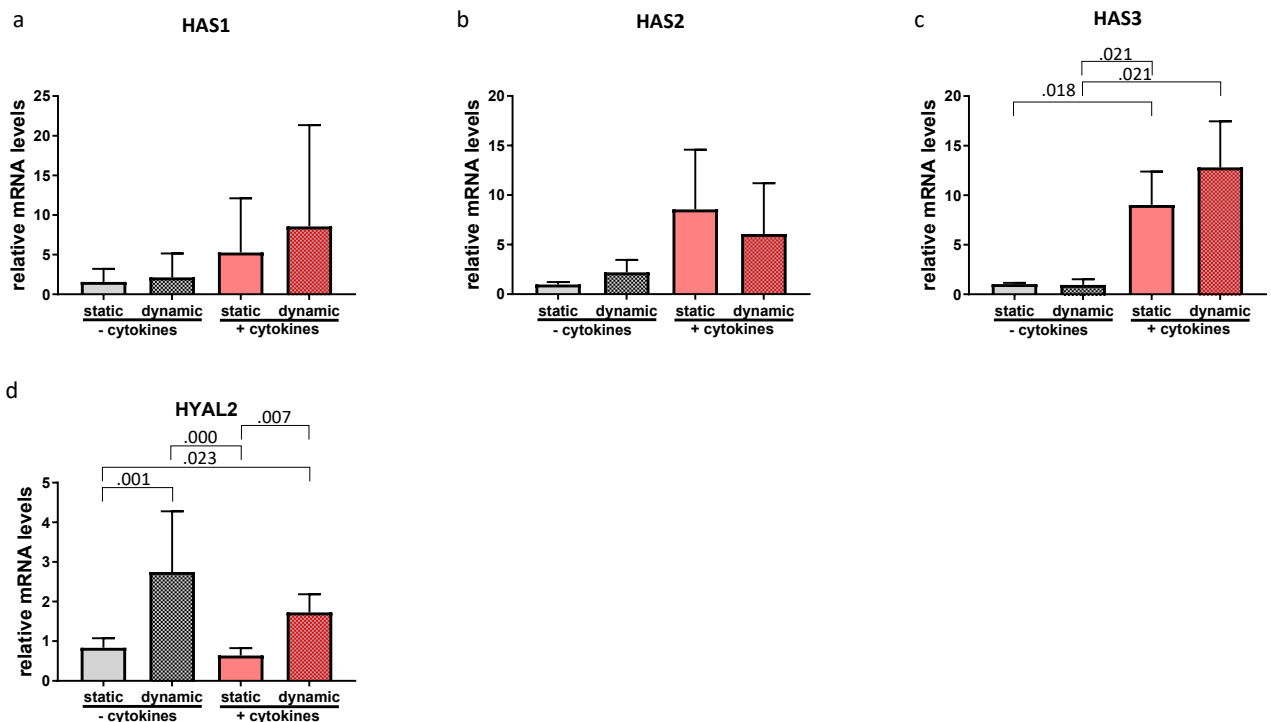


Figure 18: Effect of vibration with/without cytokine exposure on HA metabolism. qPCR was performed in order to analyze of HA-related mRNA levels. The results of the four independently conducted experiments ($N = 4$) are indicated as mean \pm S.D. A one-way ANOVA, when the data was normally distributed or Kruskal-Wallis test, when the data was non-parametric, were used for statistical analyses. A p -value <0.05 was considered statistically significant. In case of statistical significance, p -values from post-hoc tests are represented as decimal numbers above the bars;

p-values which are not shown in this figure, are complemented in the supplementary file 2. HAS1 (hyaluronan synthase 1), HAS2 (hyaluronan synthase 2), HAS3 (hyaluronan synthase 3), HYAL2 (hyaluronidase 2).

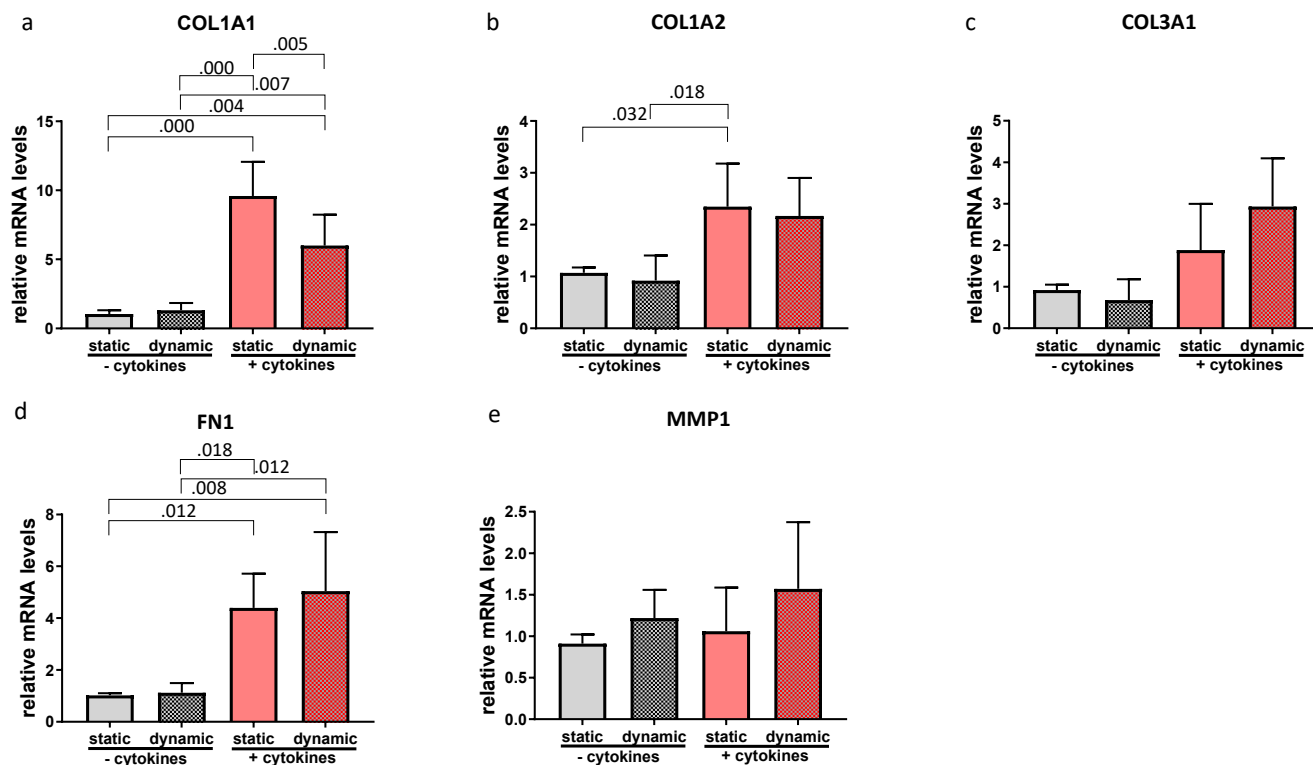


Figure 19: Effect of vibration with/without cytokine exposure on ECM-related molecules. qPCR was performed in order to analyze mRNA levels of ECM-related molecules. The results of the four independently conducted experiments ($N = 4$) are indicated as mean \pm S.D. A one-way ANOVA, when the data was normally distributed or Kruskal-Wallis test, when the data was non-parametric, were used for statistical analyses. A *p*-value < 0.05 was considered statistically significant. In case of statistical significance, *p*-values from post-hoc tests are represented as decimal numbers above the bars; *p*-values which are not shown in this figure, are complemented in the supplementary file 2. COL1A1 (collagen 1 alpha 1), COL1A2 (collagen 1 alpha 2), COL3A1 (collagen 3 alpha 1), FN1 (fibronectin 1), MMP1 (matrix metalloproteinase 1).

Inflammatory and fibrogenic markers.

Of this group of genes *IL-6* ($p = 0.003$; $\eta^2 = 0.668$) expression was significantly altered. Post hoc analysis showed that only proinflammatory/profibrotic stimuli had a significant effect, however additional vibration did not show a significant impact. Neither condition had a significant effect on the expression of *IL-1 β* ($p = 0.159$) and *TGF- β 1* ($p = 0.057$) (see figure 20).

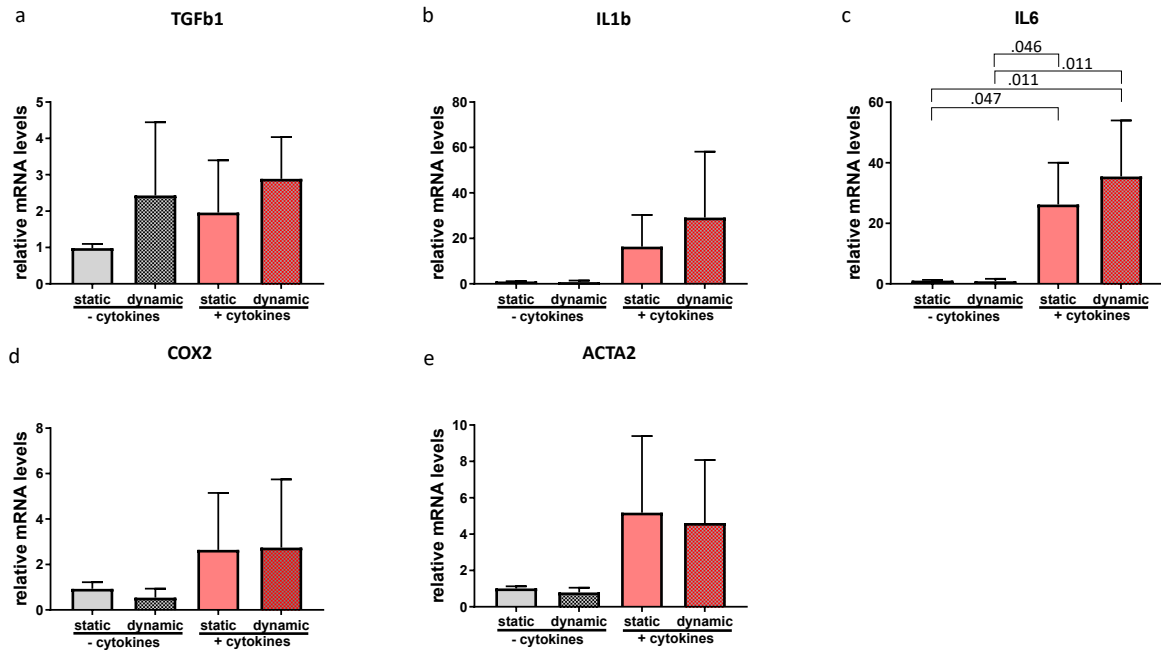


Figure 20: Effect of vibration with/without cytokine exposure on inflammatory and fibrogenic markers. qPCR was performed in order to analyze mRNA levels of ECM-related molecules. The results of the four independently conducted experiments ($N = 4$) are indicated as mean \pm S.D. A one-way ANOVA, when the data was normally distributed or Kruskal-Wallis test, when the data was non-parametric, were used for statistical analyses. A p -value < 0.05 was considered statistically significant. In case of statistical significance, p -values from post-hoc tests are represented as decimal numbers above the bars; p -values which are not shown in this figure, are complemented in the supplementary file 2. TGFb1 (transforming growth factor beta 1), IL1b (interleukin 1 β), IL6, ACTA2 (alpha smooth muscle actin).

Discussion

The present thesis elaborates the effect of mechanical stimulation on VFF under inflammatory conditions.

The early phase of wound healing comes with an inflammatory reaction, thereby promoting the healing of the wound, the recruitment of inflammatory cells as well as preventing an infection in the area of the injury. (2) Albeit a physiological process, it comes with the risk of VF tissue remodelling, thereby impairing the viscoelastic characteristics of the LP or, even more severe, leading to persistent dysphonia owing to VF scarring. (137) Therefore, the management of the wound healing phase after an injury is of utmost importance. Gaining a deeper knowledge on the biological consequences of vibration on hVFF under an inflammatory condition provides a first step towards this aim and relates directly to the clinically very relevant question of whether and for how long voice rest following phonotrauma or phonosurgical interventions should be advised. (1)

In vivo studies

The advantage of voice rest after a trauma stays highly debated in literature, since a significant number of factors influence the healing process, leading to indecisive data. (6)(138) The group around Kaneko et al. studied the role of voice rest on the basis of stroboscopic/laryngoscopic parameters. Therefore patients, who underwent phonosurgery, were put into two groups. The participants were assigned to voice rest for three or seven days, followed by voice therapy. Follow-up check-ups were performed at 1,3 and 6 months after the intervention. Objective parameters (jitter, shimmer and normalized mucosal wave amplitude) and subjective parameters (VHI-10 and GRBAS) significantly improved in the 3-day group, however not at all time points and not consistently. The authors came to the conclusion that an early postoperative phonation may have a positive effect on functional recovery and wound healing. (5) To date, no studies exist which investigate the molecular consequences after voice load or voice rest after following phonosurgery. On a molecular level in humans, the impacts of vocal overload have so far only been investigated by a small number of studies. Verdolini et al. took three vocally healthy participants, undergoing vocal loading succeeding a period of voice rest, and analyzed their laryngeal secretions. A decrease in inflammatory markers in participants following resonant voice training when compared to those respecting voice rest was described. The study protocol was however only completed by a single patient from each group, since the secretions from the larynx were gained from topically anesthetized VF in a highly complex method using cotton swabs. (1)(3)

On the contrary, the consequences of a VF trauma in animals, for the most part rats, are highly investigated. Altered expressions of many ECM-related genes (COL, HA) and some pro-fibrotic and inflammatory factors (*IL-1 β* and *TGF- β 1*) are known. (48)(139) Rousseau et al. studied wound healing processes *in vivo* in a rabbit model following an acute phonotrauma, with the focus on the VF epithelium. *TGF- β 1* and *IL-1 β* were again significantly upregulated after two hours of phonation. (140) Therefore, the increase of inflammation- and ECM-related proteins and genes in the present experiment such as *TGF- β 1*, *IL-1 β* , and *IL-6* as well as HA and COL, are in line with the above mentioned results and underline the appropriability of our model. (1)

***In vitro* studies**

To our knowledge, the effect of mechanical stimuli on VFF following an inflammatory condition has to date only been dealt with in one publication by Branski et al. They exposed VFF of lagomorpha to periodic tensile stress with or without adding *IL-1 β* and reported a reduction of the expression of MMP1, COX-2 and iNOS. The group came to the conclusion, that dynamic stimulation at adequate amplitudes could have an anti-inflammatory impact, thereby being in line with our results. In contrast to our bioreactor, which is able to cover the entire spectrum of frequencies of the human voice, their device is only able to apply a limited range. (11) (141) Another problem of *in vitro* trials, is that the cells are embedded in an aqueous environment, whereas *in vivo* they are surrounded by a plethora of MM. MM are defined as molecules with a molecular weight between 50-500 kDa. The spatial expansion of these MM results in the so-called excluded volume effect, meaning that the addition of such molecules reduces the available space for other molecules. This has a significant impact on physicochemical properties of biomolecules both intra- and extracellularly such as on the velocity of a chemical reaction or on diffusion. Moreover, experiments have shown that proteins are more stable under crowded conditions due to steric repulsion. (1)(99)(142)(143)(144) (145)

Crowded environments also influence the COL deposition and should be considered equally important as setting the optimal pH in *in vitro* fibrogenesis models. Many MM, either synthetic or natural, can be used to mimic MMC. (142)(145) In an *in vitro* fibrosis model using VFF and two synthetic MM, Fc 70 and Fc 400, Graupp et al. showed that there is a significant increase in ECM components, such as COL and HA as well as α -SMA, in contrast when compared to an uncrowded control. (98) Hence, the trials of the present thesis were carried out under crowded conditions. For this reason, comparing these results with those of other studies, which were not considering MMC, is not appropriate.

As already described in the methods section, cells were incubated in a serum free medium for one day. Even though starvation is known to influence cell susceptibility to inflammatory stimuli, it is a commonly used method, also in VF fibrosis models, to make cell populations more homogenous and consequently results more reproduceable. (1)(58)(146)(147)

Effects of vibration and cytokine-stimuli on VFF

Fibroblasts are in general diverse, a special characteristic of these cells. Depending on their location, they can complete a plethora of functions. (148) Vibration alters the ECM production of fibroblasts. This idea is supported by the studies stated above. VFF, as the predominant cell type in the LP, they are majorly responsible for the ECM composition. Moreover, in a recent publication it was stated that these cells contain high concentrations of the high-mobility group box (HMGB) 1, which is an essential DAMP. (149) Consequently, VFF are of utmost importance for a smooth phonation and play a pivotal role in wound healing. (1)

This study was preceded by pre-trials, in order to investigate the impact of IL-1 β and TGF- β 1, in combination as well as separately and at different points in time, on the expression of other ECM-related proteins and cytokines. (1)(48)(139)(141)(150)(151)(152)(153)

As a result of these preceding trials, a combination of TGF- β 1 and IL-1 β was chosen for the present study, as the role of these cytokines is known to be of high importance in tissue fibrosis and acute inflammatory processes. Their concentration were chosen on the basis of already published in vitro studies on inflammation.(1)

Besides the above-mentioned molecular changes due to cytokine treatment, also some morphological changes in the VFF were detected. It is known that some cells undergo phenotypic alterations in the area of injury. IL-1 β as well as TGF are postulated to have an impact on cell morphology.(154)(155)(156)(157) Also alterations in the nuclear structure, dependent on cellular activity and environment, are described in the literature.(158) In the present experiments as well as the preliminary trials, changes in the nuclear morphology were observed as a consequence of cytokine exposure. Additional mechanical stimulation did not cause further phenotypic alterations visible under the light-microscope. However, further studies with, for example, immunofluorescence staining may give us a more accurate image and enable a quantification of morphological alterations.

In the eight hour of mechanical stimulation setup, cytokine exposure significantly changed the *IL-6* expression. *IL-1 β* was also notably upregulated after cytokine exposure, but due to a high variance, this effect was not significant. However, *TGF- β 1* expression in the eight-hour setup did not show a trend as consequence of the proinflammatory stimulus. We traced this back to the fact that there might have been deviations in cell density between the different setups.

Previous publications have shown that TGF- β signaling as well as gene expression depend on cell density.(159)(160)(161) The variations in cell density in turn might be caused by the difference in passage number.

Moreover, we could observe a significant downregulation of COL1A1 and an upregulation of HYAL-2. Both genes are known to be mechanoresponsive.(162)(34) While a downregulation of COL1A1 might have beneficial effects on wound healing, the upregulation of HYAL-2 might be disadvantageous. Therefore, we concluded that eight hours of vibration per day might be a too intensive mechanical strain where favourable and adverse effects cancel out each other.

In the four hours vibration setup, vibration did not show a deteriorating impact on COL and HA, two very important VF ECM components. The concentration of HA in the supernatants and the gene expression of *HAS1* as well as *HAS3* were significantly upregulated following a pro-fibrotic and inflammatory stimulus. No diminishing effect of vibration on HA levels was observed.

This is a notable fact since this GAG has essential antifibrotic properties. In contrast to these results, previously published studies reported about a change in the HA metabolism after a mechanical stimulus. (10)(11) The reason for this disparity might be owed to the variations of the stimulatory duration and their patterns, since it is known that VF react differently on various types of mechanical stimulation. (163) This fact could also explain why there were differences in the results of the two groups differing in the duration of mechanical stimulation. (1)

Additionally, an increase in the expression of *COL1A1*, *COL1A2*, *COL3A1* as well as the concentration of the extracellular COL I following inflammatory stimulations was demonstrated. These results are in line with previously referenced animal studies. (1)(48)(139)

In accordance with the results of Lenselink et al., a significant upregulation under cytokine exposure of the expression of the FN1 gene as well as its encoded protein could be shown, while vibration had no impact. (1)(164)

Other cytokines, which are typically found in rat models of early VF traumata, such as COX-2, did not show any changes in the expression. (48)(139) An explanation for this phenomenon could be, that the present in vitro study did not take other cell types, apart from hVFF, into consideration (e.g macrophages). (1)

The expression of α -SMA was in our in vitro trials significantly decreased on a protein level in the four-hours of vibration per day group in contrast to the static one. The expression of *ACTA2* decreased as well, however not statistically significant. During an inflammation, it is known that VFF transform into myofibroblast. This process is accompanied by an α -SMA increase, a myofibroblasts marker. (11)(20)(77) These cells seem to be in charge of wound contraction and augmented COL deposition in a scar, thereby having a deteriorating effect for VF oscillation.

(20) The results presented in this thesis showed, that the conversion into undesired myofibroblasts was reduced, thereby further underlining the beneficial effect vibration has on wound healing.

Simultaneously, a reduction in IL-11 in supernatants under vibration could be observed, reaching statistical significance. IL-11 seems to act as an important factor in the down-streaming pathway of TGF- β 1, representing a substantial part of fibrogenesis, one example being the fibrosis of cardiovascular tissue. Moreover, it assists the differentiation of pulmonary fibroblasts to ACTA-2 positive myofibroblasts. It has also been postulated, that IL-11 plays a pivotal role in the development of multiple sclerosis. (165) As a consequence, and in line with other publications, IL-11 could be seen as a potential therapeutic approach to avoid tissue fibrosis. (1)(124)(125)(126)(166)(167)

MAPK/Erk

One major pathway which is known to be involved in mechanotransductive processes and has simultaneously an impact on inflammation is the extracellular signal-regulated kinase (Erk) signaling pathway.

The Erk belongs, besides c-Jun NH₂- terminal kinase (JNK), p38-mitogen-activated protein kinases (p38 MAPK), to the MAPK. They are serine-threonine protein kinases and regulate different cell activities such as differentiation, inflammation or apoptosis. All MAPK are organized in a multi-enzyme hierarchical construct, where an enzyme activates the down-streamed enzyme until finally the target protein, for example a transcription factor is phosphorylated. There are many ways how the pathways can be activated. One possibility is via mechanical stimuli. Whitney et al. investigated the mechanotransducing pathway in chondrocytes. Human chondrocytes were exposed to ultrasound for three minutes and compared to static controls. Integrin receptors perceive the mechanical stimulus and cause an autophosphorylation of the focal adhesion kinase (FAK). This results in the binding of kinases belonging to the Src-family which again is activated by phosphorylation. Together with the p130Cas docking protein they form the FAK-Src-p130Cas complex. This complex causes an activation of the adaptor protein CrkII. How CrkII influences Erk was not directly explored in the mentioned study. However, other studies indicate that CrkII acts on guanine nucleotide exchange factors (e.g. C3G, DOCK 180 and SOS) which transmit the signal via Ras and Raf to the Mitogen-activated protein/extracellular signal-regulated kinase (MEK) and finally to Erk. Finally, Erk influences various processes such as cell proliferation and differentiation as well as gene regulation (see Figure 21). (33)(34)(168)

Wong et al. examined the effects of mechanical forces on skin fibrosis. They demonstrated that FAK is activated after skin injury and its effect is potentiated by mechanical stress. FAK induces Erk which leads to the secretion of monocyte chemoattractant protein-1 (MCP-1), which is involved in human fibrotic disorders. The authors concluded that mechanical loads have an impact on skin fibrosis. (169)

It is known that both proteins, which were significantly downregulated due to the mechanical stimulation in our study, namely IL-11 and α -SMA, are involved in the Erk signaling pathway. (1)(166)(170)

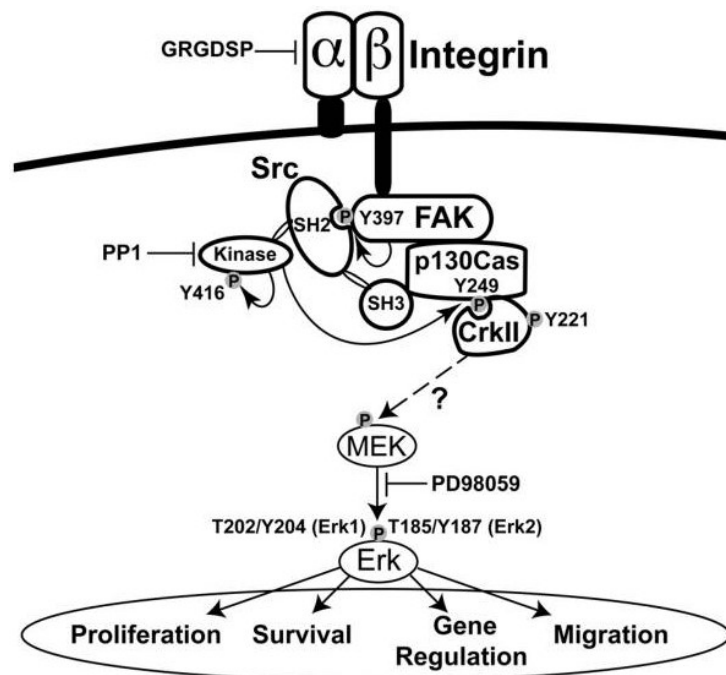


Figure 21: Illustration of possible MAPK/Erk pathway. This figure was reproduced from (32) with permission of Elsevier. This figure was published in *Ultrasound Med Biol.* 38(10), Whitney, Lamb, Louw, Subramanian, *Integrin-mediated mechanotransduction pathway of low-intensity continuous ultrasound in human chondrocytes*, pages 1734-1743, Copyright Elsevier (*Ultrasound Med Biol.*) (2012).

Limitations

The inductive reasoning of these results on the *in vivo* situation is subject to certain limitations. Firstly, since the VFF were seeded onto a flat membrane, the presented monolayer cell culture reflects a two-dimensional situation. The VF, however, are three-dimensional organs which are exposed to different forces during phonation, including tensile, inertia, aerodynamic, contractile, shear and impact stresses. At around 1MPa, tensile stress is by far the greatest force that is applied on the VF mucosa during phonation. It acts along the longitudinal axis. (40)(171)

The bioreactor used in these trials can mimic tensile and shear stresses, whereas other forces are neglected. (11) Although the present bioreactor can verifiably initiate mechanotransductive processes by exposing VFF to a wide spectrum of frequencies, it is evident that the forces acting on cells during phonation is not fully reproducible with this device because of their complexity. As a consequence, despite these promising results, further (clinical) studies are warranted in order to determine which postoperative voice exercises are most suitable for the avoidance of scarring. (1)

Moreover, in the presented trials, only VFF were used, while reality many different cell types are involved during inflammatory processes. In particular the interplay between inflammatory cells such as macrophages or fibrocytes and VFF is of major interest. (1) (172) (173)

Lastly, immortalized cells were used. A major problem in laryngology is the poor availability of resident cells. Each attempt to gain these cells might end up in a scar. Cell immortality can circumvent this issue. Various techniques have been developed to gain indefinite cell proliferation such as by mutating the cell cycle checkpoints p53 and pRb genes or introducing telomerase reverse transcriptase (TERT). (1)(174)(175)

The latter bases on the fact that the more cells divide, the shorter the ends of their chromosomes become. Therefore, the ends contain highly repetitive DNA sequences (TTAGGG) for the stabilization of the chromosomes. Shortening of these sequences is associated with cellular senescence. To prevent this aging process in hVFF, Chen and Thibeault established a method based on TERT. They harvested healthy hVFF from a male and a female donor within four hours post mortem. They achieved immortalization by transducing human TERT genes into these hVFF, which in normal somatic cells is usually absent. The immortalized cells grew without any signs of senescence. (174)(175)(176)(177) These cells were also used in the present publication. The advantages of such immortalized cells are their accessibility, the genetic homogeneity providing more consistent results and quick and continuous growth which enables the extraction of large amounts of nucleic acids and proteins. But, because of the manipulation of their genome, immortalized cells may respond differently by contrast with *in vivo* tissue or near primary VFF. (1)(177)

Conclusion

The aim of the present thesis was to investigate the effect of vibration on hVFF in a pro-fibrotic as well as inflammatory setting for the first time. The conducted trials showed a significant reduction of fibrosis-linked proteins α -SMA and IL-11 after four hours of vibration. Eight hours of vibration in turn showed significant alterations on the gene expression of *COL1A1* and *HYAL2*. The advantageous effect of a *COL1A1* downregulation as a consequence of vibration

however might be canceled out by an unfavourable upregulation of *HYAL2*. Regardless of the inherent limitations an in vitro study entails, our results imply, that, to a certain extent VF vibration following a surgical intervention could positively influence wound healing. Further studies on this topic are highly warranted and should try to approximate in vivo inflammatory conditions. The co-cultivation of VFF with other cell types as well as the development of adequate three-dimensional models would be of highest interest to this field of research. (1)

References

1. Hortobagyi D, Grossmann T, Tschernitz M, Grill M, Kirsch A, Gerstenberger C, et al. In vitro mechanical vibration down-regulates pro-inflammatory and pro-fibrotic signaling in human vocal fold fibroblasts. *PLoS One*. 2020;15(11):e0241901.
2. Ling C, Yamashita M, Waselchuk EA, Raasch JL, Bless DM, Welham NV. Alteration in cellular morphology, density and distribution in rat vocal fold mucosa following injury. *Wound Repair Regen*. 2010 Feb;18(1):89–97.
3. Verdolini Abbott K, Li NYK, Branski RC, Rosen CA, Grillo E, Steinhauer K, et al. Vocal Exercise May Attenuate Acute Vocal Fold Inflammation. *Journal of Voice*. 2012 Nov;26(6):814.e1-814.e13.
4. Chu S-H, Kim H-T, Kim M-S, Lee I-J, Park H-J. Influence of Phonation on Basement Membrane Zone Recovery after Phonomicrosurgery: A Canine Model. *Ann Otol Rhinol Laryngol*. 2000 Jul;109(7):658–66.
5. Kaneko M, Shiromoto O, Fujiu-Kurachi M, Kishimoto Y, Tateya I, Hirano S. Optimal Duration for Voice Rest After Vocal Fold Surgery: Randomized Controlled Clinical Study. *Journal of Voice*. 2017 Jan;31(1):97–103.
6. Kaneko M, Hirano S. Voice rest after laryngeal surgery: what’s the evidence? *Curr Opin Otolaryngol Head Neck Surg*. 2017 Dec;25(6):459–63.
7. Ishikawa K, Thibeault S. Voice Rest Versus Exercise: A Review of the Literature. *Journal of Voice*. 2010 Jul;24(4):379–87.
8. Guerra ML, Singh PJ, Taylor NF. Early mobilization of patients who have had a hip or knee joint replacement reduces length of stay in hospital: a systematic review. *Clin Rehabil*. 2015 Sep;29(9):844–54.
9. Yakkanti RR, Miller AJ, Smith LS, Feher AW, Mont MA, Malkani AL. Impact of early mobilization on length of stay after primary total knee arthroplasty. *Ann Transl Med*. 2019 Feb;7(4):69–69.
10. Titze IR, Hitchcock RW, Broadhead K, Webb K, Li W, Gray SD, et al. Design and validation of a bioreactor for engineering vocal fold tissues under combined tensile and vibrational stresses. *Journal of Biomechanics*. 2004 Oct;37(10):1521–9.
11. Kirsch A, Hortobagyi D, Stachl T, Karbiener M, Grossmann T, Gerstenberger C, et al. Development and validation of a novel phonomimetic bioreactor. *PLoS ONE*. 2019;14(3):e0213788.

12. Minoru Hirano. Phonosurgery: basic and clinical investigations. *Otologia*21(Suppl 1): 239-442. 1975.
13. Gugatschka M, Grossmann T, Hortobagyi D. Molekulare Laryngologie: Ein neues Kapitel im Verständnis laryngealer Erkrankungen. *HNO* [Internet]. 2021 Apr 6 [cited 2021 Jul 4]; Available from: <http://link.springer.com/10.1007/s00106-021-01016-1>
14. Gray SD, Alipour F, Titze IR, Hammond TH. Biomechanical and Histologic Observations of Vocal Fold Fibrous Proteins. *Ann Otol Rhinol Laryngol*. 2000 Jan;109(1):77–85.
15. Gray SD, Titze IR, Chan R, Hammond TH. Vocal fold proteoglycans and their influence on biomechanics. *Laryngoscope*. 1999 Jun;109(6):845–54.
16. Catten M, Gray SD, Hammond TH, Zhou R, Hammond E. Analysis of cellular location and concentration in vocal fold lamina propria. *Otolaryngol Head Neck Surg*. 1998 May;118(5):663–7.
17. Levendoski EE, Leydon C, Thibeault SL. Vocal Fold Epithelial Barrier in Health and Injury: A Research Review. *J Speech Lang Hear Res*. 2014 Oct;57(5):1679–91.
18. Gray SD, Pignatari SS, Harding P. Morphologic ultrastructure of anchoring fibers in normal vocal fold basement membrane zone. *J Voice*. 1994 Mar;8(1):48–52.
19. Duscher D, Maan ZN, Wong VW, Rennert RC, Januszyk M, Rodrigues M, et al. Mechanotransduction and fibrosis. *Journal of Biomechanics*. 2014 Jun;47(9):1997–2005.
20. Jetté ME, Hayer SD, Thibeault SL. Characterization of human vocal fold fibroblasts derived from chronic scar. *The Laryngoscope*. 2013 Mar;123(3):738–45.
21. Sato K, Umeno H, Ono T, Nakashima T. Histopathologic study of human vocal fold mucosa unphonated over a decade. *Acta Oto-Laryngologica*. 2011 Dec;131(12):1319–25.
22. Fishman JM, Long J, Gugatschka M, De Coppi P, Hirano S, Hertegard S, et al. Stem cell approaches for vocal fold regeneration: Stem Cell Approaches Vocal Regeneration. *The Laryngoscope*. 2016 Aug;126(8):1865–70.
23. Lass NJ. *Speech and language: advances in basic research and practice....* 7 7. 1982.
24. Thomas LB, Harrison AL, Stemple JC. Aging Thyroarytenoid and Limb Skeletal Muscle: Lessons in Contrast. *Journal of Voice*. 2008 Jul;22(4):430–50.
25. von LEDEN H. The Mechanism of Phonation: A Search for a Rational Theory of Voice Production. *Archives of Otolaryngology - Head and Neck Surgery*. 1961 Dec 1;74(6):660–76.
26. van den Berg J. Myoelastic-Aerodynamic Theory of Voice Production. *Journal of Speech and Hearing Research*. 1958 Sep;1(3):227–44.

27. Titze IR. Comments on the Myoelastic - Aerodynamic Theory of Phonation. *J Speech Lang Hear Res.* 1980 Sep;23(3):495–510.
28. Noordzij JP, Ossoff RH. Anatomy and physiology of the larynx. *Otolaryngol Clin North Am.* 2006 Feb;39(1):1–10.
29. Vahabzadeh-Hagh AM, Zhang Z, Chhetri DK. Hirano's cover-body model and its unique laryngeal postures revisited. *The Laryngoscope.* 2018 Jun;128(6):1412–8.
30. Harrington J, Cassidy S. The Acoustic Theory of Speech Production. In: *Techniques in Speech Acoustics* [Internet]. Dordrecht: Springer Netherlands; 1999 [cited 2021 Jul 4]. p. 29–56. (Ide N, Véronis J, editors. *Text, Speech and Language Technology*; vol. 8). Available from: http://link.springer.com/10.1007/978-94-011-4657-9_3
31. Titze IR. Nonlinear source-filter coupling in phonation: Theory. *The Journal of the Acoustical Society of America.* 2008 May;123(5):2733–49.
32. Tsata V, Beis D. In Full Force. *Mechanotransduction and Morphogenesis during Homeostasis and Tissue Regeneration. JCDD.* 2020 Oct 1;7(4):40.
33. Whitney NP, Lamb AC, Louw TM, Subramanian A. Integrin-Mediated Mechanotransduction Pathway of Low-Intensity Continuous Ultrasound in Human Chondrocytes. *Ultrasound in Medicine & Biology.* 2012 Oct;38(10):1734–43.
34. Wang JH-C, Thampatty BP, Lin J-S, Im H-J. Mechanoregulation of gene expression in fibroblasts. *Gene.* 2007 Apr;391(1–2):1–15.
35. Jaalouk DE, Lammerding J. Mechanotransduction gone awry. *Nat Rev Mol Cell Biol.* 2009 Jan;10(1):63–73.
36. Barry SP, Davidson SM, Townsend PA. Molecular regulation of cardiac hypertrophy. *Int J Biochem Cell Biol.* 2008;40(10):2023–39.
37. Zhou S-B, Wang J, Chiang C-A, Sheng L-L, Li Q-F. Mechanical stretch upregulates SDF-1 α in skin tissue and induces migration of circulating bone marrow-derived stem cells into the expanded skin. *Stem Cells.* 2013 Dec;31(12):2703–13.
38. Chin MS, Lancerotto L, Helm DL, Dastouri P, Prsa MJ, Ottensmeyer M, et al. Analysis of neuropeptides in stretched skin. *Plast Reconstr Surg.* 2009 Jul;124(1):102–13.
39. Bartlett RS, Gaston JD, Ye S, Kendzierski C, Thibeault SL. Mechanotransduction of vocal fold fibroblasts and mesenchymal stromal cells in the context of the vocal fold mechano. *Journal of Biomechanics.* 2019 Jan;83:227–34.
40. Li N. Current Understanding and Future Directions for Vocal Fold Mechanobiology. *J*

- Cytol Mol Biol [Internet]. 2013 [cited 2020 Feb 15]; Available from: <http://www.avensonline.org/fulltextarticles/JCMB-2325-4653-01-0001.html>
41. Huber-Lang M, Lambris JD, Ward PA. Innate immune responses to trauma. *Nat Immunol*. 2018 Apr;19(4):327–41.
 42. Wang P-H, Huang B-S, Horng H-C, Yeh C-C, Chen Y-J. Wound healing. *J Chin Med Assoc*. 2018 Feb;81(2):94–101.
 43. Barrientos S, Stojadinovic O, Golinko MS, Brem H, Tomic-Canic M. Growth factors and cytokines in wound healing. *Wound Repair Regen*. 2008 Oct;16(5):585–601.
 44. Roh JS, Sohn DH. Damage-Associated Molecular Patterns in Inflammatory Diseases. *Immune Netw*. 2018;18(4):e27.
 45. Sorg H, Tilkorn DJ, Hager S, Hauser J, Mirastschijski U. Skin Wound Healing: An Update on the Current Knowledge and Concepts. *Eur Surg Res*. 2017;58(1–2):81–94.
 46. Werner S, Grose R. Regulation of wound healing by growth factors and cytokines. *Physiol Rev*. 2003 Jul;83(3):835–70.
 47. Hackam DJ, Ford HR. Cellular, biochemical, and clinical aspects of wound healing. *Surg Infect (Larchmt)*. 2002;3 Suppl 1:S23-35.
 48. Lim X, Tateya I, Tateya T, Muñoz-Del-Río A, Bless DM. Immediate Inflammatory Response and Scar Formation in Wounded Vocal Folds. *Ann Otol Rhinol Laryngol*. 2006 Dec;115(12):921–9.
 49. Berse, Hunt, Diegel, Morganelli, Yeo, Brown, et al. Hypoxia augments cytokine (transforming growth factor-beta (TGF-beta) and IL-1)-induced vascular endothelial growth factor secretion by human synovial fibroblasts. *Clin Exp Immunol*. 1999 Jan;115(1):176–82.
 50. Wallace HA, Basehore BM, Zito PM. Wound Healing Phases. In: *StatPearls* [Internet]. Treasure Island (FL): StatPearls Publishing; 2021 [cited 2021 Jul 4]. Available from: <http://www.ncbi.nlm.nih.gov/books/NBK470443/>
 51. Goligorsky MS. Restitutio ad integrum: a dream or a real possibility? *Nephrol Dial Transplant*. 2013 Nov;28(11):2682–7.
 52. Leung A, Crombleholme TM, Keswani SG. Fetal wound healing: implications for minimal scar formation. *Curr Opin Pediatr*. 2012 Jun;24(3):371–8.
 53. Eming SA, Wynn TA, Martin P. Inflammation and metabolism in tissue repair and regeneration. *Science*. 2017 Jun 9;356(6342):1026–30.

54. Thibeault SL, Gray SD, Bless DM, Chan RW, Ford CN. Histologic and rheologic characterization of vocal fold scarring. *J Voice*. 2002 Mar;16(1):96–104.
55. Friedrich G, Gugatschka M. [Vocal fold scars: pathogenesis, diagnosis, therapy]. *HNO*. 2013 Feb;61(2):94, 96–101.
56. Friedrich G, Dikkers FG, Arens C, Remacle M, Hess M, Giovanni A, et al. Vocal fold scars: current concepts and future directions. Consensus report of the Phonosurgery Committee of the European Laryngological Society. *Eur Arch Otorhinolaryngol*. 2013 Sep;270(9):2491–507.
57. Hirschi SD, Gray SD, Thibeault SL. Fibronectin: an interesting vocal fold protein. *J Voice*. 2002 Sep;16(3):310–6.
58. Kishimoto Y, Kishimoto AO, Ye S, Kendzioriski C, Welham NV. Modeling fibrosis using fibroblasts isolated from scarred rat vocal folds. *Lab Invest*. 2016 Jul;96(7):807–16.
59. Chao S, Song SA. Videostroboscopy. In: StatPearls [Internet]. Treasure Island (FL): StatPearls Publishing; 2021 [cited 2021 Jul 4]. Available from: <http://www.ncbi.nlm.nih.gov/books/NBK567774/>
60. Costello D. Acoustic Assessment. *Adv Otorhinolaryngol*. 2020;85:55–8.
61. Branski RC, Cukier-Blaj S, Pusic A, Cano SJ, Klassen A, Mener D, et al. Measuring Quality of Life in Dysphonic Patients: A Systematic Review of Content Development in Patient-Reported Outcomes Measures. *Journal of Voice*. 2010 Mar;24(2):193–8.
62. Schneider B, Denk D-M, Bigenzahn W. Acoustic assessment of the voice quality before and after medialization thyroplasty using the titanium vocal fold medialization implant (tvfmi)★. *Otolaryngology - Head and Neck Surgery*. 2003 Jun;128(6):815–22.
63. Olson DE, Goding GS, Michael DD. Acoustic and perceptual evaluation of laryngeal reinnervation by ansa cervicalis transfer. *Laryngoscope*. 1998 Dec;108(12):1767–72.
64. Francis DO, McKiever ME, Garrett CG, Jacobson B, Penson DF. Assessment of Patient Experience With Unilateral Vocal Fold Immobility: A Preliminary Study. *Journal of Voice*. 2014 Sep;28(5):636–43.
65. Schneider-Stickler B, Gaechter J, Bigenzahn W. Long-term results after external vocal fold medialization thyroplasty with titanium vocal fold medialization implant (TVFMI). *European Archives of Oto-Rhino-Laryngology*. 2013 May;270(5):1689–94.
66. Schneider B, Denk D-M, Bigenzahn W. Functional results after external vocal fold medialization thyroplasty with the titanium vocal fold medialization implant. *Laryngoscope*. 2003

Apr;113(4):628–34.

67. Friedrich G. Titanium vocal fold medializing implant: introducing a novel implant system for external vocal fold medialization. *Ann Otol Rhinol Laryngol*. 1999 Jan;108(1):79–86.
68. Okui A, Konomi U, Kanazawa T, Komazawa D, Nakamura K, Matsushima K, et al. Therapeutic Efficacy of Basic Fibroblast Growth Factor in Patients With Vocal Fold Atrophy. *The Laryngoscope*. 2020 Dec;130(12):2847–52.
69. Kumai Y. Pathophysiology of Fibrosis in the Vocal Fold: Current Research, Future Treatment Strategies, and Obstacles to Restoring Vocal Fold Pliability. *IJMS*. 2019 May 24;20(10):2551.
70. Ohno T, Hirano S, Kanemaru S, Yamashita M, Umeda H, Suehiro A, et al. Drug delivery system of hepatocyte growth factor for the treatment of vocal fold scarring in a canine model. *Ann Otol Rhinol Laryngol*. 2007 Oct;116(10):762–9.
71. Long JL. Tissue engineering for treatment of vocal fold scar. *Curr Opin Otolaryngol Head Neck Surg*. 2010 Dec;18(6):521–5.
72. Mattei A, Magalon J, Velier M, Dignat-George F, Giovanni A, Sabatier F. Commentary about mesenchymal stem cells and scarred vocal folds. *Stem Cell Res Ther*. 2020 May 7;11(1):173.
73. Li L, Stiadle JM, Lau HK, Zerdoum AB, Jia X, Thibeault SL, et al. Tissue engineering-based therapeutic strategies for vocal fold repair and regeneration. *Biomaterials*. 2016;108:91–110.
74. Ling C, Li Q, Brown ME, Kishimoto Y, Toya Y, Devine EE, et al. Bioengineered vocal fold mucosa for voice restoration. *Sci Transl Med*. 2015 Nov 18;7(314):314ra187.
75. Maeder ML, Gersbach CA. Genome-editing Technologies for Gene and Cell Therapy. *Mol Ther*. 2016 Mar;24(3):430–46.
76. Nikam RR, Gore KR. Journey of siRNA: Clinical Developments and Targeted Delivery. *Nucleic Acid Therapeutics*. 2018 Aug;28(4):209–24.
77. Kishimoto Y, Yamashita M, Wei A, Toya Y, Ye S, Kendzierski C, et al. Reversal of Vocal Fold Mucosal Fibrosis Using siRNA against the Collagen-Specific Chaperone Serpinh1. *Mol Ther Nucleic Acids*. 2019 Jun 7;16:616–25.
78. White A. Management of benign vocal fold lesions: current perspectives on the role for voice therapy. *Current Opinion in Otolaryngology & Head and Neck Surgery*. 2019 Jun;27(3):185–90.

79. Ogawa M, Inohara H. Is voice therapy effective for the treatment of dysphonic patients with benign vocal fold lesions? *Auris Nasus Larynx*. 2018 Aug;45(4):661–6.
80. Tang SS, Thibeault SL. Timing of Voice Therapy: A Primary Investigation of Voice Outcomes for Surgical Benign Vocal Fold Lesion Patients. *Journal of Voice*. 2017 Jan;31(1):129.e1-129.e7.
81. Cheuy VA, Foran JRH, Paxton RJ, Bade MJ, Zeni JA, Stevens-Lapsley JE. Arthrofibrosis Associated With Total Knee Arthroplasty. *The Journal of Arthroplasty*. 2017 Aug;32(8):2604–11.
82. Whitling S, Lyberg-Åhlander V, Rydell R. Absolute or relative voice rest after phonosurgery: a blind randomized prospective clinical trial. *Logopedics Phoniatrics Vocology*. 2018 Oct 2;43(4):143–54.
83. Dhaliwal SS, Doyle PC, Failla S, Hawkins S, Fung K. Role of voice rest following laser resection of vocal fold lesions: A randomized controlled trial. *The Laryngoscope*. 2020 Jul;130(7):1750–5.
84. Rihkanen H, Geneid A. Voice rest and sick leave after phonosurgical procedures: surveys among European laryngologists and phoniatricians. *Eur Arch Otorhinolaryngol*. 2019 Feb;276(2):483–7.
85. Tateya T, Tateya I, Sohn JH, Bless DM. Histological Study of Acute Vocal Fold Injury in a Rat Model. *Ann Otol Rhinol Laryngol*. 2006 Apr;115(4):285–92.
86. Wolchok JC, Brokopp C, Underwood CJ, Tresco PA. The effect of bioreactor induced vibrational stimulation on extracellular matrix production from human derived fibroblasts. *Biomaterials*. 2009 Jan;30(3):327–35.
87. Kutty JK, Webb K. Vibration stimulates vocal mucosa-like matrix expression by hydrogel-encapsulated fibroblasts. *Journal of Tissue Engineering and Regenerative Medicine*. 2009;n/a-n/a.
88. Gaston J, Quinchia Rios B, Bartlett R, Berchtold C, Thibeault SL. The Response of Vocal Fold Fibroblasts and Mesenchymal Stromal Cells to Vibration. Van Wijnen A, editor. *PLoS ONE*. 2012 Feb 16;7(2):e30965.
89. Farran AJE, Teller SS, Jia F, Clifton RJ, Duncan RL, Jia X. Design and characterization of a dynamic vibrational culture system: Vibrational culture system. *Journal of Tissue Engineering and Regenerative Medicine*. 2013 Mar;7(3):213–25.
90. Latifi N, Heris HK, Thomson SL, Taher R, Kazemirad S, Sheibani S, et al. A Flow

Perfusion Bioreactor System for Vocal Fold Tissue Engineering Applications. *Tissue Engineering Part C: Methods*. 2016 Sep;22(9):823–38.

91. Kim D, Lim J-Y, Kwon S. Development of Vibrational Culture Model Mimicking Vocal Fold Tissues. *Annals of Biomedical Engineering*. 2016 Oct;44(10):3136–43.
92. Zhang H, Wang Y, Bai X, Lv Z, Zou J, Xu W, et al. Cyclic Tensile Strain on Vocal Fold Fibroblasts Inhibits Cigarette Smoke-Induced Inflammation: Implications for Reinke Edema. *Journal of Voice*. 2015 Jan;29(1):13–21.
93. Graupp M, Rinner B, Frisch MT, Weiss G, Fuchs J, Sundl M, et al. Towards an in vitro fibrogenesis model of human vocal fold scarring. *Eur Arch Otorhinolaryngol*. 2018 May;275(5):1211–8.
94. Branco A, Bartley SM, King SN, Jetté ME, Thibeault SL. Vocal fold myofibroblast profile of scarring: Scar Vocal Fold Myofibroblast. *The Laryngoscope*. 2016 Mar;126(3):E110–7.
95. Xiao L. TGF-beta 1 induced fibroblast proliferation is mediated by the FGF-2/ERK pathway. *Front Biosci*. 2012;17(7):2667.
96. Wang X, Waldeck H, Kao WJ. The effects of TGF- α , IL-1 β and PDGF on fibroblast adhesion to ECM-derived matrix and KGF gene expression. *Biomaterials*. 2010 Mar;31(9):2542–8.
97. Branski RC, Zhou H, Sandulache VC, Chen J, Felsen D, Kraus DH. Cyclooxygenase-2 signaling in vocal fold fibroblasts. *The Laryngoscope*. 2010 Sep;120(9):1826–31.
98. Graupp M, Gruber H-J, Weiss G, Kiesler K, Bachna-Rotter S, Friedrich G, et al. Establishing principles of macromolecular crowding for in vitro fibrosis research of the vocal fold lamina propria. *Laryngoscope*. 2015 Jun;125(6):E203-209.
99. Ellis RJ. Macromolecular crowding: obvious but underappreciated. *Trends in Biochemical Sciences*. 2001 Oct;26(10):597–604.
100. Ricard-Blum S. The collagen family. *Cold Spring Harb Perspect Biol*. 2011 Jan 1;3(1):a004978.
101. Tang SS, Mohad V, Gowda M, Thibeault SL. Insights Into the Role of Collagen in Vocal Fold Health and Disease. *Journal of Voice*. 2017 Sep;31(5):520–7.
102. Rousseau B, Ge P, French LC, Zeale DL, Thibeault SL, Ossoff RH. Experimentally induced phonation increases matrix metalloproteinase-1 gene expression in normal rabbit vocal fold. *Otolaryngol Head Neck Surg*. 2008 Jan;138(1):62–8.

103. Klein T, Bischoff R. Physiology and pathophysiology of matrix metalloproteases. *Amino Acids*. 2011 Jul;41(2):271–90.
104. Nagase H, Visse R, Murphy G. Structure and function of matrix metalloproteinases and TIMPs. *Cardiovasc Res*. 2006 Feb 15;69(3):562–73.
105. Yang H, Makaroff K, Paz N, Aitha M, Crowder MW, Tierney DL. Metal Ion Dependence of the Matrix Metalloproteinase-1 Mechanism. *Biochemistry*. 2015 Jun 16;54(23):3631–9.
106. Dettori-Gera C, Ronner P, Scarpa A. Difference in dose-response curves for glucose-induced insulin and somatostatin release in rat pancreas. *Biochim Biophys Acta*. 1985 May 8;839(3):281–6.
107. Rousseau B, Sohn J, Montequin DW, Tateya I, Bless DM. Functional outcomes of reduced hyaluronan in acute vocal fold scar. *Ann Otol Rhinol Laryngol*. 2004 Oct;113(10):767–76.
108. Tateya I, Tateya T, Watanuki M, Bless DM. Homeostasis of Hyaluronic Acid in Normal and Scarred Vocal Folds. *Journal of Voice*. 2015 Mar;29(2):133–9.
109. Gaston J, Thibeault SL. Hyaluronic acid hydrogels for vocal fold wound healing. *Biomatter*. 2013 Jan;3(1):e23799.
110. Fallacara A, Baldini E, Manfredini S, Vertuani S. Hyaluronic Acid in the Third Millennium. *Polymers (Basel)*. 2018 Jun 25;10(7):E701.
111. Salwowska NM, Bebenek KA, Żądło DA, Wcisło-Dziadecka DL. Physicochemical properties and application of hyaluronic acid: a systematic review. *J Cosmet Dermatol*. 2016 Dec;15(4):520–6.
112. Pankov R, Yamada KM. Fibronectin at a glance. *J Cell Sci*. 2002 Oct 15;115(Pt 20):3861–3.
113. Zollinger AJ, Smith ML. Fibronectin, the extracellular glue. *Matrix Biol*. 2017 Jul;60–61:27–37.
114. Ferrara N. Vascular endothelial growth factor: basic science and clinical progress. *Endocr Rev*. 2004 Aug;25(4):581–611.
115. Apte RS, Chen DS, Ferrara N. VEGF in Signaling and Disease: Beyond Discovery and Development. *Cell*. 2019 Mar 7;176(6):1248–64.
116. Eltzschig HK, Carmeliet P. Hypoxia and inflammation. *N Engl J Med*. 2011 Feb 17;364(7):656–65.

117. Gugatschka M, Darnhofer B, Grossmann T, Schittmayer M, Hortobagyi D, Kirsch A, et al. Proteomic Analysis of Vocal Fold Fibroblasts Exposed to Cigarette Smoke Extract: Exploring the Pathophysiology of Reinke's Edema. *Mol Cell Proteomics*. 2019 Aug;18(8):1511–25.
118. Hinz B, Celetta G, Tomasek JJ, Gabbiani G, Chaponnier C. Alpha-smooth muscle actin expression upregulates fibroblast contractile activity. *Mol Biol Cell*. 2001 Sep;12(9):2730–41.
119. Fletcher DA, Mullins RD. Cell mechanics and the cytoskeleton. *Nature*. 2010 Jan 28;463(7280):485–92.
120. Calder PC. Eicosanoids. *Essays Biochem*. 2020 Sep 23;64(3):423–41.
121. Borish LC, Steinke JW. 2. Cytokines and chemokines. *J Allergy Clin Immunol*. 2003 Feb;111(2 Suppl):S460-475.
122. Fitzpatrick FA. Cyclooxygenase enzymes: regulation and function. *Curr Pharm Des*. 2004;10(6):577–88.
123. Lim X, Bless DM, Muñoz-Del-Río A, Welham NV. Changes in Cytokine Signaling and Extracellular Matrix Production Induced by Inflammatory Factors in Cultured Vocal Fold Fibroblasts. *Ann Otol Rhinol Laryngol*. 2008 Mar;117(3):227–38.
124. Kido S, Kuriwaka-Kido R, Imamura T, Ito Y, Inoue D, Matsumoto T. Mechanical stress induces Interleukin-11 expression to stimulate osteoblast differentiation. *Bone*. 2009 Dec;45(6):1125–32.
125. Ng B, Dong J, D'Agostino G, Viswanathan S, Widjaja AA, Lim W-W, et al. Interleukin-11 is a therapeutic target in idiopathic pulmonary fibrosis. *Sci Transl Med*. 2019 Sep 25;11(511):eaaw1237.
126. Chen H, Chen H, Liang J, Gu X, Zhou J, Xie C, et al. TGF- β 1/IL-11/MEK/ERK signaling mediates senescence-associated pulmonary fibrosis in a stress-induced premature senescence model of Bmi-1 deficiency. *Exp Mol Med*. 2020 Jan;52(1):130–51.
127. Murakami S. Periodontal tissue regeneration by signaling molecule(s): what role does basic fibroblast growth factor (FGF-2) have in periodontal therapy? *Periodontol* 2000. 2011 Jun;56(1):188–208.
128. Nugent MA, Iozzo RV. Fibroblast growth factor-2. *Int J Biochem Cell Biol*. 2000 Feb;32(2):115–20.
129. Tateya I, Tateya T, Sohn J-H, Bless DM. Histological Effect of Basic Fibroblast Growth Factor on Chronic Vocal Fold Scarring in a Rat Model. *Clin Exp Otorhinolaryngol*. 2016 Mar 7;9(1):56–61.

130. Grossmann T, Steffan B, Kirsch A, Grill M, Gerstenberger C, Gugatschka M. Exploring the Pathophysiology of Reinke's Edema: The Cellular Impact of Cigarette Smoke and Vibration. *Laryngoscope*. 2020 Jun 22;
131. Titze IR, Hunter EJ, Svec JG. Voicing and silence periods in daily and weekly vocalizations of teachers. *J Acoust Soc Am*. 2007 Jan;121(1):469–78.
132. Chan A, Mongeau L, Kost K. Vocal fold vibration measurements using laser Doppler vibrometry. *The Journal of the Acoustical Society of America*. 2013 Mar;133(3):1667–76.
133. Karbiener M, Darnhofer B, Frisch M-T, Rinner B, Birner-Gruenberger R, Gugatschka M. Comparative proteomics of paired vocal fold and oral mucosa fibroblasts. *Journal of Proteomics*. 2017 Feb;155:11–21.
134. Livak KJ, Schmittgen TD. Analysis of Relative Gene Expression Data Using Real-Time Quantitative PCR and the $2^{-\Delta\Delta CT}$ Method. *Methods*. 2001 Dec;25(4):402–8.
135. Vandesompele J, De Preter K, Pattyn F, Poppe B, Van Roy N, De Paepe A, et al. Accurate normalization of real-time quantitative RT-PCR data by geometric averaging of multiple internal control genes. *Genome Biol*. 2002 Jun 18;3(7):RESEARCH0034.
136. Dheda K, Huggett JF, Bustin SA, Johnson MA, Rook G, Zumla A. Validation of housekeeping genes for normalizing RNA expression in real-time PCR. *BioTechniques*. 2004 Jul;37(1):112–9.
137. Hansen JK, Thibeault SL. Current Understanding and Review of the Literature: Vocal Fold Scarring. *Journal of Voice*. 2006 Mar;20(1):110–20.
138. Joshi A, Johns MM. Current practices for voice rest recommendations after phonomicrosurgery: Postsurgical Voice Rest Recommendations. *The Laryngoscope*. 2018 May;128(5):1170–5.
139. Welham NV, Lim X, Tateya I, Bless DM. Inflammatory Factor Profiles One Hour following Vocal Fold Injury. *Ann Otol Rhinol Laryngol*. 2008 Feb;117(2):145–52.
140. Rousseau B, Kojima T, Novaleski CK, Kimball EE, Valenzuela CV, Mizuta M, et al. Recovery of Vocal Fold Epithelium after Acute Phonotrauma. *Cells Tissues Organs (Print)*. 2017;204(2):93–104.
141. Branski RC, Perera P, Verdolini K, Rosen CA, Hebda PA, Agarwal S. Dynamic biomechanical strain inhibits IL-1beta-induced inflammation in vocal fold fibroblasts. *J Voice*. 2007 Nov;21(6):651–60.

142. Ellis RJ. Macromolecular crowding: an important but neglected aspect of the intracellular environment. *Current Opinion in Structural Biology*. 2001 Feb;11(1):114–9.
143. Gnutt D, Ebbinghaus S. The macromolecular crowding effect--from in vitro into the cell. *Biol Chem*. 2016 Jan;397(1):37–44.
144. Rivas G, Minton AP. Macromolecular Crowding In Vitro, In Vivo, and In Between. *Trends Biochem Sci*. 2016 Nov;41(11):970–81.
145. Chen C, Loe F, Blocki A, Peng Y, Raghunath M. Applying macromolecular crowding to enhance extracellular matrix deposition and its remodeling in vitro for tissue engineering and cell-based therapies. *Adv Drug Deliv Rev*. 2011 Apr 30;63(4–5):277–90.
146. Pirkmajer S, Chibalin AV. Serum starvation: *caveat emptor*. *American Journal of Physiology-Cell Physiology*. 2011 Aug;301(2):C272–9.
147. Krishna P, Regner M, Palko J, Liu F, Abramowitch S, Jiang J, et al. The effects of decorin and HGF-primed vocal fold fibroblasts in vitro and ex vivo in a porcine model of vocal fold scarring. *The Laryngoscope*. 2010 Nov;120(11):2247–57.
148. Foote AG, Wang Z, Kendzioriski C, Thibeault SL. Tissue specific human fibroblast differential expression based on RNAsequencing analysis. *BMC Genomics*. 2019 Dec;20(1):308.
149. Li-Jessen NYK, Powell M, Choi A-J, Lee B-J, Thibeault SL. Cellular source and pro-inflammatory roles of high-mobility group box 1 in surgically injured rat vocal folds: HMGB1 in Vocal Folds. *The Laryngoscope*. 2017 Jun;127(6):E193–200.
150. Verdolini K, Branski RC, Rosen CA, Hebda PA. Shifts in Biochemical Markers Associated with Wound Healing in Laryngeal Secretions following Phonotrauma: A Preliminary Study. *Ann Otol Rhinol Laryngol*. 2003 Dec;112(12):1021–5.
151. Branski RC, Rosen CA, Verdolini K, Hebda PA. Biochemical Markers Associated With Acute Vocal Fold Wound Healing: A Rabbit Model. *Journal of Voice*. 2005 Jun;19(2):283–9.
152. Lifshitz V, Frenkel D. TGF- β . In: *Handbook of Biologically Active Peptides* [Internet]. Elsevier; 2013 [cited 2021 Jul 4]. p. 1647–53. Available from: <https://linkinghub.elsevier.com/retrieve/pii/B9780123850959002256>
153. Lichtman MK, Otero-Vinas M, Falanga V. Transforming growth factor beta (TGF- β) isoforms in wound healing and fibrosis: TGF- β and wound healing. *Wound Rep and Reg*. 2016 Mar;24(2):215–22.
154. Cooke JP. Inflammation and Its Role in Regeneration and Repair: A Caution for Novel Anti-Inflammatory Therapies. *Circ Res*. 2019 Apr 12;124(8):1166–8.

155. Wang J, Fan T-J, Yang X-X, Chang S-M. Transforming growth factor- β 2 induces morphological alteration of human corneal endothelial cells in vitro. *Int J Ophthalmol.* 2014;7(5):759–63.
156. Chen X, Thibeault SL. Response of Fibroblasts to Transforming Growth Factor- β 1 on Two-Dimensional and in Three-Dimensional Hyaluronan Hydrogels. *Tissue Engineering Part A.* 2012 Dec;18(23–24):2528–38.
157. Pita I, Jelaso AM, Ide CF. IL-1 β increases intracellular calcium through an IL-1 type 1 receptor mediated mechanism in C6 astrocytic cells. *Int J Dev Neurosci.* 1999 Dec;17(8):813–20.
158. Skinner BM, Johnson EEP. Nuclear morphologies: their diversity and functional relevance. *Chromosoma.* 2017 Mar;126(2):195–212.
159. Paulsson Y, Karlsson C, Heldin CH, Westermark B. Density-dependent inhibitory effect of transforming growth factor-beta 1 on human fibroblasts involves the down-regulation of platelet-derived growth factor alpha-receptors. *J Cell Physiol.* 1993 Oct;157(1):97–103.
160. Nallet-Staub F, Yin X, Gilbert C, Marsaud V, Ben Mimoun S, Javelaud D, et al. Cell density sensing alters TGF- β signaling in a cell-type-specific manner, independent from Hippo pathway activation. *Dev Cell.* 2015 Mar 9;32(5):640–51.
161. Inoue T, Nabeshima K, Shimao Y, Kataoka H, Koono M. Cell density-dependent regulation of fibronectin splicing at the EDA region in fibroblasts: cell density also modulates the responses of fibroblasts to TGF-beta and cancer cell-conditioned medium. *Cancer Lett.* 1998 Jul 3;129(1):45–54.
162. Kitamura R, Tanimoto K, Tanne Y, Kamiya T, Huang Y-C, Tanaka N, et al. Effects of mechanical load on the expression and activity of hyaluronidase in cultured synovial membrane cells. *J Biomed Mater Res.* 2010 Jan;92A(1):87–93.
163. Kojima T, Valenzuela CV, Novaleski CK, Van Deusen M, Mitchell JR, Garrett CG, et al. Effects of phonation time and magnitude dose on vocal fold epithelial genes, barrier integrity, and function: Time and Dose Effects on Vocal Fold Function. *The Laryngoscope.* 2014 Dec;124(12):2770–8.
164. Lenselink EA. Role of fibronectin in normal wound healing: Role of fibronectin in normal wound healing. *Int Wound J.* 2015 Jun;12(3):313–6.
165. Zhang X, Putoczki T, Markovic-Plese S. IL-11 in multiple sclerosis. *Oncotarget [Inter-*

- net]. 2015 Oct 20 [cited 2020 Feb 15];6(32). Available from: <http://www.oncotarget.com/fulltext/6027>
166. Schafer S, Viswanathan S, Widjaja AA, Lim W-W, Moreno-Moral A, DeLaughter DM, et al. IL-11 is a crucial determinant of cardiovascular fibrosis. *Nature*. 2017 Dec;552(7683):110–5.
167. Judd LM, Ulaganathan M, Howlett M, Giraud AS. Cytokine signalling by gp130 regulates gastric mucosal healing after ulceration and, indirectly, antral tumour progression. *J Pathol*. 2009 Mar;217(4):552–62.
168. Kim EK, Choi E-J. Compromised MAPK signaling in human diseases: an update. *Arch Toxicol*. 2015 Jun;89(6):867–82.
169. Wong VW, Rustad KC, Akaishi S, Sorkin M, Glotzbach JP, Januszyk M, et al. Focal adhesion kinase links mechanical force to skin fibrosis via inflammatory signaling. *Nat Med*. 2011 Dec 11;18(1):148–52.
170. Shi Z-D, Abraham G, Tarbell JM. Shear Stress Modulation of Smooth Muscle Cell Marker Genes in 2-D and 3-D Depends on Mechanotransduction by Heparan Sulfate Proteoglycans and ERK1/2. Agarwal S, editor. *PLoS ONE*. 2010 Aug 16;5(8):e12196.
171. Titze IR. Mechanical stress in phonation. *J Voice*. 1994 Jun;8(2):99–105.
172. Ling C, Yamashita M, Zhang J, Bless DM, Welham NV. Reactive response of fibrocytes to vocal fold mucosal injury in rat. *Wound Repair Regen*. 2010 Oct;18(5):514–23.
173. King SN, Chen F, Jetté ME, Thibeault SL. Vocal fold fibroblasts immunoregulate activated macrophage phenotype. *Cytokine*. 2013 Jan;61(1):228–36.
174. Maqsood MI, Matin MM, Bahrami AR, Ghasroldasht MM. Immortality of cell lines: challenges and advantages of establishment. *Cell Biol Int*. 2013 Oct;37(10):1038–45.
175. Honegger P. Overview of cell and tissue culture techniques. *Curr Protoc Pharmacol*. 2001 May;Chapter 12:Unit12.1.
176. Chen X, Thibeault SL. Novel isolation and biochemical characterization of immortalized fibroblasts for tissue engineering vocal fold lamina propria. *Tissue Eng Part C Methods*. 2009 Jun;15(2):201–12.
177. Carter M, Shieh JC. Cell Culture Techniques. In: *Guide to Research Techniques in Neuroscience* [Internet]. Elsevier; 2010 [cited 2021 Jul 4]. p. 281–96. Available from: <https://linkinghub.elsevier.com/retrieve/pii/B9780123748492000136>

Supplementary appendix

Supplementary file 1: raw data from statistical tests four hours of vibration per day

qPCR		
Shapiro-Wilk		significance
COL1A1	Static without cytokines	0,117
	Dynamic without cytokines	0,932
	Static with cytokines	0,551
	Dynamic with cytokines	0,121
COL1A2	Static without cytokines	0,755
	Dynamic without cytokines	0,338
	Static with cytokines	0,177
	Dynamic with cytokines	0,899
COL3A1	Static without cytokines	0,331
	Dynamic without cytokines	0,972
	Static with cytokines	0,772
	Dynamic with cytokines	0,962
COX2	Static without cytokines	0,702
	Dynamic without cytokines	0,011
	Static with cytokines	0,385
	Dynamic with cytokines	0,507
FN1	Static without cytokines	0,446
	Dynamic without cytokines	0,525
	Static with cytokines	0,566
	Dynamic with cytokines	0,984
HAS1	Static without cytokines	0,931
	Dynamic without cytokines	0,656
	Static with cytokines	0,212
	Dynamic with cytokines	0,018
HAS2	Static without cytokines	0,28
	Dynamic without cytokines	0,572

	Static with cytokines	0,93
	Dynamic with cytokines	0,981
HAS3	Static without cytokines	0,31
	Dynamic without cytokines	0,061
	Static with cytokines	0,92
	Dynamic with cytokines	0,695
HYAL2	Static without cytokines	0,687
	Dynamic without cytokines	0,394
	Static with cytokines	0,539
	Dynamic with cytokines	0,564
IL1b	Static without cytokines	0,24
	Dynamic without cytokines	0,119
	Static with cytokines	0,09
	Dynamic with cytokines	0,06
IL6	Static without cytokines	0,629
	Dynamic without cytokines	0,363
	Static with cytokines	0,984
	Dynamic with cytokines	0,588
MMP1	Static without cytokines	0,705
	Dynamic without cytokines	0,61
	Static with cytokines	0,924
	Dynamic with cytokines	0,374
TGFb1	Static without cytokines	0,086
	Dynamic without cytokines	0,393
	Static with cytokines	0,596
	Dynamic with cytokines	0,719
ACTA2	Static without cytokines	0,808
	Dynamic without cytokines	0,246
	Static with cytokines	0,072
	Dynamic with cytokines	0,297

1-way ANOVA	between groups F-value	between groups p-value
COL1A1	18,901	0,000
COL1A2	15,485	0,000
COL3A1	7,116	0,005
FN1	16,449	0,000
HAS2	2,341	0,125
HAS3	15,209	0,000
HYAL2	2,093	0,155
IL1b	5,166	0,016
IL6	8,133	0,003
MMP1	6,105	0,009
TGFb1	5,679	0,012
ACTA2	12,266	0,001

Kruskal-Wallis	Kruskal-Wallis H	p-value
COX2	2,537	0,506
HAS1	7,456	0,043

Man-U-Whit-ney			p-value
HAS1	Static without cytokines	Dynamic without cytokines	0,486
		Static with cytokines	0,029
		Dynamic with cytokines	0,029
	Dynamic without cytokines	Static with cytokines	0,343
		Dynamic with cytokines	0,343
	Static with cytokines	Dynamic with cytokines	0,886

Tukey-post hoc			p-value
COL1A1	Static without cytokines	Dynamic without cytokines	0,996
		Static with cytokines	0,000
		Dynamic with cytokines	0,007
	Dynamic without cytokines	Static without cytokines	0,996
		Static with cytokines	0,000
		Dynamic with cytokines	0,010
	Static with cytokines	Static without cytokines	0,000
		Dynamic without cytokines	0,000
		Dynamic with cytokines	0,179
	Dynamic with cytokines	Static without cytokines	0,007
		Dynamic without cytokines	0,010
		Static with cytokines	0,179
COL1A2	Static without cytokines	Dynamic without cytokines	0,893
		Static with cytokines	0,003
		Dynamic with cytokines	0,001
	Dynamic without cytokines	Static without cytokines	0,893
		Static with cytokines	0,010
		Dynamic with cytokines	0,002
	Static with cytokines	Static without cytokines	0,003
		Dynamic without cytokines	0,010
		Dynamic with cytokines	0,764
	Dynamic with cytokines	Static without cytokines	0,001
		Dynamic without cytokines	0,002
		Static with cytokines	0,764
COL3A1	Static without cytokines	Dynamic without cytokines	0,999
		Static with cytokines	0,058
		Dynamic with cytokines	0,014
	Dynamic without cytokines	Static without cytokines	0,999
		Static with cytokines	0,073
		Dynamic with cytokines	0,018

	Static with cytokines	Static without cytokines	0,058
		Dynamic without cytokines	0,073
		Dynamic with cytokines	0,850
	Dynamic with cytokines	Static without cytokines	0,014
		Dynamic without cytokines	0,018
		Static with cytokines	0,850
FN1	Static without cytokines	Dynamic without cytokines	0,923
		Static with cytokines	0,002
		Dynamic with cytokines	0,001
	Dynamic without cytokines		
		Static without cytokines	0,923
		Static with cytokines	0,007
		Dynamic with cytokines	0,001
	Static with cytokines	Static without cytokines	0,002
		Dynamic without cytokines	0,007
		Dynamic with cytokines	0,786
	Dynamic with cytokines	Static without cytokines	0,001
		Dynamic without cytokines	0,001
		Static with cytokines	0,786
HAS3	Static without cytokines	Dynamic without cytokines	1,000
		Static with cytokines	0,002
		Dynamic with cytokines	0,002
	Dynamic without cytokines		
		Static without cytokines	1,000
		Static with cytokines	0,003
		Dynamic with cytokines	0,002
	Static with cytokines	Static without cytokines	0,002
		Dynamic without cytokines	0,003
		Dynamic with cytokines	0,999
	Dynamic with cytokines	Static without cytokines	0,002
		Dynamic without cytokines	0,002
		Static with cytokines	0,999
IL1b	Static without cytokines	Dynamic without cytokines	1,000
		Static with cytokines	0,232

		Dynamic with cytokines	0,030
	Dynamic without cytokines	Static without cytokines	1,000
		Static with cytokines	0,233
		Dynamic with cytokines	0,030
	Static with cytokines	Static without cytokines	0,232
		Dynamic without cytokines	0,233
		Dynamic with cytokines	0,618
	Dynamic with cytokines	Static without cytokines	0,030
		Dynamic without cytokines	0,030
		Static with cytokines	0,618
IL6	Static without cytokines	Dynamic without cytokines	1,000
		Static with cytokines	0,023
		Dynamic with cytokines	0,016
	Dynamic without cytokines	Static without cytokines	1,000
		Static with cytokines	0,025
		Dynamic with cytokines	0,017
	Static with cytokines	Static without cytokines	0,023
		Dynamic without cytokines	0,025
		Dynamic with cytokines	0,997
	Dynamic with cytokines	Static without cytokines	0,016
		Dynamic without cytokines	0,017
		Static with cytokines	0,997
MMP1	Static without cytokines	Dynamic without cytokines	0,389
		Static with cytokines	0,011
		Dynamic with cytokines	0,026
	Dynamic without cytokines	Static without cytokines	0,389
		Static with cytokines	0,179
		Dynamic with cytokines	0,370
	Static with cytokines	Static without cytokines	0,011
		Dynamic without cytokines	0,179
		Dynamic with cytokines	0,956

	Dynamic with cytokines	Static without cytokines	0,026
		Dynamic without cytokines	0,370
		Static with cytokines	0,956
TGFb1	Static without cytokines	Dynamic without cytokines	0,920
		Static with cytokines	0,014
		Dynamic with cytokines	0,129
	Dynamic without cytokines	Static without cytokines	0,920
		Static with cytokines	0,042
		Dynamic with cytokines	0,331
	Static with cytokines	Static without cytokines	0,014
		Dynamic without cytokines	0,042
		Dynamic with cytokines	0,585
	Dynamic with cytokines	Static without cytokines	0,129
		Dynamic without cytokines	0,331
		Static with cytokines	0,585
ACTA2	Static without cytokines	Dynamic without cytokines	1,000
		Static with cytokines	0,001
		Dynamic with cytokines	0,046
	Dynamic without cytokines	Static without cytokines	1,000
		Static with cytokines	0,001
		Dynamic with cytokines	0,042
	Static with cytokines	Static without cytokines	0,001
		Dynamic without cytokines	0,001
		Dynamic with cytokines	0,238
	Dynamic with cytokines	Static without cytokines	0,046
		Dynamic without cytokines	0,042
		Static with cytokines	0,238

Luminex		
Shapiro-Wilk		significance
COL1A1	Dynamic without cytokines	0,736
	Dynamic with cytokines	0,858
	Static without cytokines	0,301
	Static with cytokines	0,918
Fibronectin	Dynamic without cytokines	0,222
	Dynamic with cytokines	0,191
	Static without cytokines	0,011
	Static with cytokines	0,711
TIMP1	Dynamic without cytokines	0,458
	Dynamic with cytokines	0,943
	Static without cytokines	0,451
	Static with cytokines	0,716
VEGF-C	Dynamic without cytokines	0,488
	Dynamic with cytokines	0,886
	Static without cytokines	0,254
	Static with cytokines	0,512
FGF	Dynamic without cytokines	0,651
	Dynamic with cytokines	0,869
	Static without cytokines	0,563
	Static with cytokines	0,549
IL11	Dynamic without cytokines	0,78
	Dynamic with cytokines	0,167
	Static without cytokines	0,062
	Static with cytokines	0,755
VEGF-A	Dynamic without cytokines	0,802
	Dynamic with cytokines	0,887
	Static without cytokines	0,347
	Static with cytokines	0,231

1-way ANOVA	between groups F-value	between groups p-value
COL1A1	7,468	0,004
TIMP1	0,596	0,629
VEGF-C	0,876	0,481
FGF	24,311	0,000
IL11	24,864	0,000
VEGF-A	0,389	0,763

Kruskal-Wallis	Kruskal-Wallis H	p-value
Fibronectin	11,029	0,012

Man-U-Whitney			p-value
Fibronectin	Dynamic without cytokines	Dynamic with cytokines	0,057
		Static without cytokines	0,200
		Static with cytokines	0,029
	Dynamic with cytokines	Static without cytokines	0,057
		Static with cytokines	0,343
	Static without cytokines	Static with cytokines	0,029

Tukey-post hoc			p-value
COL1A1	Dynamic without cytokines	Dynamic with cytokines	0,050
		Static without cytokines	0,772
		Static with cytokines	0,093
	Dynamic with cytokines	Dynamic without cytokines	0,050
		Static without cytokines	0,009
		Static with cytokines	0,983
	Static without cytokines	Dynamic without cytokines	0,772
		Dynamic with cytokines	0,009
		Static with cytokines	0,018
	Static with cytokines	Dynamic without cytokines	0,093
		Dynamic with cytokines	0,983
		Static without cytokines	0,018
FGF	Dynamic without cytokines	Dynamic with cytokines	0,007
		Static without cytokines	0,982
		Static with cytokines	0,000
	Dynamic with cytokines	Dynamic without cytokines	0,007
		Static without cytokines	0,004
		Static with cytokines	0,067
	Static without cytokines	Dynamic without cytokines	0,982
		Dynamic with cytokines	0,004
		Static with cytokines	0,000
	Static with cytokines	Dynamic without cytokines	0,000
		Dynamic with cytokines	0,067
		Static without cytokines	0,000
IL11	Dynamic without cytokines	Dynamic with cytokines	0,298
		Static without cytokines	0,994
		Static with cytokines	0,000

	Dynamic with cytokines	Dynamic without cytokines	0,298
		Static without cytokines	0,418
		Static with cytokines	0,000
	Static without cytokines	Dynamic without cytokines	0,994
		Dynamic with cytokines	0,418
		Static with cytokines	0,000
	Static with cytokines	Dynamic without cytokines	0,000
		Dynamic with cytokines	0,000
		Static without cytokines	0,000

Western Blot		
Shapiro-Wilk		significance
aSMA	Dynamic without cytokines	0,213
	Dynamic with cytokines	0,162
	Static without cytokines	0,412
	Static with cytokines	0,482
COL	Dynamic without cytokines	0,792
	Dynamic with cytokines	0,469
	Static without cytokines	0,278
	Static with cytokines	0,779

1-way ANOVA	between groups F-value	between groups p-value
aSMA	14,514	0,000
COL	3,008	0,076

Tukey-post hoc			p-value
aSMA	Dynamic without cytokines	Dynamic with cytokines	0,264
		Static without cytokines	0,990
		Static with cytokines	0,000
	Dynamic with cytokines	Dynamic without cytokines	0,264
		Static without cytokines	0,394
		Static with cytokines	0,007
	Static without cytokines	Dynamic without cytokines	0,990
		Dynamic with cytokines	0,394
		Static with cytokines	0,001
	Static with cytokines	Dynamic without cytokines	0,000
		Dynamic with cytokines	0,007
		Static without cytokines	0,001

ELISA		
Shapiro-Wilk		significance
Hyaluronic Acid	Dynamic without cytokines	0,806
	Dynamic with cytokines	0,941
	Static without cytokines	0,023
	Static with cytokines	0,412

Kruskal-Wallis	Kruskal-Wallis H	p-value
Hyaluronic Acid	11,934	0,008

Man-U-Whitney			p-value
Hyaluronic Acid	Dynamic without cytokines	Dynamic with cytokines	0,029
		Static without cytokines	0,686
		Static with cytokines	0,029
	Dynamic with cytokines	Static without cytokines	0,029
		Static with cytokines	0,200
	Static without cytokines	Static with cytokines	0,029

Supplementary file 2: raw data from statistical tests - eight hours of vibration per day

qPCR		
Shapiro-Wilk		
COL1A1	Static without cytokines	0,372
	Dynamic without cytokines	0,754
	Static with cytokines	0,135
	Dynamic with cytokines	0,422
COL1A2	Static without cytokines	0,362
	Dynamic without cytokines	0,087
	Static with cytokines	0,988
	Dynamic with cytokines	0,71
COL3A1	Static without cytokines	0,899
	Dynamic without cytokines	0,523
	Static with cytokines	0,011
	Dynamic with cytokines	0,631
COX2	Static without cytokines	0,445
	Dynamic without cytokines	0,106
	Static with cytokines	0,826
	Dynamic with cytokines	0,355
FN1	Static without cytokines	0,073
	Dynamic without cytokines	0,632
	Static with cytokines	0,683
	Dynamic with cytokines	0,404
HAS1	Static without cytokines	0,466
	Dynamic without cytokines	0,013
	Static with cytokines	0,114
	Dynamic with cytokines	0,031
HAS2	Static without cytokines	0,949
	Dynamic without cytokines	0,755

	Static with cytokines	0,293
	Dynamic with cytokines	0,786
HAS3	Static without cytokines	0,036
	Dynamic without cytokines	0,378
	Static with cytokines	0,329
	Dynamic with cytokines	0,371
HYAL2	Static without cytokines	0,601
	Dynamic without cytokines	0,508
	Static with cytokines	0,351
	Dynamic with cytokines	0,635
IL1b	Static without cytokines	0,919
	Dynamic without cytokines	0,282
	Static with cytokines	0,31
	Dynamic with cytokines	0,232
IL6	Static without cytokines	0,915
	Dynamic without cytokines	0,235
	Static with cytokines	0,933
	Dynamic with cytokines	0,817
MMP1	Static without cytokines	0,223
	Dynamic without cytokines	0,462
	Static with cytokines	0,663
	Dynamic with cytokines	0,581
TGFb1	Static without cytokines	0,878
	Dynamic without cytokines	0,252
	Static with cytokines	0,039
	Dynamic with cytokines	0,16
ACTA2	Static without cytokines	0,338
	Dynamic without cytokines	0,579
	Static with cytokines	0,5
	Dynamic with cytokines	0,041

1-way ANOVA	between groups F-value	between groups p-value
COL1A1	33,100	0,000
COL1A2	6,025	0,010
COX2	1,621	0,236
FN1	9,491	0,002
HAS2	3,153	0,065
IL1b	2,064	0,159
IL6	8,044	0,003
MMP1	1,066	0,400
HYAL2	16,310	0,000

Kruskal-Wallis	Kruskal-Wallis H	p-value
COL3A1	9,816	0,006
HAS1	3,115	0,411
HAS3	11,846	0,000
TGFb1	7,037	0,057
ACTA2	2,912	0,437

Man-U-Whitney			p-value
COL3A1	Static without cytokines	Dynamic without cytokines	0,248
		Static with cytokines	0,069
		Dynamic with cytokines	0,248
	Dynamic without cytokines	Static with cytokines	0,083
		Dynamic with cytokines	0,050
	Static with cytokines	Dynamic with cytokines	0,564
HAS3	Static without cytokines	Dynamic without cytokines	0,248
		Static with cytokines	0,018
		Dynamic with cytokines	0,248
	Dynamic without cytokines	Static with cytokines	0,021
		Dynamic with cytokines	0,021

	Static with cytokines	Dynamic with cytokines	0,386
--	-----------------------	------------------------	-------

Tukey-post hoc			p-value
COL1A1	Static without cytokines	Dynamic without cytokines	0,993
		Static with cytokines	0,000
		Dynamic with cytokines	0,004
	Dynamic without cytokines	Static without cytokines	0,993
		Static with cytokines	0,000
		Dynamic with cytokines	0,007
	Static with cytokines	Static without cytokines	0,000
		Dynamic without cytokines	0,000
		Dynamic with cytokines	0,005
	Dynamic with cytokines	Static without cytokines	0,004
		Dynamic without cytokines	0,007
		Static with cytokines	0,005
COL1A2	Static without cytokines	Dynamic without cytokines	0,987
		Static with cytokines	0,032
		Dynamic with cytokines	0,159
	Dynamic without cytokines	Static without cytokines	0,987
		Static with cytokines	0,018
		Dynamic with cytokines	0,093
	Static with cytokines	Static without cytokines	0,032
		Dynamic without cytokines	0,018
		Dynamic with cytokines	0,774
	Dynamic with cytokines	Static without cytokines	0,159
		Dynamic without cytokines	0,093
		Static with cytokines	0,774
FN1	Static without cytokines	Dynamic without cytokines	0,996

		Static with cytokines	0,012
		Dynamic with cytokines	0,008
	Dynamic without cytokines	Static without cytokines	0,996
		Static with cytokines	0,018
		Dynamic with cytokines	0,012
	Static with cytokines	Static without cytokines	0,012
		Dynamic without cytokines	0,018
		Dynamic with cytokines	0,996
	Dynamic with cytokines	Static without cytokines	0,008
		Dynamic without cytokines	0,012
		Static with cytokines	0,996
IL6	Static without cytokines	Dynamic without cytokines	1,000
		Static with cytokines	0,047
		Dynamic with cytokines	0,011
	Dynamic without cytokines	Static without cytokines	1,000
		Static with cytokines	0,046
		Dynamic with cytokines	0,011
	Static with cytokines	Static without cytokines	0,047
		Dynamic without cytokines	0,046
		Dynamic with cytokines	0,842
	Dynamic with cytokines	Static without cytokines	0,011
		Dynamic without cytokines	0,011
		Static with cytokines	0,842
HYAL2	Static without cytokines	Dynamic without cytokines	0,001
		Static with cytokines	0,892
		Dynamic with cytokines	0,023
	Dynamic without cytokines	Static without cytokines	0,001
		Static with cytokines	0,000
		Dynamic with cytokines	0,273
	Static with cytokines	Static without cytokines	0,892

		Dynamic without cytokines	0,000
		Dynamic with cytokines	0,007
	Dynamic with cytokines	Static without cytokines	0,023
		Dynamic without cytokines	0,273
		Static with cytokines	0,007

Supplementary file 3: Catalogue numbers

General laboratory equipment

Product	Company	CAS/Red
Cell culture flask 250mL 75 cm ²	Greiner Bio-One GmbH; Germany	658175
Cell culture flask 50mL 50 cm ²	Greiner Bio-One GmbH; Germany	690175
Bioflex® culture plate + pron-ectin, C557155	Flexcell® Int. Corp.; USA	BF3001P
Nunclon Multidish 24 well	Thermo Scientific; Denmark	142475
Serological Pipette 5mL	Corning Incorporated; USA	4051
Serological Pipette 10mL	Corning Incorporated; USA	4101
Serological Pipette 25mL	Corning Incorporated; USA	4251
ART® 10µL Barriere tip, sterile	Thermo Scientific; USA	2140
ART® 20µL Barriere tip, sterile	Thermo Scientific; USA	2149P
ART® 100µL Barriere tip, sterile	Thermo Scientific; USA	2065E
ART® 200µL Barriere tip, sterile	Thermo Scientific; USA	2069
ART® 1000µL Barriere tip, ster-ile	Thermo Scientific; USA	2079-05-HR
Cell scraper, sterile	Corning Incorporated; USA	3010
Falcon 15mL Polypropylene Conical Tube	Corning Science; Mexico	352095
Falcon 50mL Polypropylene Conical Tube	Corning Science; Mexico	352070
Millipak® Express 0,22µm	Merck KGaA, Germany	MPGP02001
CombiTips advanced 10mL	Eppendorf, Germany	0030089464
CombiTip 5mL	Eppendorf, Germany	0030089456
Ethanol denaturated ≥99,8%	Roth GmbH &Co KG; Germany	K928.3
Nitril® 3000 Gloves	Meditrade	1280
Milli-Q® Reference A+ Water Purification System	Merck KGaA, Germany	
Bacillol 30 Tissues	Hartmann	
0,2µm filter unit	Whatman™; GE Healthcare UK	10462200
QIAzol® Lysis Reagent	QIAGEN Sciences; USA	56008534

RNase AWAY	Molecular BioProducts; USA	#7003
QuantiTect® Reverse Transcription Kit	QUIAGEN GmbH; Germany	64-17-5
Ethanol absolute 99,9% for analysis, Rotipur®	AustrAlco	1.009.832.511
Chloroform Rotipuran® ≥99%, p.a.	Carl Roth, Germany	

LDH Assay

Pierce™ LDH Cytotoxicity Assay Kit	Thermo Scientific; USA	88954
96 well BRANDplates, clear	BRAND, Germany	781602

qPCR

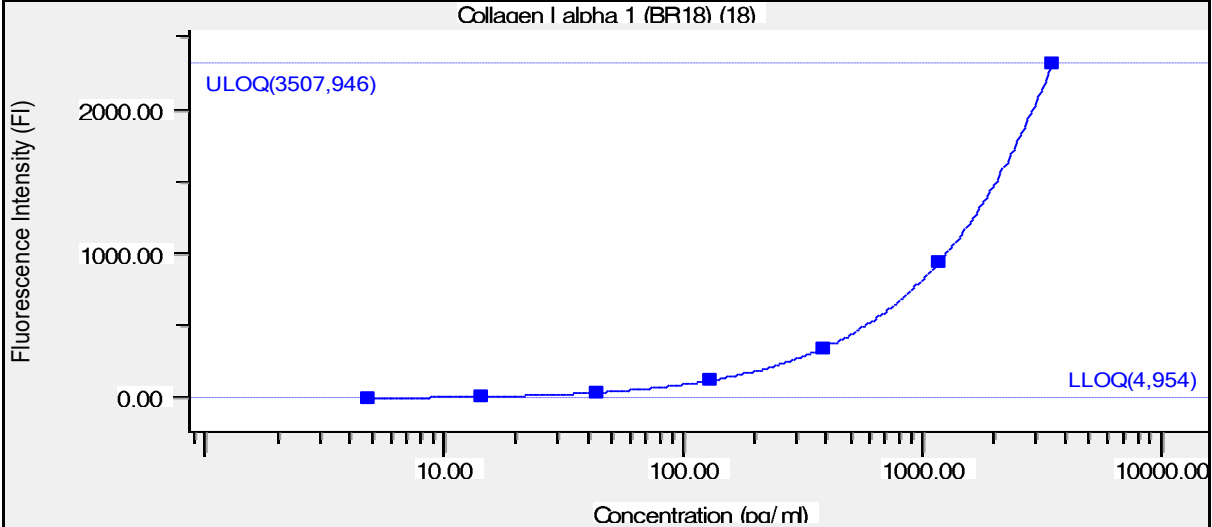
GoTaq qPCR Mastermix (2x)	Promega; USA	A600A
Nuclease-Free Water	Promega; USA	P119E
FrameStar® 384 Well Skirted PCR Plate; Roche Style, Plus qPCR Seal	4titude Ltd.; UK	4ti-0382

Western Blot

RIPA Buffer (5x)	Cell Biolabs INC.	AKR-191
SuperSignal™ West PicoPLUS Chemiluminescent Substrate	Thermo Scientific; USA	34578
Precision Plus Protein™ Standard Dual Color	Biorad	#161-0374
Tris Buffered Saline (TBS, 10x)	Biorad	#1706435
Tris/Glycerin/SDS buffer (TGS 10x)	Biorad	#161-0732
Restore™ PLUS Western Blot Stripping Buffer	Thermo Scientific; USA	46430
Tween® 20 viscous liquid	Sigma-Aldrich	P1379
Laemmli Sample Buffer (4x)	Biorad	#161-0747

Supplementary file 4: Standard Curves of Luminex Samples - four hours of vibration per day

COL1A1



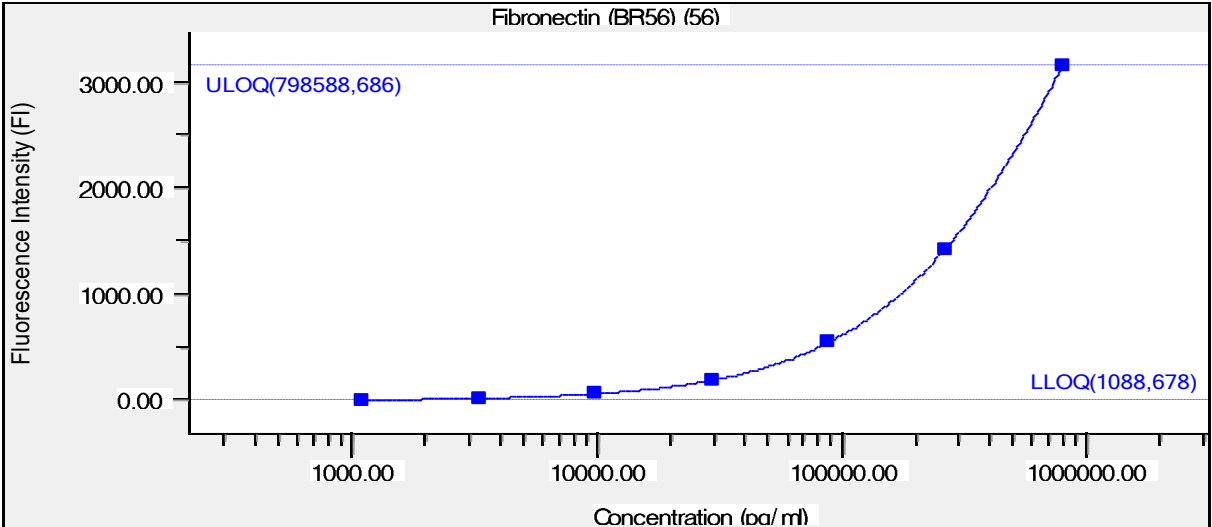
■ Standard □ Partial Outlier ⊠ Outlier

Regression Type: Logistic - 5PL

Std. Curve: $FI = -0,642674 + (29302,2 + 0,642674) / ((1 + (Conc / 28404)^{-0,580408})^{1,71943})$

FitProb. = 0,9643, ResVar. = 0,0364

FN1



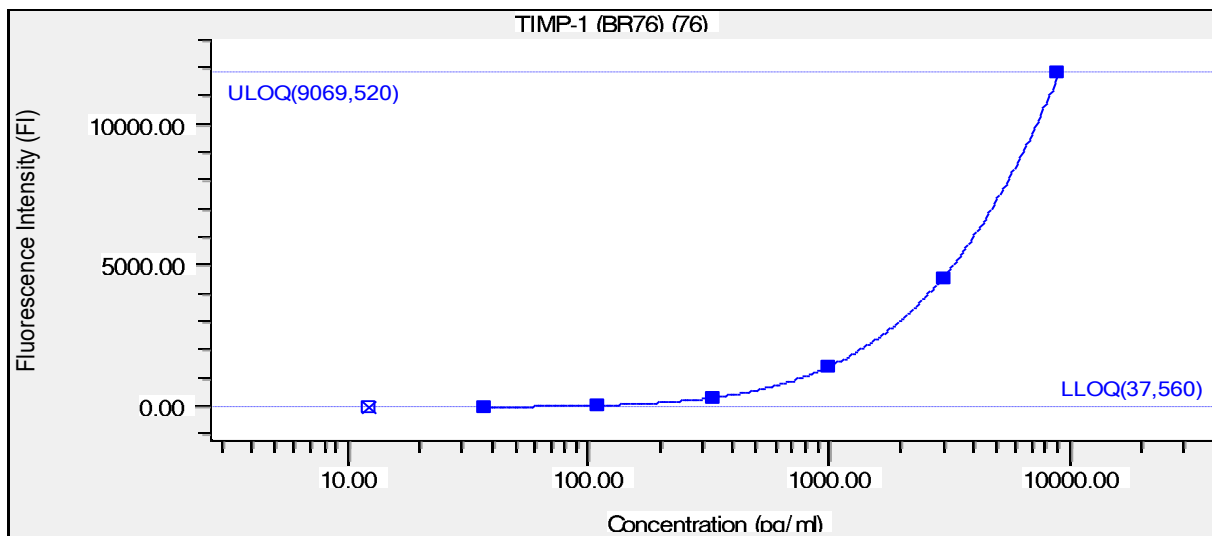
■ Standard □ Partial Outlier ⊠ Outlier

Regression Type: Logistic - 5PL

Std. Curve: $FI = 0,687694 + (7573,04 - 0,687694) / ((1 + (\text{Conc} / 1,18955E+006)^{-1,044}))^{0,945819}$

FitProb. = 0,9430, ResVar. = 0,0586

TIMP1



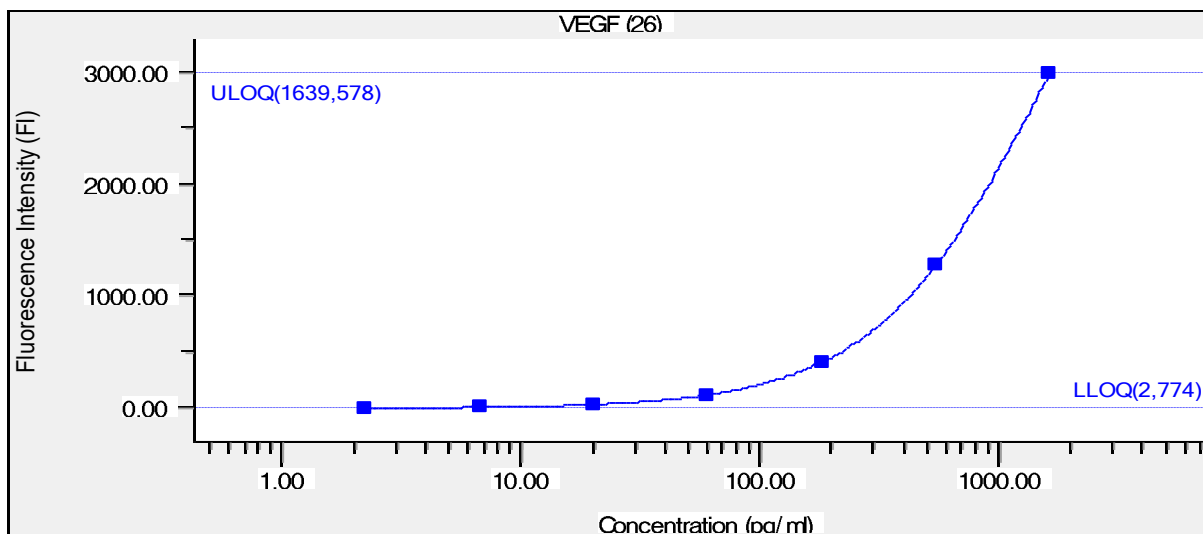
■ Standard □ Partial Outlier ⊠ Outlier

Regression Type: Logistic - 5PL

Std. Curve: $FI = 4,16841 + (192067 - 4,16841) / ((1 + (\text{Conc} / 226,583)^{-0,307883}))^{10}$

FitProb. = 0,5967, ResVar. = 0,2801

VEGF A



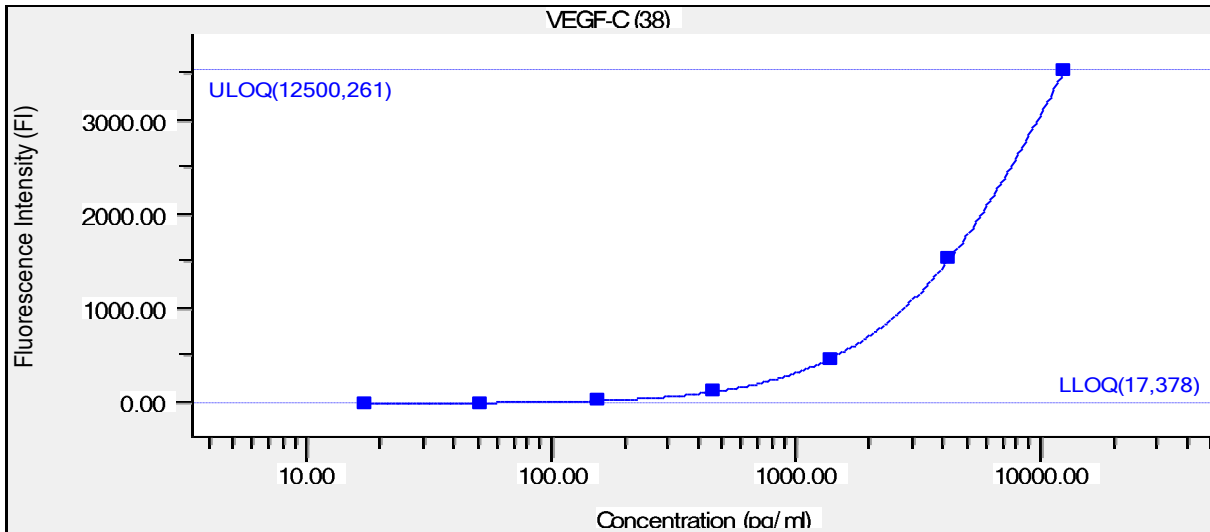
■ Standard □ Partial Outlier ☒ Outlier

Regression Type: Logistic - 5PL

Std. Curve: $FI = 0,800005 + (5003,9 - 0,800005) / ((1 + (Conc / 1613,94)^{-1,50279}))^{0,753571}$

FitProb. = 0,8189, ResVar. = 0,1997

VEGF C



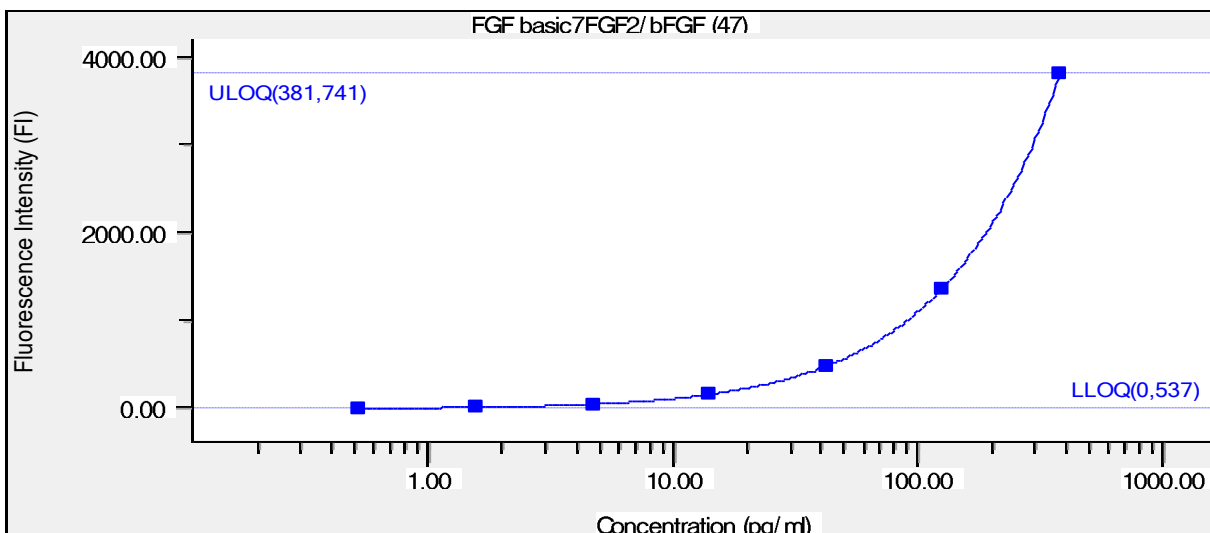
■ Standard □ Partial Outlier ⊗ Outlier

Regression Type: Logistic - 5PL

Std. Curve: $FI = 2,94227 + (8729,96 - 2,94227) / ((1 + (\text{Conc} / 10052,7)^{-0,902707}))^{1,5024}$

FitProb. = 0,4831, ResVar. = 0,7276

bFGF



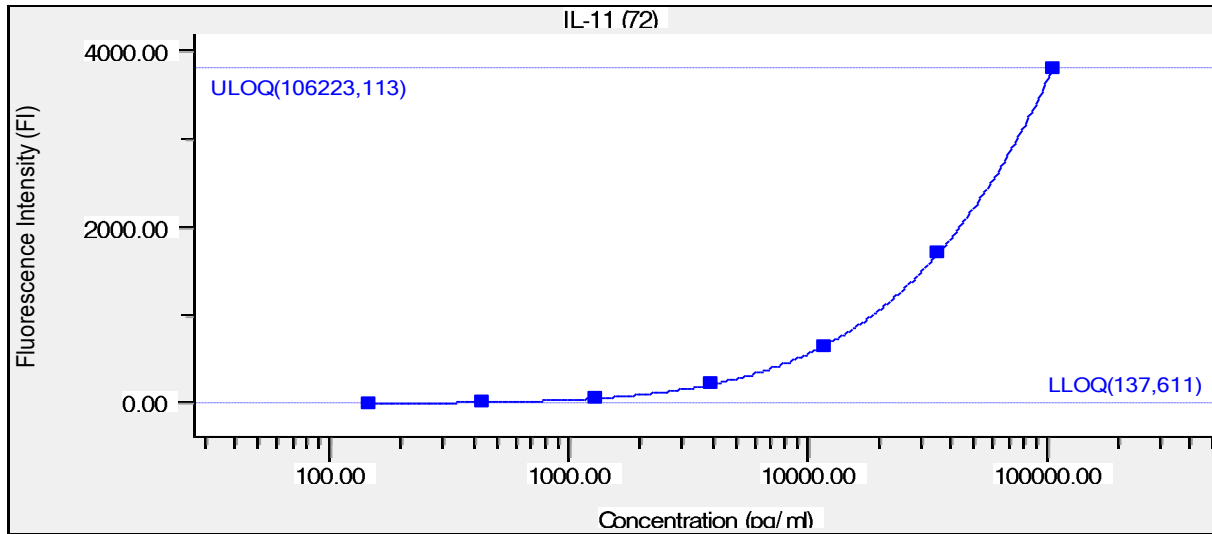
■ Standard □ Partial Outlier ⊗ Outlier

Regression Type: Logistic - 5PL

Std. Curve: $FI = 1,0247 + (3,86125E+007 - 1,0247) / ((1 + (\text{Conc} / 420764)^{-0,195664}))^{5,77412}$

FitProb. = 0,6418, ResVar. = 0,4435

IL11



■ Standard □ Partial Outlier ⊠ Outlier

Regression Type: Logistic - 5PL

Std. Curve: $FI = 4,90078 + (69355,7 - 4,90078) / ((1 + (\text{Conc} / 7286,84)^{-0,273837}))^{7,39831}$

FitProb. = 0,6694, ResVar. = 0,4014